THE IMPACT OF NETWORK CHANGES ON POWER QUALITY AND COMPENSATION DEVICE PERFORMANCE

By

Mbulelo Busani Edmund Ngcamu. Pr Eng

BSc Eng, University of kwa Zulu Natal, South Africa 2001

A Dissertation

A Postgraduate thesis submitted to the Discipline of Electrical Engineering at the University of kwa Zulu Natal in partial fulfillment for the requirements of the degree of Master of Science (Electrical Engineering)

EXAMINER'S COPY

Supervised by: Professor N. M Ijumba (PhD, Pr Eng, CEng)

July 2012

"As the candidate's Supervisor I agree/do not agree to the submission of this thesis.

DECLARATION

I..... declare that

(i) The research reported in this dissertation/thesis, except where otherwise indicated, is my original work.

(ii) This dissertation/thesis has not been submitted for any degree or examination at any other university.

(iii) This dissertation/thesis does not contain other persons" data, pictures, graphs or other information, unless specifically acknowledged as being sourced from other persons.

(iv) This dissertation/thesis does not contain other persons" writing, unless specifically acknowledged as being sourced from other researchers. Where other written sources have been quoted, then:

a) their words have been re-written but the general information attributed to them has been referenced;

b) where their exact words have been used, their writing has been placed inside quotation marks, and referenced.

(v) Where I have reproduced a publication of which I am an author, co-author or editor, I have indicated in detail which part of the publication was actually written by myself alone and have fully referenced such publications.

(vi) This dissertation/thesis does not contain text, graphics or tables copied and pasted from the Internet, unless specifically acknowledged, and the source being detailed in the dissertation/thesis and in the References sections.

Signed:

ACKNOWLEDGEMENTS

First and foremost I would like to thank my Lord Jesus Christ for His guidance and protection through the years and without whom this work would have never materialised. I wish to extend a special thanks to Professor N M Ijumba for his consistent support and guidance throughout the Master‟s program.

I would like to express my sincere gratitude to Mike Nene, Nombuso Gumede, Ezekiel Matlou and Tshokolo Motlala for their assistance and encouragement throughout the compilation of this thesis.

I dedicate this Work to my late Mother, A.N Ngcamu who was supporting me but passed away before completion of this work.

Finally, my deepest appreciation for the love, patience, support, prayers and encouragement I received from my wife Nokubonga Ngcamu.

ABSTRACT

This dissertation describes the impact of changing network configuration on power quality and performance of existing compensation devices in the transmission network. The underlying theory was assessed and thereafter the Everest substation network case scenario was selected to study the above due to; the number of reconfigurations it has experienced in the past, increased capacitor bank failures and also due to the harmonics problems experienced.

The study involved the installation of harmonic current measuring instruments at Everest 132kV feeders to identify the potential sources of harmonics and to determine the dominant harmonics. A dig Silent Power Factory model was then constructed to perform various simulations in order to determine the impact of the changes done on the Everest network as well as the impact of capacitor switching on the harmonics amplification at Everest 132kV Bus-bars. The study also focussed on analysing the performance history of the capacitor banks at Everest and to determine if high harmonic amplification had an impact on capacitor bank performance.

The simulation results revealed that network reconfigurations have negatively impacted power quality at Everest. The results showed that there is also a correlation between the switching of the two 72MVAR capacitor banks and the amplification of the harmonics at Everest. The highest amplification occurred when both capacitor banks were switched in and the resonance point occurred around the 5^{th} harmonic which coincided with the data from field measurements. There was a 61% increase in 5^{th} harmonic impedance amplitude after the Everest network was reconfigured, for the condition when both capacitors are switched in. The lowest amplification occurred when none of the capacitor banks were switched in.

Three options were assessed to eliminate the problem of harmonics at Everest, the first one was to prohibit the switching in of both capacitors at Everest and utilise other available means around the Everest network for voltage support. The second option was to change the capacitor size, thus moving the resonance point away from the 5^{th} harmonic. The last option was to install a harmonic filter at Everest to filter out the problematic harmonics. The first option is recommended as it has been successfully tested, can be readily implemented and is much more cost effective compared to the others.

Table of Contents

List of Figures

List of Tables

List of Abbreviations

THD	Total Harmonic Distortion
PCC	Point of Common Coupling
TDD	Total Demand Distortion
CRT	Cathode Ray Tube
RMS	Root Mean Square
UPS	Uninterruptible Power Supply
AC	Alternating Current
DC	Direct Current
GMR	Geometric Mean Radius
TIPPS	Transmission Information for Performance and Protection System
ENMAC	Energy Management system
HD	Harmonic Distortion
Trfr	Transformer
FFT	Fast Fourier Transform
EMS	Network Control Operating and Alarms Log System

CHAPTER 1: INTRODUCTION

1.1 Background

Since South Africa became a democratic country in year 1994, there has been a steady increase in the number of foreign investors investing in the country. Local companies have also been expanding their operations which initiated a steady slump in electricity generation reserve margins, thereby necessitating additional power generation. Coupled with this was the government‟s social responsibility to provide formal housing for the homeless including free basic electricity. All these factors have led to the escalating energy demands and Eskom, being the main electricity producer has to ensure that the energy needs of all sectors in the country are adequately met.

The growing power demands coupled with the limited generating capacity in the country has introduced undue pressure on Eskom‟s ability to balance power supply and demand. Customers continue to submit new or additional power supply applications and Eskom is expected to honour their promise of powering the nation. In most cases, Eskom network planners try their level best to strengthen, reconfigure and re-design electricity distribution and transmission systems in order to grant required power to the customers.

However, holistic quality of supply analysis was sometimes overlooked in the past, as feasibility studies were often need orientated and normally focused on assessing the availability of capacity, good voltage regulation and financially justifiable solutions. As a result, other power quality aspects were often overlooked, resulting in the network being configured in any manner without conducting adequate quality of supply impact analysis. Also in some cases a number of harmonic producing loads were connected to the network without conducting proper impact analysis and sometimes without imposing and enforcing adherence to necessary contractual emission limits as stipulated in the NRS048 and IEEE 519-1992 standards. This in some cases has led to the deterioration of power quality in a number of Eskom distribution and transmission networks. Literature surveyed indicates that exposure to excessive harmonic voltages and currents over time may have a negative impact on equipment performance [1]. Other harmonics effects include excessive heating and higher stress on the capacitor‟s dielectric/insulation, Waveform distortions can cause relay malfunctioning thereby affecting relay performance and overheating of transformers and neutral conductors particularly caused by third order harmonics.

1.2 Network changes

Everest substation is a 275/132/22kV Transmission station situated in the Free State North West Transmission Grid; it was built in the year 1988 and consists of: two 275/132/22kV 500MVA transformers, 2 x 72MVAR Capacitor Banks and three 275kV supplying lines and nine outgoing 132kV feeders. The substation mainly supplies mines and some industrial customers in the Welkom area of the Free-State Province, as highlighted in figure 3.1 below showing the actual layout of the Everest network

In the year 2005/6 the Welkom Distribution Network which is supplied from Leander, Everest and Theseus transmission stations underwent reconfiguration when one of the main distribution stations, Alma was decommissioned. Most of the load that was supplied by Alma was transferred away from Everest to Euclid substation. The Everest network was also reconfigured when Witpan and Virginia Terminal substations were linked to Leander and Theseus substations due to sensitive customers around the area complaining about poor quality of supply. It was after these reconfigurations that the harmonics levels increase was noticed at Everest substation [2]. Eskom‟s national control centre started receiving THD exceedance alarms (THD levels exceeding NRS048 limits), leading to speculation that the Everest networks have high harmonic voltage content.

A study then had to be conducted to analyse the Everest situation and determine suitable remedial action. The study involved the installation of harmonic current measuring instruments at Everest 132kV feeders to identify the potential sources of harmonics and to determine the dominant harmonics. A dig Silent Power Factory model was then constructed to perform simulations in order to determine the impact of the changes done on the Everest network as well as the impact of capacitor switching on the harmonics amplification at Everest 132kV Bus-bars. Once the impact is fully understood, it is then that suitable mitigation measures could be proposed.

The study also focussed on analysing the performance history of the capacitor banks at Everest and to determine if high harmonic amplification had an impact on capacitor bank performance.

CHAPTER 2: LITERATURE REVIEW

2.1 Harmonics

Harmonics can be described as a phenomenon that causes distortion to the utilities‟ sinusoidal supply voltage. This distortion is caused by non-linear customer loads that draw non-sinusoidal currents [3], [4], [5]. A non-linear load is a type of load that draws a current that is not proportional to the voltage supplied. Figure 2.1 shows graphical representation of a non-linear load.

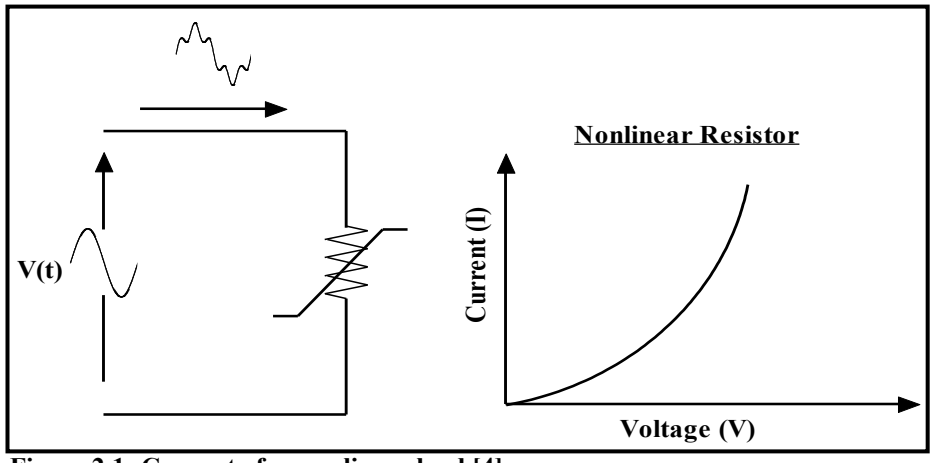

Figure 2.1: Concept of a non-linear load [4].

Typical customer loads that draw non sinusoidal currents from the utilities supply include the following: arc furnaces, welders, electric discharge lamps, electronic power supplies, variable speed drives, static Var compensators etc [3], [4], [5].The non-sinusoidal currents drawn by such loads, flow through the impedance of the supply network and introduce a distortion to the supply voltage at other points in the network. Figure 2.2 below depicts this concept.

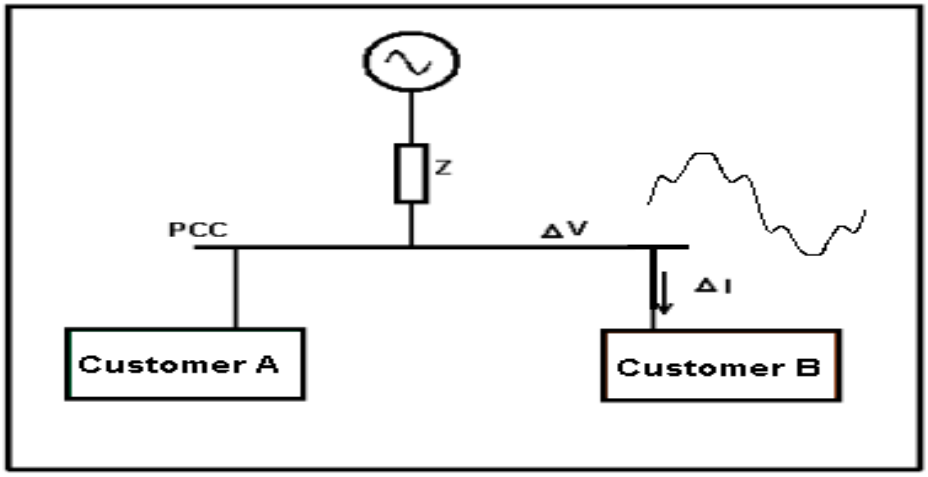

Figure 2.2: Impact of non-linear load on PCC [3]

In figure 2.2 above customer B‟s load draws non-sinusoidal currents from the point of common coupling (PCC) thereby causing a distortion to the source voltage. This distorted voltage is then seen by and can negatively affect customer A in the network.

A harmonic is defined as an integer multiple of the fundamental frequency and is given by the formula [3], [4], [5]:

$f_0 = h.\ f_0$ .....(1)

Where f_0 is the fundamental frequency of the power system and (h) is an integer. In the case of a 50Hz power system, the 3rd harmonic is a 150Hz component.
According to Fourier theory, any stationary, periodic waveform can be obtained by the superposition of individual sinusoidal waves of given magnitude and phase angle [3], [4], [5] Figure 2.3 shows the concept of the Fourier series.

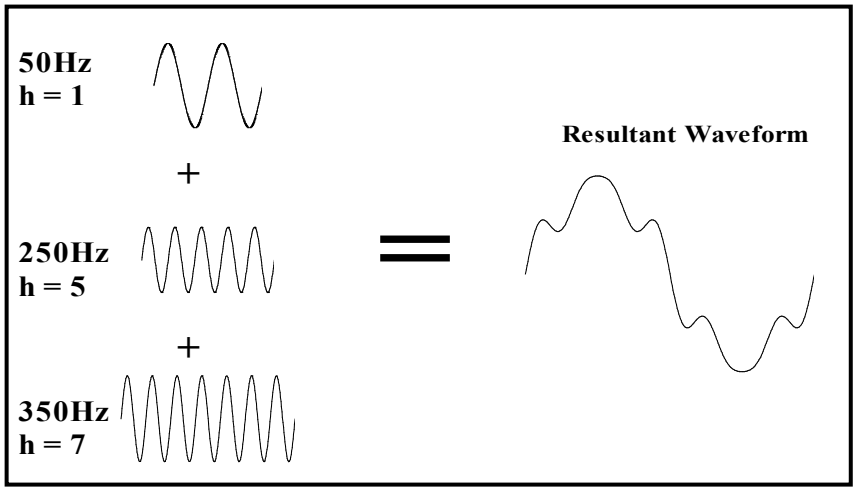

Figure 2.3: Fourier series representation of a distorted waveform [4].

The amplitudes of the harmonic components are inversely proportional to the frequency of the harmonic component [3], [6], [7]. In the case of a 50Hz power system, the 3rd harmonic would give 150Hz component with amplitude of 1/3. This implies that as the harmonic frequencies increase, the corresponding amplitudes tend to decrease.

Frequency domain harmonic analysis algorithms can be derived by means of Discrete Fourier Transform (DFT) or Fast Fourier Transform (FFT) in order to determine the voltage and current frequency spectra from discrete time samples [3], [6], [7].

According to Fourier; a waveform f (t) of period T angular frequency $\omega = 2\pi / T$, can be expanded by [3], [6], [7]:

$$F(t) = a_0/2 + \sum_{n+1}^{\infty} (C_n \sin(n\omega t + \varphi n)$$

The sequence of Fourier coefficients (a_n and b_n) are known as the spectrum of F.

Where; $a_n = 2 / T \int_0^T F(t) \cos(n\omega t dt)$ $\quad C_n = (a_n^2 + b_n^2)^{1/2}$

Where; $b_n = 2 / T \int_0^T F(t) \sin(n\omega t dt)$ $\quad \varphi_n = \tan^{-1}\{a_n/b_n\}$

The periodic waveforms consist of a sum sinusoids at integer multiples of the fundamental frequency f = 1/T, thus the signals at frequencies above the fundamental are called harmonics, where the kth harmonic is the signal at kf [3], [6], [7].

The dc component a_0 is normally zero in a power system; therefore harmonic distortion management focuses on minimising the individual frequency components C_n.

2.2 Application of the Fourier series for harmonic measurement

The application of the Fast Fourier Transform (FFT) is utilised for the accurate digital approximation of an input signal and there are three parameters that are critical for the success of the approximation process [3], [8]:

i. Sampling window length – refers to a finite sample of data obtained from a continuous current or voltage signals. For accurate representation of the true signal, when the sample window is repeated, it should approximate the true signal
ii. Sampling rate – determines the maximum frequency that the FFT can accurately depict the underlying signal. There are two principles that should be applied:
    a. Adherence to Nyquist criterion which prescribes that the sampling frequency must be twice the maximum frequency to be extracted by the FFT.
    b. All frequencies above the defined maximum frequency must be negligible in magnitude; otherwise the FFT will reflect them as lower frequency components.
iii. The vertical resolution of the A/D converter - defines the number of "steps" that can be vertically displayed; thus indicating signal accuracy.

2.2.1 Challenges in applying the FFT

The FFT suffers from a number of pitfalls that might negatively impact on the accuracy of the sampled signals, these include [3], [8]:

- Aliasing – occurs when signals of higher frequency than the sampling frequency are present in in the waveform. This tends to cause lower harmonics to be indicated higher than they really are. Therefore, it is critical that the sampling rate of a digital recorder be at least twice the frequency of the maximum frequency component of the input signal, in order to avoid aliasing errors. Aliasing problems can be resolved by increasing the sampling frequency, by pre-filtering the analogue signal, or using digital recorders that employ anti-aliasing filters.
- Picket fence effect – occurs when the resultant waveform includes frequencies that are not one of the discrete frequencies. This can be corrected by adequately adjusting the sampling frequency.
- Round off noise – refers to errors in the FFT output caused by rounding off and truncation errors during signal approximation. Such errors are not easily predictable, hence amplitude bit resolution and sampling frequency must be adjusted higher to address this phenomenon.

2.3 Total Harmonic Distortion (THD)

Total harmonic distortion gives an indication of the total distortion at a certain bus bar within the power system. THD is defined as the r.m.s value of the individual harmonic components; where $V_{(h)}$ is the magnitude (%) of harmonic component (h) [3], [4], [9]:

$$V_{(h)} = \sqrt{\sum V(h)^2} \quad \text{.....(2)}$$

THD does not give details of which harmonic components are more dominant.

2.4 Propagation of Harmonic Distortion in a Power System

A first order representation of a power system at harmonic frequencies defines the impedance of generators, lines and transformers as equivalent reactance-s of magnitude given by [3], [4], [9]:

$$X_{(h)} = h * X_0 \quad \text{.....(3)}$$

Where; h is the harmonic order and X_0 refers to the reactance at fundamental frequency.

It is then possible to determine the Thevenin equivalent of the network at each harmonic frequency. Since the harmonic voltages generated by the generators are normally considered as negligible, therefore the Thevenin voltage source is zero (short circuit). Figure 2.4 below depicts the Thevenin equivalent circuit for the network. The impedance of the network at certain frequencies determines the flow of harmonic currents. The harmonic currents will naturally flow through the least impedance path in the network, and then flow back towards the system generators [3], [4], [9].

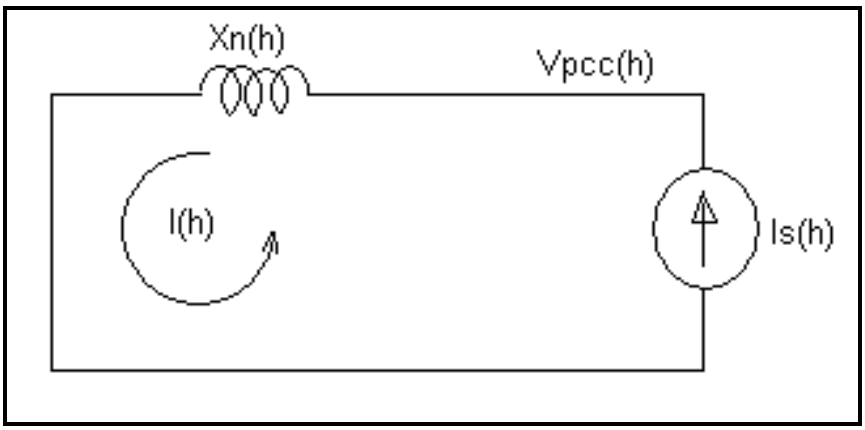

Figure 2.4: First order Thevenin network representation at harmonic frequencies [3].

The harmonic voltage is given by:

Vpcc(h)= Xn(h). Is(h) volts ..... (4)

Where *Vpcc(h)* is the harmonic voltage at the point of common coupling, $X_n(h)$ is the Thevenin equivalent impedance, and $I_s(h)$ characteristic load current.

The harmonic voltages in the system tend to be highest in magnitude at the load side and appear reduced in magnitude as one approach the generators [3], [4], [9]. *Vpcc(h)* is that point in the network where harmonic distortion will affect other customers connected to that point. Figure 2.5 below depicts the resultant voltage distortions in the network, where the resulting harmonic voltages are largest in magnitude at the load side and decrease in magnitude when moving closer to the generators [3], [4], [9]. $I_a(h)$ indicates the characteristic harmonic load current, while 3%, 1% and 0.1% indicates the typical reduction in harmonic voltages as one moves from the nonlinear load to the generators. This would be mainly caused by the change in network impedance as the harmonic current flows through the network.

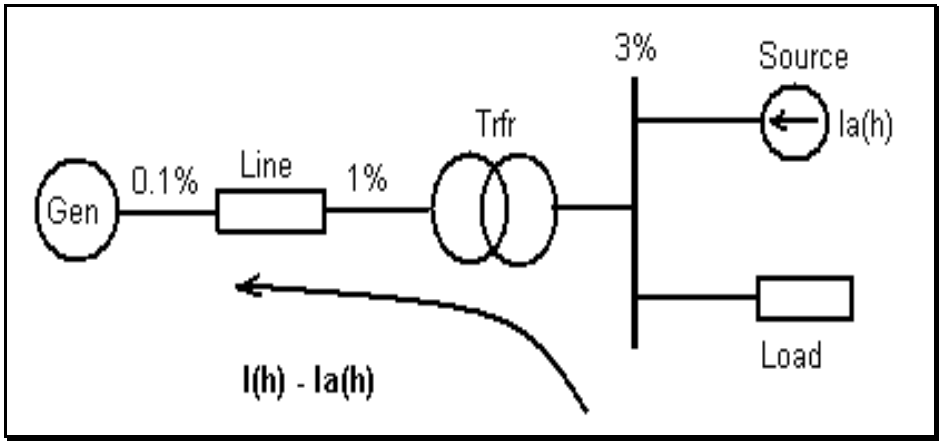

Figure 2.5: Resulting distribution of harmonic voltages in the supply network [3]

2.5 Harmonic Resonance

The harmonic levels in the system can also be influenced by resonant conditions; therefore it becomes critical to monitor and control these conditions in order to reduce voltage distortions. Resonance causes the levels of harmonics to be amplified in the network. Resonance occurs at specific frequencies, which is determined by the component impact of the capacitive (e.g. capacitor banks) and Inductive (e.g. Transformers and rest of the network) components of the network [3], [4], [10].

At the resonance frequency the inductance and capacitance reactance are the same. The reactance of these components is dependent on frequency. The formulas for these impedances are given below.

$$X_L = j2\pi fL \quad \text{.....(5)}$$

$$X_C = \frac{1}{j2\pi fC} \quad \text{.....(6)}$$

Where L and C are the inductance and capacitance values respectively, f is the frequency. The resistive part of the network changes with the square root of the harmonic; this is done to roughly take into consideration the skin effect. From these equations it can be seen that as the frequency increases the inductive impedance increases and the capacitive impedance decreases and vice versa. The resonant frequency can be calculated as follows [3], [4], [10]:

$$f_{resonance} = \frac{1}{2\pi\sqrt{LC}} \quad \text{.....(7)}$$

In equation (7) above, the resonant frequency is calculated using the networks inductive and capacitive component values.

Resonance can either be parallel or series depending on where the harmonic source is situated in the network. The difference between series and parallel resonance is in the harmonic impedance at the resonance frequency. Parallel resonance is manifested by high impedance which hinders the flow of harmonic currents, while on the other hand series resonance is manifested by low impedance [3], [4], [10].

Figures 2.6 and 2.7 below depict the parallel and Series impedances under resonance conditions.

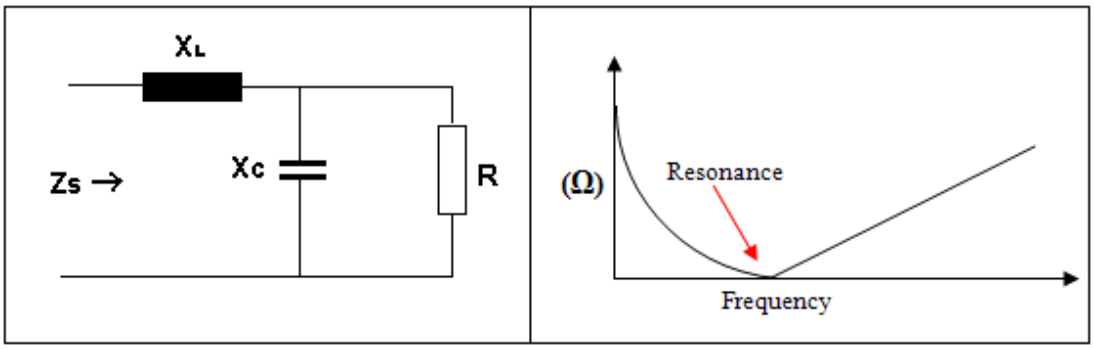

Figure 2.6: Series harmonic network and impedance [3]

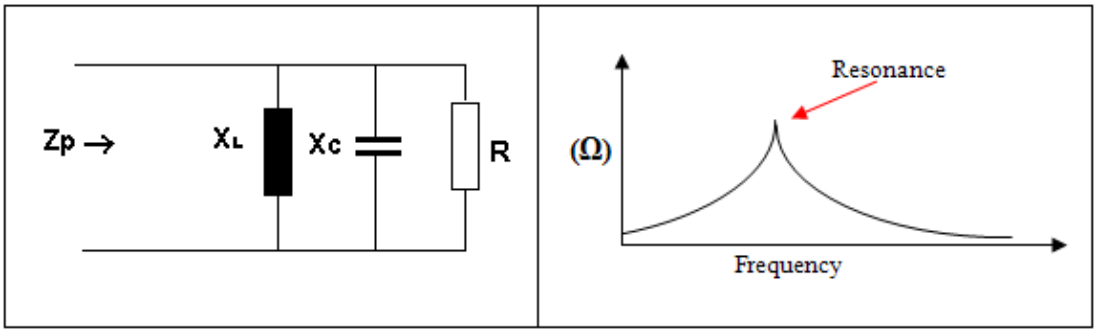

Figure 2.7: Parallel harmonic network and impedance [3]

2.5.1 Effect of Load Damping

Another important consideration is network loading which plays a critical role in the damping of harmonics. High network loading provides adequate load damping which results in significantly reduced impedance at resonant frequency. A resonance point may exist at a

certain PCC; however the consequences may not be detrimental if there is adequate load damping that may reduce the size of the harmonic distortion to acceptable levels [3], [4].
High amplification of harmonic impedance will occur if the characteristic frequency of the harmonic producing load coincides with the resonance frequency of the network. Therefore, it is necessary to study the system resonance conditions before connecting any new harmonic producing loads in order to avoid system resonance problems. One can use the following rule of thumb to predict the frequency at which resonance may occur [3], [4].

The parallel resonance frequency can be calculated by using the following formula:

$$f_{parallel\_resonance} = f_1\sqrt{\frac{S_{sc}}{Q_c}} \quad \text{.....(8)}$$

Where f_1 refers to the fundamental frequency, S_{SC} the short circuit power at the bus-bar of the system and Q_C the total reactive power generated by capacitors and cables in the system.

The series resonance frequency can be calculated by making use of the following formula:

$$f_{series\_resonance} = \sqrt{\frac{S_{TRFR}}{Q_C} * \frac{100}{X_{TRFR}}} \quad \text{.....(9)}$$

Where; S_{TRFR} is the transformer power rating, Q_C the capacitor bank rating and X_{TRFR} the impedance of the transformer in percent. The assumption made here is that the transformer impedance is large relative to the impedance of the upper network.
Non-linear loads are main sources of harmonics in the network, and these should be modelled as current sources for accurate harmonic analysis [3], [4].

2.6 Effect of Harmonics on the Power System

Harmonics distortions have various effects on the power system; these include [3], [11], [12]:

- Harmonics are known to cause excessive heating and higher stress on the capacitor"s dielectric/insulation.
- Waveform distortions can cause relay malfunctioning thereby affecting relay performance.

- Overheating of transformers and neutral conductors particularly caused by third order harmonics.
- They result in increased I^2R losses in the transmission system, due to the flow of harmonic currents.
- They increase the losses in transformers especially the eddy current losses,

2.7 Mitigation of the Effects of Harmonics

The power system harmonics can be mitigated by doing the following [3], [4], [12]:

- Power System Design:
  - ✓ Limiting the non-linear load to 30% of the maximum transformer‟s capacity
  - ✓ Limiting non-linear loads to 15% of the transformer‟s capacity, when power factor correction capacitors are installed.
  - ✓ Determining if resonant condition on the distribution could occur:

- Changing capacitor size can result in significantly reduced amplification at resonant frequency
- Installation of harmonic filters tuned to filter out specific harmonics
- Network reconfiguration

2.8 IEEE 519 1992 “Harmonic Limits”

This standard aims to establish “harmonic voltage limits for transmission and distribution networks as well as set harmonic currents limits in the industrial distribution networks” [13]. When harmonic currents flow in the network impedances, it causes harmonic voltages which distort the utilities‟ supply voltage; therefore it becomes important to control the harmonic currents and impedances in order to control harmonic voltages. The harmonic limits discussed in the IEEE 519 1992 standard are aimed at [13]:

- Limiting the harmonic currents from non-linear loads to prevent excessive voltage distortion levels
- Limiting the harmonic distortions utilities‟ supply voltage

The limits for voltage and current harmonics defined in IEEE 519 1992 depend on various variables such as:

- **PCC:** Point of common coupling. This refers to the point of interface between the utility and a particular customer [13], [14]. It is the electrical point of connection between the utility and customer, where meaningful harmonic measurements can be taken.
- $\mathbf{I_{SC}}$**:** short circuit current.
- $\mathbf{I_L}$**:** average maximum demand current.
- **TDD:** Total demand distortion. which is similar to Total Harmonic Distortion

2.8.1 Voltage Distortion Limits

Voltage distortion limits recommended by IEEE519 1992 define the minimum quality of the utilities‟ supply voltage. Table 2.1 below shows voltage distortion limits for various distribution and transmission systems.

***PCC* Voltage**	**Individual Harmonic Magnitude (%)**	**THDv (%)**
≤69kV	3	5
69 - 161kV	1.5	2.5
≥ 161kV	1	1.5

Table 2.1: Voltage Distortion Limits (in % of V1) [13]

Voltage distortions are created when harmonic currents flow through the distribution network‟s impedances thereby causing voltage drops at each harmonic frequency. The harmonic voltages created sum up and lead to the distortion of the fundamental frequency supply voltage. Equation (5) above, tells us that the system reactance is proportional to the system frequency, therefore at 5^{th} harmonic frequency the reactance will also be five times the fundamental reactance figure. Therefore even if small amounts of harmonic currents flow in the network, they would cause high levels of harmonic voltage distortions.

The IEEE 519, 1992 standard indicates that the network can be represented by a short-circuit impedance, where the impact of capacitors is neglected. Capacitors tend to introduce low-impedance paths for harmonic currents to flow at high frequencies [13]. At lower frequencies capacitors tend to introduce resonant conditions that could amplify the system impedance to exceed the short-circuit impedance [13].

The network‟s harmonic voltage distortion is influenced by the injected harmonic current and the network impedance at each harmonic frequency [13]. The quantity and the size of non-linear loads/customers determine the total injected harmonic currents. The IEEE 519, 1992 standard establishes a guideline for limiting harmonic currents injection based on the non-linear load size. The larger the non-linear load/customers the stricter the emission limits are since the larger non-linear load contributes more to the distortion [13].

The current distortion limits developed takes into account that the harmonic currents injected by individual customers vary in harmonic components injected and in harmonic currents phase angles [13]. Therefore, the harmonic current limits stipulated in Table 2.1 above are used to monitor and control the individual frequency harmonic voltage distortions triggered by a particular customer.

Voltage distortion levels can be further reduced by implementing filters in the network especially in cases where individual customers do meet the stipulated current distortion limits, but due to insufficient diversity between harmonic injections, high voltage distortion levels still persist [13]. The network‟s frequency response characteristics can sometimes cause voltage distortion problems leading to harmonic current amplification at a certain harmonic frequency. The network‟s frequency characteristic results from the system‟s physical configuration that can be corrected by network reconfiguration, relocating capacitors, changing capacitor sizes or by installing a harmonic filter [13].

2.8.2 Current Distortion Limits

According to the IEEE 519, 1992 standard it is important to limit the harmonic distortions caused by any customer at any location in the network in order to ensure that the network‟s harmonic levels are acceptable at any point [13].

The harmonic current distortion limits recommended by IEEE519, 1992 standard depict the acceptable distortion by any customer at any location in the network. The following indices are recommended [13]:

- TDD: Total demand distortion - harmonic current distortion is represented as % of peak demand load current
- Maximum Harmonic Current Distortion represented as Percent of I_L
- Individual Harmonic Order

Is/IL	<11	11<h<17	17<h<23	23<h<35	35<h	TDD
<20	2	1	0.75	0.3	0.15	2.5
20<50	3.5	1.75	1.25	0.5	0.25	4
50<100	5	2.25	2	0.75	0.35	6
100<1000	6	2.75	2.5	1	0.5	7.5
>1000	7.5	3.5	3	1.25	0.7	10

Table 2.2: Current Distortion Limits for Sub transmission Systems [13]

- Even harmonics are restricted to 25% of the odd harmonics.
- Dc offsets that emanate from current distortions a, e.g., half-wave rectifiers, are not permitted.
- Despite the value of $I_{sc}/I_{L;}$ power generation plant is restricted to the current distortion limits above.

Where

- I_{sc} = Maximum short-circuit current at PCC.
- I_L = maximum demand load current

In Table 2.2 above, the ratio of the short circuit current capacity to the customer‟s maximum load current at the point of common coupling is used to express customer size [13]. These harmonic current limits indicated are aimed at limiting the individual frequency voltage harmonic to 3% of the fundamental and the voltage THD to 5% of the fundamental frequency voltage [13].

2.9 Harmonic Trap Filters

Harmonic filtering is often necessary in cases where non-linear loads constitute more than 20% of the electrical load connected to a distribution system, in order to ensure that harmonic current distortions are acceptable [14], [15], [16]. The most common or easiest to implement is a series tuned L-C shunt filter, also known as “harmonic trap filer.” These types of filters can be constructed using special tuning reactors (L) and capacitors (C).

The important characteristic of a series L-C filter is such that its impedance is very low at the tuning, or resonant frequency [14]. The harmonic filter needs to be tuned at the characteristic harmonic frequency drawn by a non-linear load; this will enable the harmonic current to be

drawn from the trap filter therefore allowing the fundamental frequency current to be drawn from the distribution network. This situation will ensure that most of the harmonic current demanded by the non-linear load will be supplied by the harmonic trap filter and therefore less harmonic current will be drawn from the distribution network. This will therefore lead to the reduction of the harmonic current distortion at PCC.

When an isolation transformer or a series line reactor is installed before the harmonic filter, it will increase the network impedance at certain harmonic frequencies. This will therefore lead to the diversion of larger amount of harmonic currents to the filter. This will lead to the reduction of harmonic currents in the network.

Figures 2.8 and 2.9 depict simplified harmonic trap filters diagrams and indicate necessary connections for effective harmonic reduction [14], [15], [16].

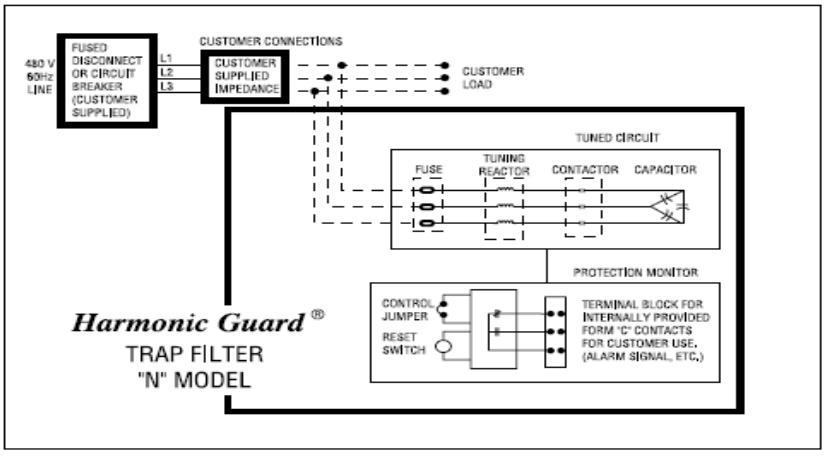

Figure 2.8: Trap filter without line reactor [14]

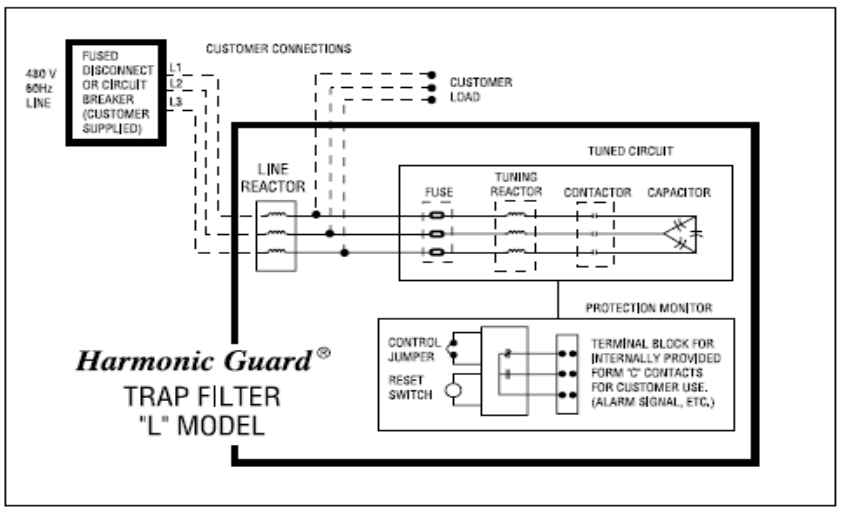

Figure 2.9: Trap filter with line reactor in series [14]

2.9.1 Harmonic Filter Tuning

The most appropriate way to tune a trap filter is to tune it just below the lowest harmonic present in the distribution network. For instance in a 3-phase 6-pulse rectifier, the 5^{th} harmonic (300 Hz) is the lowest characteristic harmonic, therefore the trap filter can be tuned at 282Hz [14], [15], [16]. This will enable the most of the 5^{th} harmonic currents to flow into the trap filter. Since harmonic trap filters are broad band, a 5^{th} harmonic tuned filter is capable of also absorbing significant amounts of 7^{th} harmonic currents. Higher harmonic frequencies will be significantly reduced by the series impedance. Therefore a 5^{th} harmonic tuned trap filter is capable of limiting the harmonic currents at PCC to acceptable levels.

2.9.2 Harmonic Trap Filter Disadvantages

Harmonic trap filters tend to try to filter the entire distribution network of harmonic components, as such if additional non-linear loads are connected to the network without filtering, the previously installed filters may become overloaded. However a line reactor can be used in conjunction with the filter to minimize the likelihood of this occurring and to improve the filter performance. Other disadvantages include [14], [17]:

- The cost of harmonic trap filters is relatively high
- Reliability may be reduced due to the larger number of components making up the filter
- Increased protection requirements and possibility of inferior reliability
- Network changes such as adding nonlinear loads could lead to overloading therefore caution is required to the overloading of the filter

2.10 Voltage Unbalance

Voltage unbalance occurs when the magnitude and/or phase angle differs between the phases of a three phase power system [18].

The voltage unbalance in a power system is given by:

$$\%\text{V-unbalance} = \frac{\text{Maximum Deviation from the average line voltage} \quad \text{X } 100}{\text{Average Line Voltage}} \qquad \ldots\ldots(10)$$

Or

$$\%\text{V-unbalance} = \frac{\text{Maximum Deviation from the average phase voltage} \quad \text{X } 100}{\text{Average Phase Voltage}} \qquad \ldots\ldots(11)$$

2.10.1 Causes of Voltage Unbalance

Voltage unbalance is mainly caused by any of the following [18], [19]:

- Unbalanced distribution of loads across the three phases of the distribution network
- Long transmission lines that are not transposed (the impedance of the centre phase differs from that of the outer phases, resulting in differing voltages at the receiving end – even if the load itself is balanced)
- Unequal transformer tap settings
- Arc furnaces (particularly when the electrode breaks in the middle of a melt cycle)
- A blown fuse on a 3 phase bank of power factor correction improvement capacitors.

2.10.2 Effects of Voltage Unbalance

The main impact of voltage unbalance is on motors and generators, the effects appear as follows [3], [19]:

- Increased heating of the rotor and the stator, resulting in higher temperatures that impact the life span of the insulation.
- Motor tripping (Where motor unbalance protection or over current protection is installed).
- Reduced average torque supplied by the motor.
- Increase vibration and noise.

Figure 2.10 below, shows the percentage of temperature rise as related to the voltage unbalance. The relationship is exponential, and approximately increases by twice the square of the percent of voltage unbalance [3], [19].

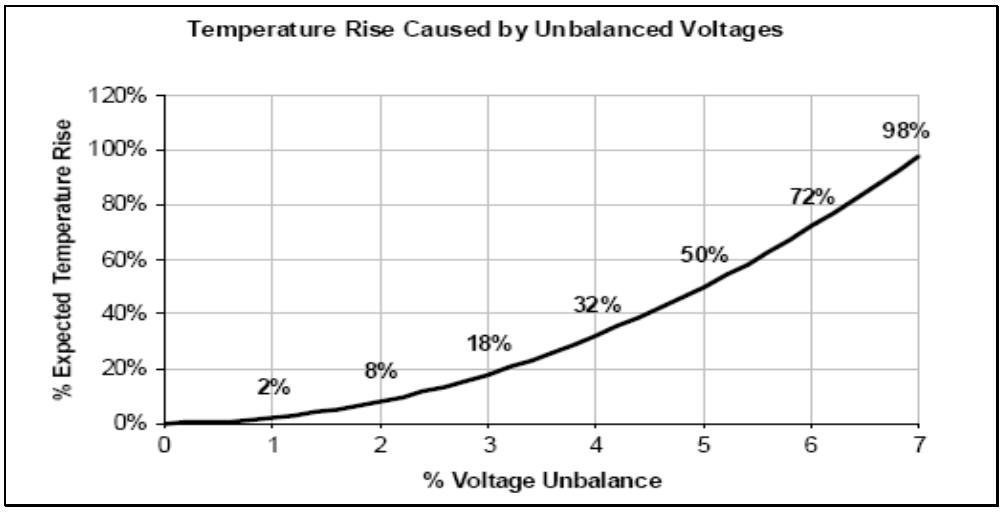

Figure 2.10: Percent Temperature Rise Due to Voltage Unbalance [19]

2.10.3 Mitigation of Voltage Unbalance

As indicated above, voltage unbalance can be very harmful to the health of motors and detrimental to operation, it critical to mitigate the voltage unbalance problem as soon as it is identified. Voltage unbalance can be mitigated by doing the following [3], [19]:

- Motor De-rating – to reduce the possibility of damage
- Application of appropriate motor protection
- Correcting unbalance system loading problems
- Transposition of un-transposed long lines
- Installation of phase shifting transformers

2.11 Flicker and Voltage Fluctuation Phenomenon

Flicker can be described as the fluctuation in the supply voltage and is visible in the momentary dimming/ fluctuations in the light intensity [3], [20].

2.11.1 Measurement of Voltage Flicker

Because the voltage fluctuations are random in nature it becomes difficult to compare the frequency sensitivity of the human eye to the voltage fluctuations. Therefore flicker is measured by an instrument that simulates for any fluctuating voltages supplied to its terminals. The IEC 61000-4-15 specifies the flicker measurement instrument which provides an output P_{st} that describes the flicker severity over a short term (10 minutes) [3], [20].

The figure below shows P_{st} =1 curve for rectangular voltage changes (%) for (60W), 120 A and 230 V lamps. This figure indicates that the human perception of voltage flicker is greatest around 1000 changes per minute.

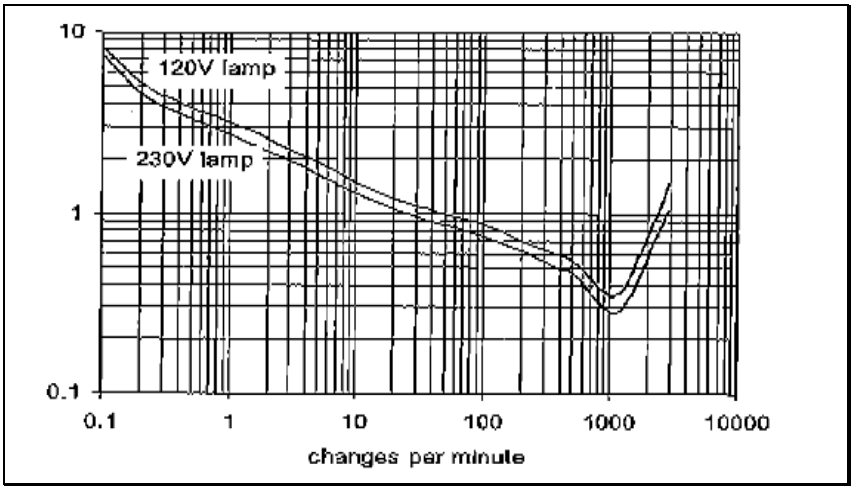

Figure 2.11: P_{st} = 1 Curves for Rectangular voltage Changes [3]

Pst is given as: $Pst = \frac{Pst(LV) \times Ssc(LV)}{Ssc(HV)}$ .....(12)

Where: $S_{sc}(LV)$ = Short Circuit MVA at LV

$S_{sc}(HV)$ = Short Circuit MVA at HV

$P_{st}(LV)$ = Flicker Severity at LV

$P_{st}(HV)$ = Flicker Severity at HV

2.11.2 Causes of Voltage Flicker

Flicker is mainly caused by loads that draw fluctuating currents; these loads include [3] [21]:

- Arc Furnaces and Welders
- Motor loads which drive loads that vary with time (Saw mills, rolling mills and crushers).
- Controlled loads (Burst heating, Thermostat controlled heating such as Geysers).

2.11.3 Effects of Voltage Flicker

Flicker mainly affects the human eye; other effects include [3], [21]:

- Problems with online balancing technologies
- The image on some older CRT displays

2.11.4 Mitigation of Voltage Flicker Problems

The mitigation of the flicker problem is largely dependent on the cause and the effect of the flicker phenomenon. The following are some of the mitigation strategies that may be employed [3], [21]:

- Increasing the fault level at the HV bus bar

- Installation of shunt compensation at the arc furnace MV bus bar
- Application of alternative furnace technologies e.g. DC furnaces generates significantly less flicker than AC furnaces.
- Higher wattage lamps can be used where individual customers complain.

2.12 Voltage Dips

A voltage dip is a short-term reduction (typically less than 3seconds) in at least one of the three phase or line voltages, below a specified dip threshold. Voltage dips are normally specified according to the duration and magnitude of the retained voltage, which is given as a percentage of nominal RMS voltage sustained at the lowest point during the dip [3], [22].

2.12.1 Voltage Dips Detection

Voltage dips are normally detected when the nominal rms voltage drops below a certain threshold which is usually defined as a percentage of a reference voltage. The reference voltage can be the nominal voltage, the declared voltage, or a value representing the voltage magnitude just before the dip event is initiated [3], [22].

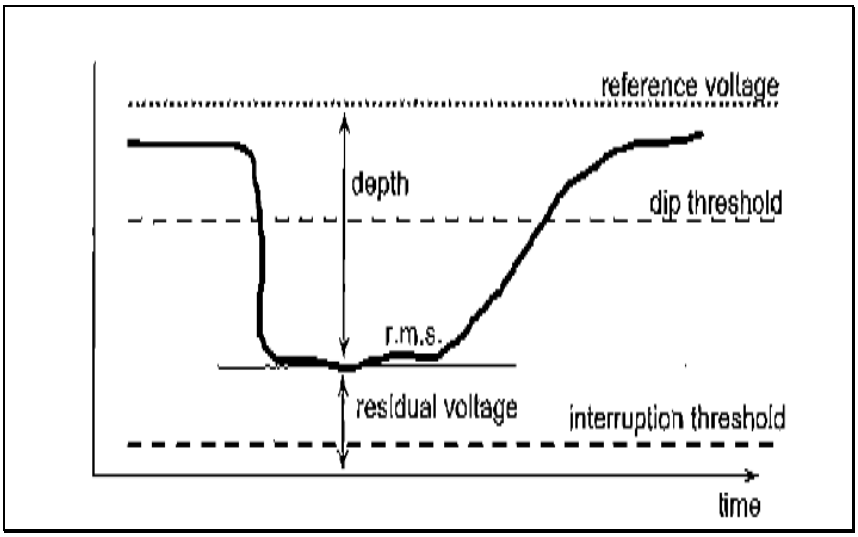

Figure 2.12: Dip and Interruption Thresholds [3]

2.12.2 Causes of Voltage Dips

Voltage dips are normally caused by faults on the supply network or the customer‟s plant or facility. The dip magnitude is dependent on the fault level and the fault location in relation to the measurement point. The dip duration is dependent on the response times of protection equipment to isolate the fault from the network [3], [23].

Typical network faults are caused by bird activity on the lines, line hardware failures, lightning activity and fires.

2.12.3 Effects of Voltage Dips

Voltage dip events very often affect voltage dip sensitive customers and they can be costly, effects include [3], [23]:

- Malfunctioning of control circuits resulting in the tripping of the process.
- Physical damage or failure of power electronic devices and fuses due to high currents.
- Stalling of Motors (when attempting to accelerate on a weak system after a fault).
- Motor contactors to drop out due to a lack of voltage to the magnetic coils that keep the contacts connected.
- Variable speed drives to trip due to operation of their under voltage protection or over current protection.

2.12.4 Mitigation of Voltage Dips

When a voltage dip occurs on the network a considerable retained voltage exist in the network, such that there is some energy available however it is useless to the load since the voltage is very low. There are various voltage dip mitigation devices that can be implemented to reduce the effect of many types of voltage dips in the network. Such devices function by generating full voltage from the available energy during the dip. They are generally known as automatic voltage stabilisers [3], [23], [24].

The typical types of automatic voltage stabilisers include [3], [23], [24]:

- **Changing the motor starter contactors from AC to DC to extend ride-through**. A DC contactor or relay is stronger because the flux is constant. A rectifier is required to change AC to DC. A small storage capacitor could be added to DC contactor to extend ride-through energy. Disadvantage of DC is increased arcing due to lack of zero crossing to break the arc.

- **Off-line UPS, uninterruptible power supply,** on a PC, PLC or controls to switch to battery on a dip below 105 volts or an interruption. An advantage is that the UPS will ride through not only sags, but also momentary and extended interruptions up to the limit of the battery capacity, maybe 5 to 10 minutes.

- **Ferro-resonant (constant voltage) transformer** on PC, PLC or controls to provide sag ride-through. They also provide filtering of transients. They will not ride through a momentary or sustained interruption.

- **Thyristor switched-line voltage regulator** on computers and other three phase sensitive equipment, not on motor controls. It utilizes thyristor control of buck and boost transformers in combination with parametric filters to provide regulated sinusoidal output even with nonlinear loads typical of computer systems.

CHAPTER 3: METHODOLOGY

3.1 Network Model Development

Everest substation is a 275/132/22kV Transmission station situated in the Free State North West Transmission Grid; it was built in the year 1988 and consists of: two 275/132/22kV 500MVA transformers, 2 x 72MVAR Capacitor Banks and three 275kV supplying lines and eleven outgoing 132kV feeders. The substation mainly supplies mines and some industrial customers in the Welkom area of the Free-State Province. Since year 2005 the Eskom"s national control centre has been receiving THD exceedance alarms (THD levels exceeding NRS048 limit of 3%), leading to speculation that the Everest networks have high harmonic voltage content. Figure 3.1 below shows the actual layout of the Everest network

This dissertation investigates the root causes of the high harmonics problem at Everest substation. It also investigates the impact of high harmonics on Everest capacitor banks performance. The Everest network model was created using Dig-silent Power Factory Modelling tool.

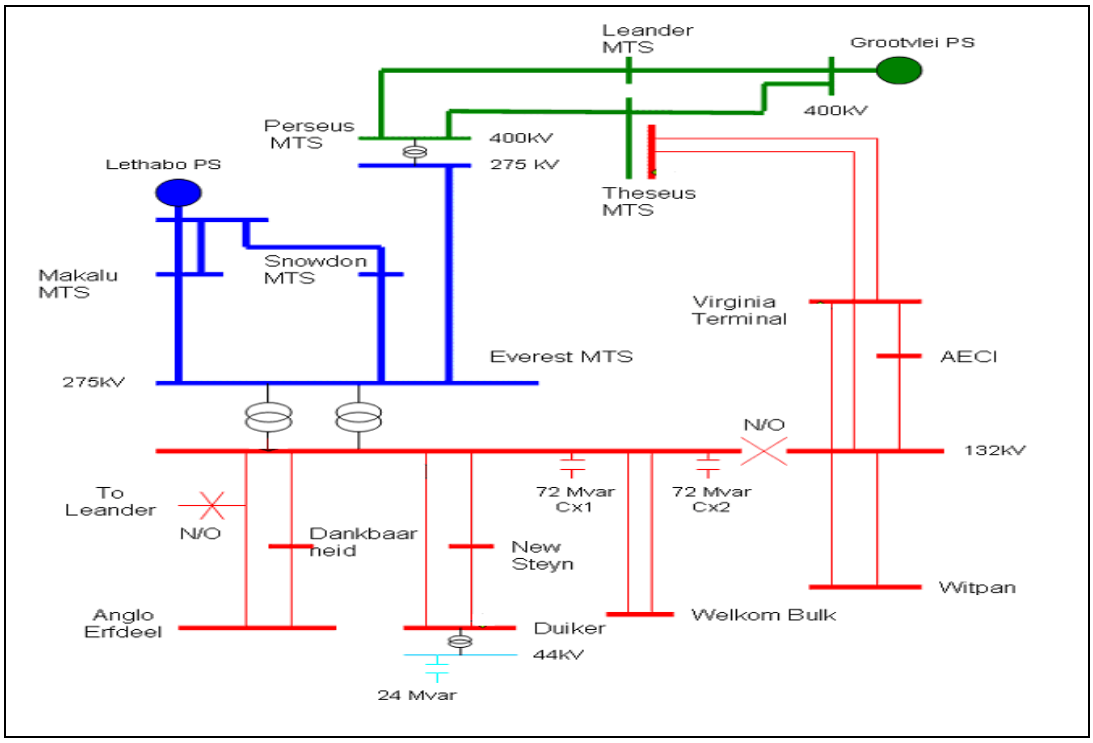

Figure 3.1: Everest network diagram [2]

The figure above shows Welkom Transmission network diagram which depicts Everest substation interconnection with Makalu, Snowdon, Theseus, Leander, and Peseus Main

Transmission Stations (MTS). Lethabo and Grootvlei Power Stations are also shown as main source of power in to the network.

Figure 3.2 below depicts the Everest Substation as seen from ENMAC (system used by controllers to monitor and control the network). The figure shows the snapshot of the network during day time when both capacitor banks were switched out.

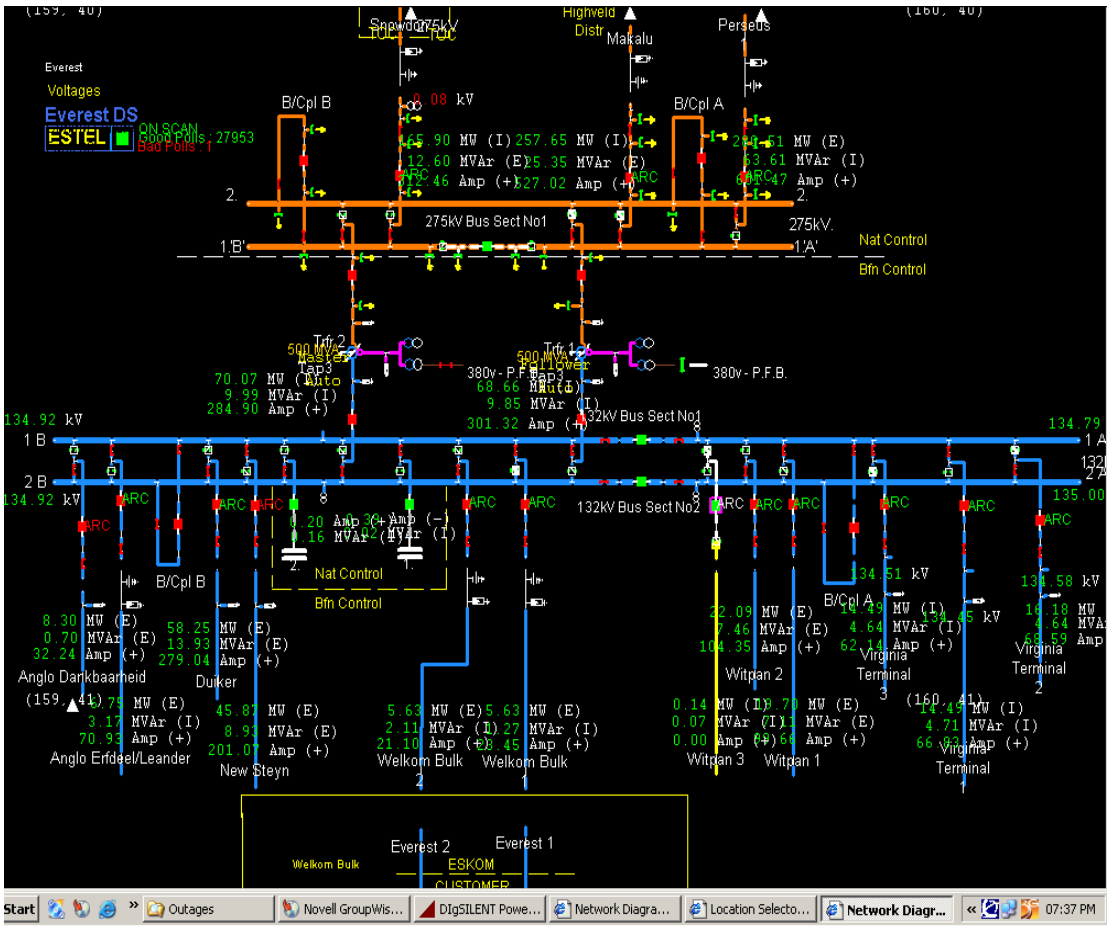

Figure 3.2: Everest network schematic diagram

3.1.1 Dig-silent Power Factory Network Model

In order to simulate various network conditions it was necessary to build a Dig-silent Power Factory Model to match the real life network. Figure 3.3 below shows the Everest network model in Dig-silent Power Factory where the equipment drawn in light blue colour indicates 132kV network. The dark green colour indicates 400kV network.

The orange colour indicates the 275kV network, while the purple colour indicates the 66kV network.

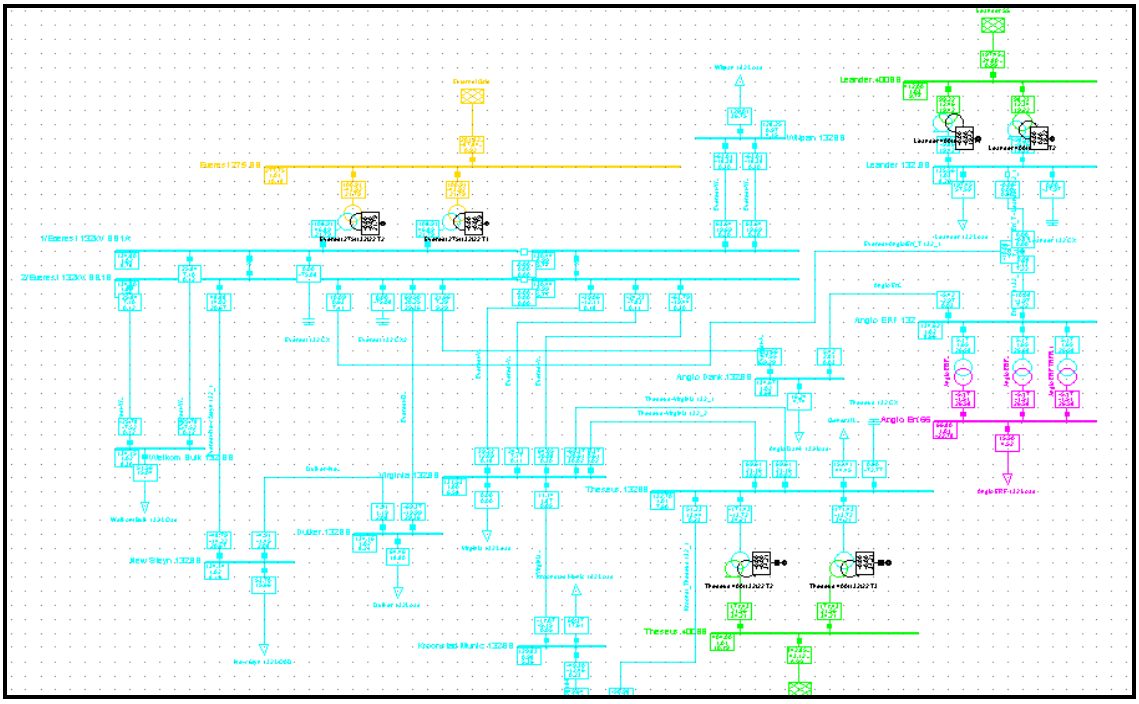

Figure 3.3: Everest network model in Dig-silent Power Factory [26]

3.1.2 Loading Data Used For Simulations

The loading information for the Everest network was obtained from the winter 2010 load test report. This report outlines the loading of all equipment in the distribution network as obtained from various online metering systems in the field during winter system peak.

The table below depicts the current Welkom main transmission stations peak transformer loadings

Transformer Name	Maximum Loading	Rated Power	Total Apparent Power	Total Active Power	Total Reactive Power
	%	MVA	MVA	MW	MVAR
Everest 275/132/22 T1	22.25	500	111.27	100.91	46.89
Everest 275/132/22 T2	22.25	500	111.27	100.91	46.89
Leander 400/132/22 T1	19.94	500	99.71	99.22	9.86
Leander 400/132/22 T2	19.94	500	99.71	99.22	9.86
Theseus 400/132/22 T1	34.40	500	171.98	171.43	13.72
Theseus 400/132/22 T1	34.40	500	171.98	171.43	13.72

Table3.1: Loading of Everest Network

The table below depicts the Welkom network peak distribution line loadings

Line Name	Loading	Rated Power	Apparent Power	Active Power	Reactive Power
	%	MVA	MVA	MW	Mvar
Anglo-Erf_T - Leander 132_1	0.00	196.39	0.00	0	0
Everest-Anglo Dank 132_1	9.45	241.89	22.85	21.66	7.29
Everest-Anglo/Erf_T 132_1	7.25	139.46	10.11	10.09	0.63
Everest-Duiker 132_1	29.93	241.89	72.39	69.5	20.25
Everest-New Steyn 132_1	21.02	241.89	50.85	48.88	14.02
Everest-Virginia 132_1	20.82	196.39	40.89	39.06	-12.11
Everest-Virginia 132_2	12.97	196.39	25.46	-24.23	-7.83
Everest-Virginia 132_3	33.96	196.39	66.69	-63.79	-19.44
Everest-Welkom Bulk 132_1	13.62	196.39	26.74	25.78	7.1
Everest-Welkom Bulk 132_2	13.75	196.39	27.00	25.84	7.84
Everest-Witpan 132_1	33.87	196.39	66.52	-63.54	-19.69
Everest-Witpan 132_2	33.87	196.39	66.52	-63.54	-19.69
Kroonst_Theseus 132_1	26.97	196.39	52.96	51.23	13.44
Theseus-Virginia 132_1	30.08	241.89	72.76	69.61	21.16
Theseus-Virginia 132_2	30.08	241.89	72.76	69.61	21.16

Table3.2: Loading of Everest & other Welkom Networks

3.1.3 Modelling of Transmission and Distribution Lines

The actual data used to build the all line models was obtained from Eskom‟s Phoenix plant database that is used to store specific plant data. Everest substation is supplied via three 275kV lines namely:

1) The Perseus – Everest 275kV line 1 is 146.8km in length and is constructed in twin bare conductor which has a thermal rating of 1058A translating to 504MVA.
2) The Snowdon – Everest 275kV line 1 is 157km in length and is constructed in twin bare conductor which has a thermal rating of 1768A translating to 842MVA.
3) The Makalu – Everest 275kV line 1 is 158.3km in length and is constructed in twin bare conductor which has a thermal rating of 1768A translating to 842MVA.

Figure 3.4 below shows the input parameters required to model all 275kV lines in Dig-silent Power Factory simulation tool.

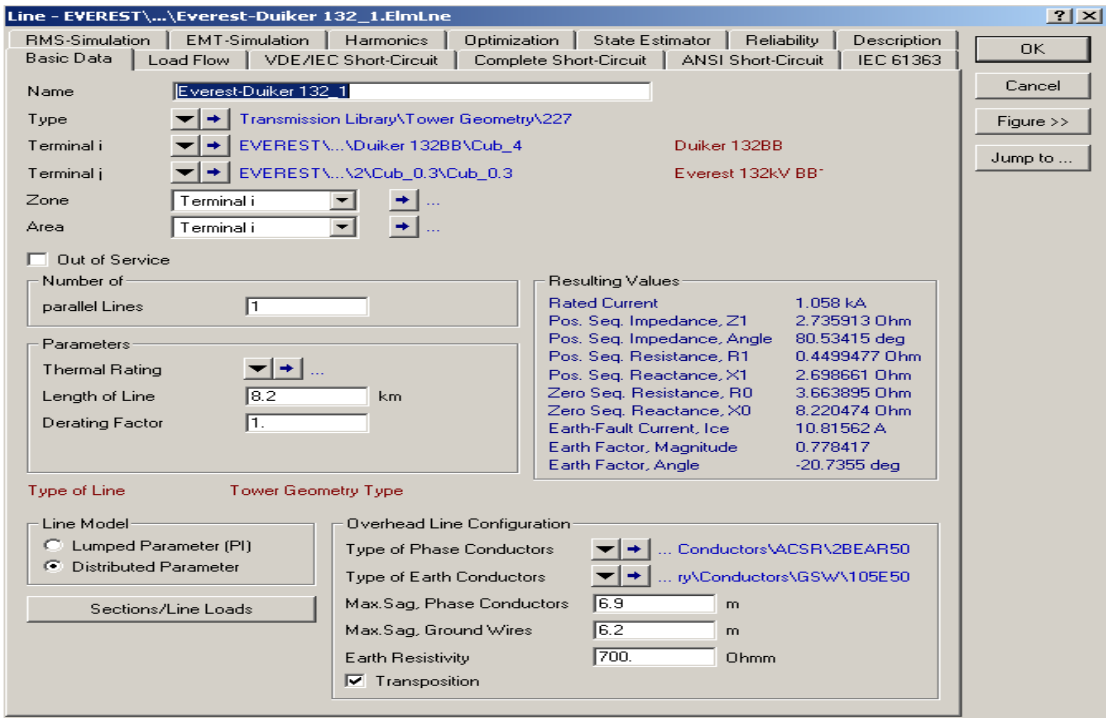

Figure 3.4: Dig-silent required data for transmission line model – 1

Figure 3.4 above shows the modelling of the Perseus – Everest 275kV line from Perseus 275kV bus bar to Everest 275kV bus bar. In order to model any line in Dig-silent, certain parameters are required i.e. basic data essential for load-flow. The basic data needed includes: from and to bus-bar names (terminal i and terminal j), number of lines running in parallel (if more than one), the line length, the line model (lumped PI model or distributed parameter model) and the overhead line configuration information (type of phase conductors, type of earth conductors, maximum sag of phase conductors, maximum sag of ground wires, earth resistivity and transposition).

Basic data also includes the type data and Figure 3.5 below indicates the phase conductor type data parameters that are needed in order to complete the line model.

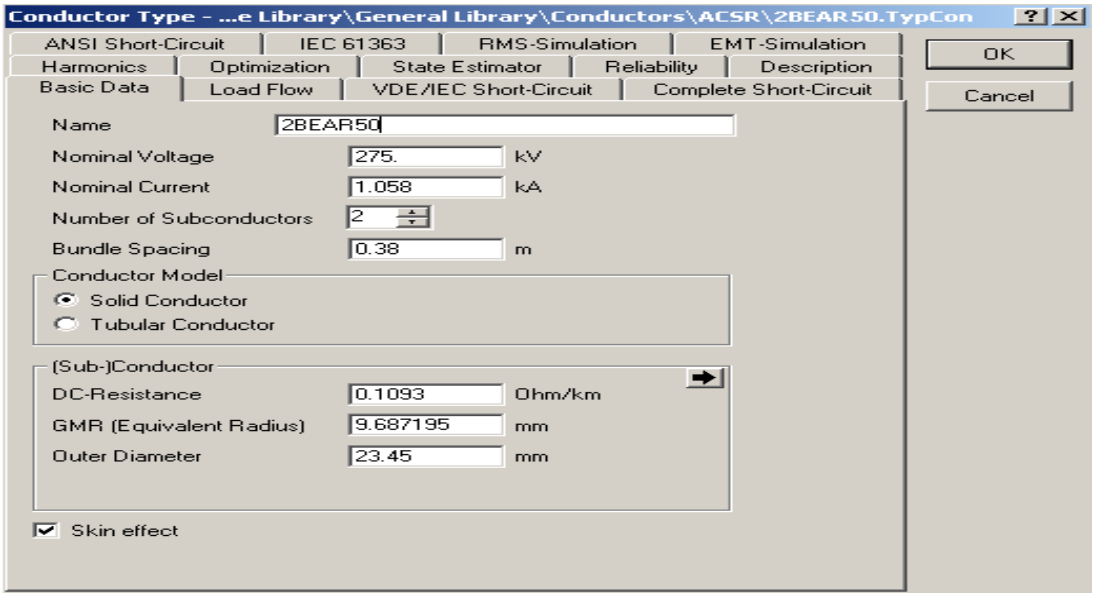

Figure 3.5: Dig-silent required data for transmission line model - 2

The line type data required for a transmission line phase conductor model includes the following: name, nominal voltage, nominal current, number of Sub conductors, bundle spacing, Sub conductor (DC resistance, Diameter and GMR).

Figure 3.6 below indicates the earth conductor type data parameters that are needed in order to complete the line model.

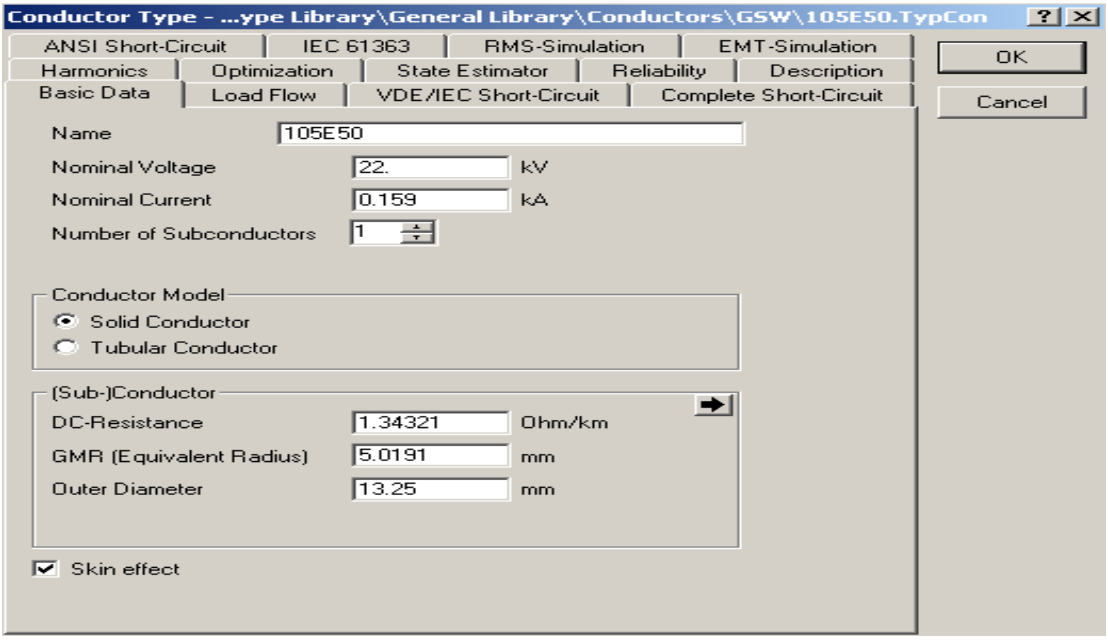

Figure 3.6: Dig-silent required data for transmission line model - 3

The line type data required for a transmission line earth wire model includes the following: name, nominal voltage, nominal current, number of Sub conductors, Sub conductor (DC resistance, Diameter and GMR). Once all the input parameters for the type data have been specified, Dig-Silent then uses the specified ohms per km parameters and the total line length in order to calculate the actual line parameters in ohms.

There are eleven outgoing 132kV lines at Everest and it should be noted that the same procedure as explained above that was used in developing all the other line models which included the following lines: Everest – Virginia 132kV lines 1, 2 and 3; Everest – Duiker 132kV line, Everest – New Steyn 132kV line, Everest – Welkom Bulk 132kV lines 1&2, Everest – Anglo Dankbarheid 132kV line, Everest Witpan 1&2 and Everest – Anglo Erfdeel 132kV line.

3.1.4 Modelling of Transformers

In order to model any transformer in Dig-silent, certain parameters are required i.e. basic data essential for load-flow. The actual data used to build all transformer models was obtained from Eskom‟s Phoenix plant database that is used to store specific plant data.

The following Figure 3.7 shows the Dig-silent model that was used in modelling the 275/88/22kV 500MVA transformers at Everest substation.

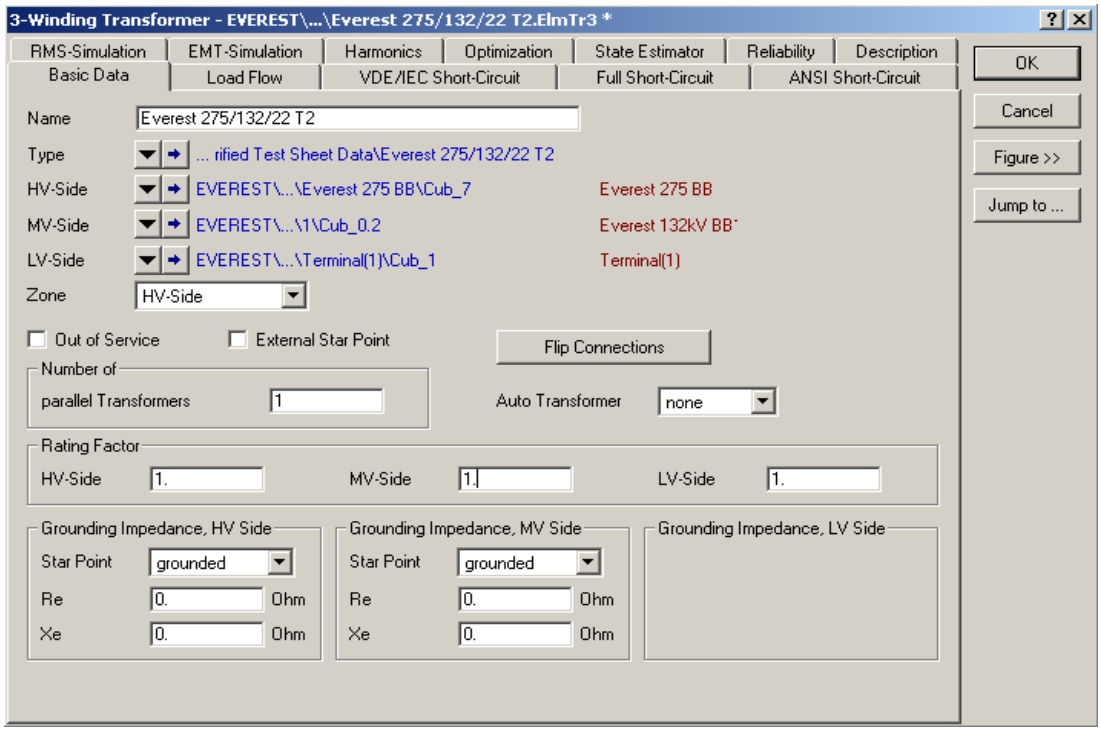

Figure 3.7: Dig-silent required data Everest 275/132/22kV transformer-1

This transformer was modelled using the three-winding transformer model. The basic data required for this model includes the following: Name, transformer type, HV and LV bus-bars, number of transformers running in parallel (if more than one), Whether it is an auto transformer, Rating factor, grounding impedance for the HV and MV star points.

Figure 3.8 below shows the load flow data required for the transformer model.

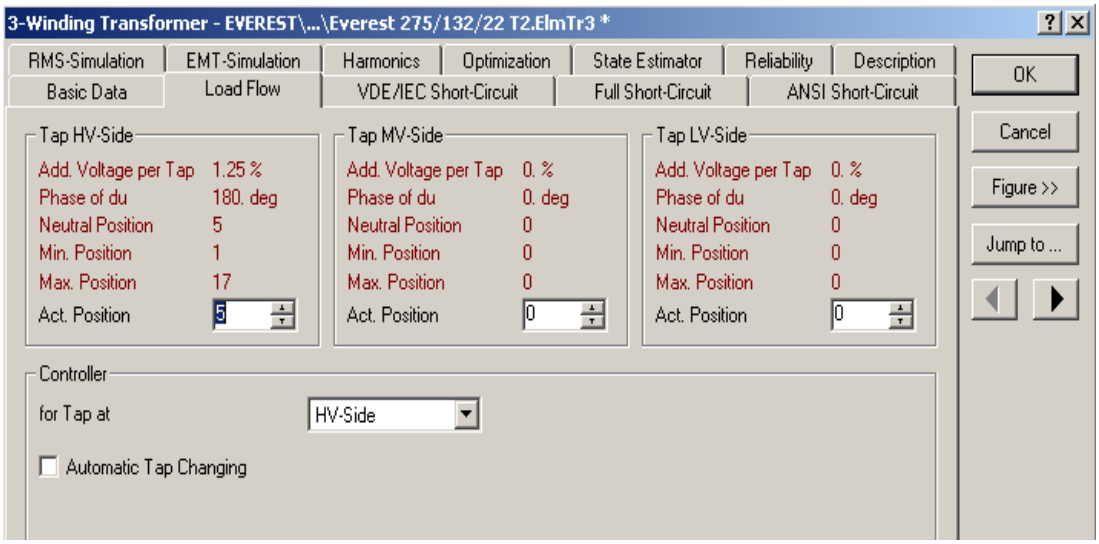

Figure 3.8: Load flow data required as part of basic data for Everest 275/132/22kV trfr

The load flow data required as part of basic data includes the following: additional voltage per tap, phase shift and the actual tap position. The transformer type data also needs to be specified and the Figure 3.9 below indicates the basic data that is required as part of the transformer type data.

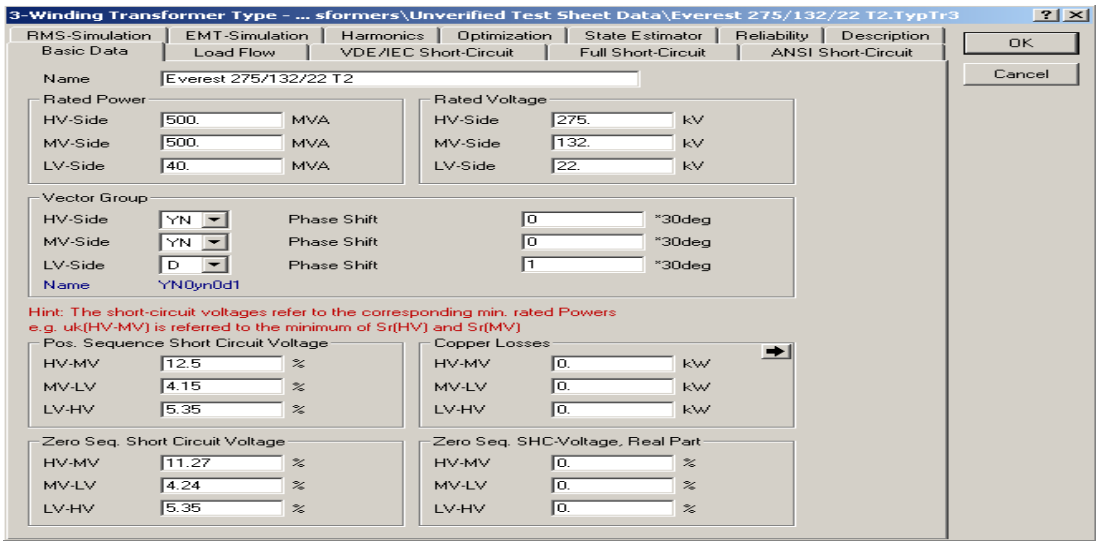

Figure 3.9: Basic data required as part of basic data for Everest 275/132/22kV transformer-3

The input basic data that is required as part of the transformer type data includes the following: Name, rated power, rated voltage, vector grouping and phase shift, positive and zero sequence short circuit voltages. Figure 3.10 below shows the load flow data that is required as part of the transformer type data.

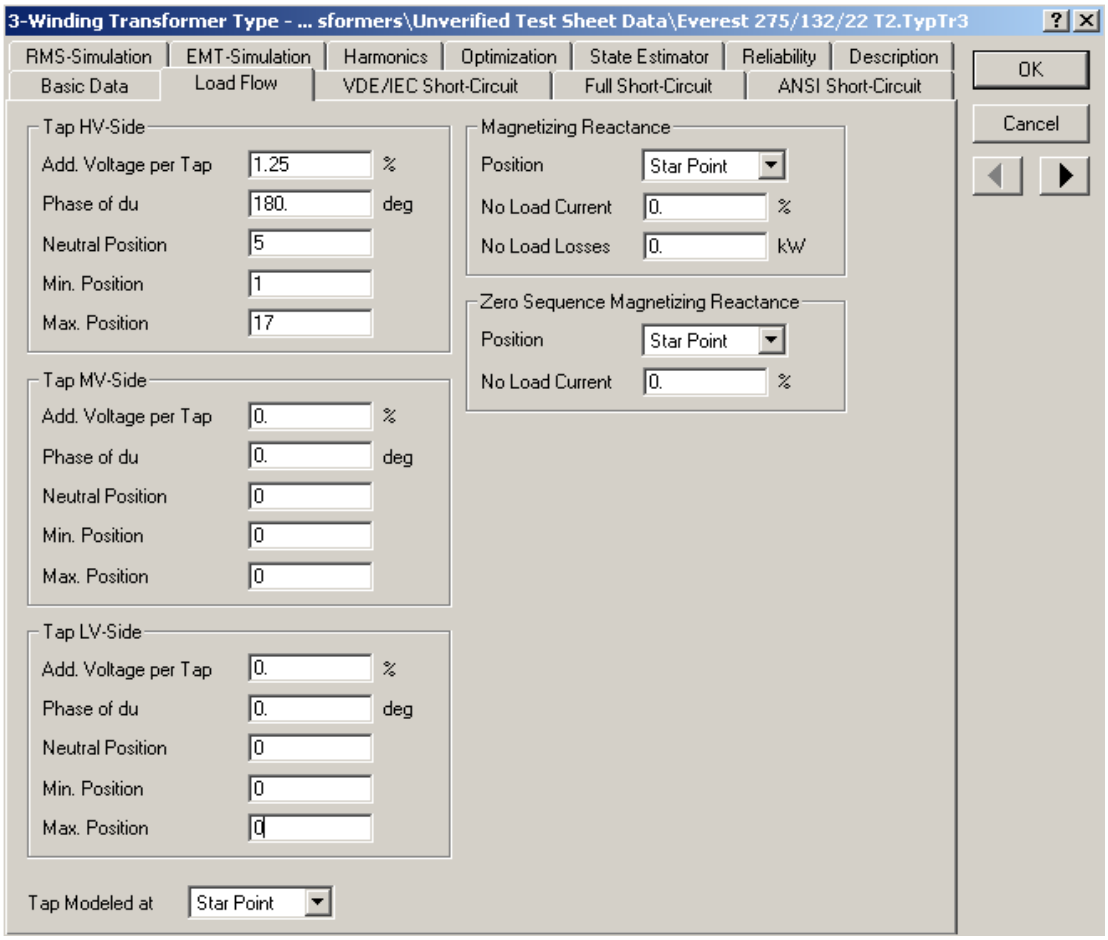

Figure 3.10: Load flow data required for the Everest 275/132/22kV transformer Model-4

The load flow data required as part of the transformer type data is the tap changer information. This transformer has seventeen tap positions i.e. 1 is the minimum, 5 is nominal/neutral and 17 is the maximum. The additional voltage per tap step is 1.25% and the phase shifting is 180 degrees since the transformer has a vector grouping of the YN0yn0d1 type. The values for the magnetizing impedance of this transformer were defaulted to zero.

Similarly the transformers at other substations in the network were modelled using the data stipulated above.

3.1.5 Modelling of Capacitor Banks

The basic data required to model the Everest 132kV 2 x 72MVAR capacitor banks is shown in figure 3.11 below. The actual data used to build all capacitor bank models was obtained from Eskom's Phoenix plant database that is used to store specific plant data.

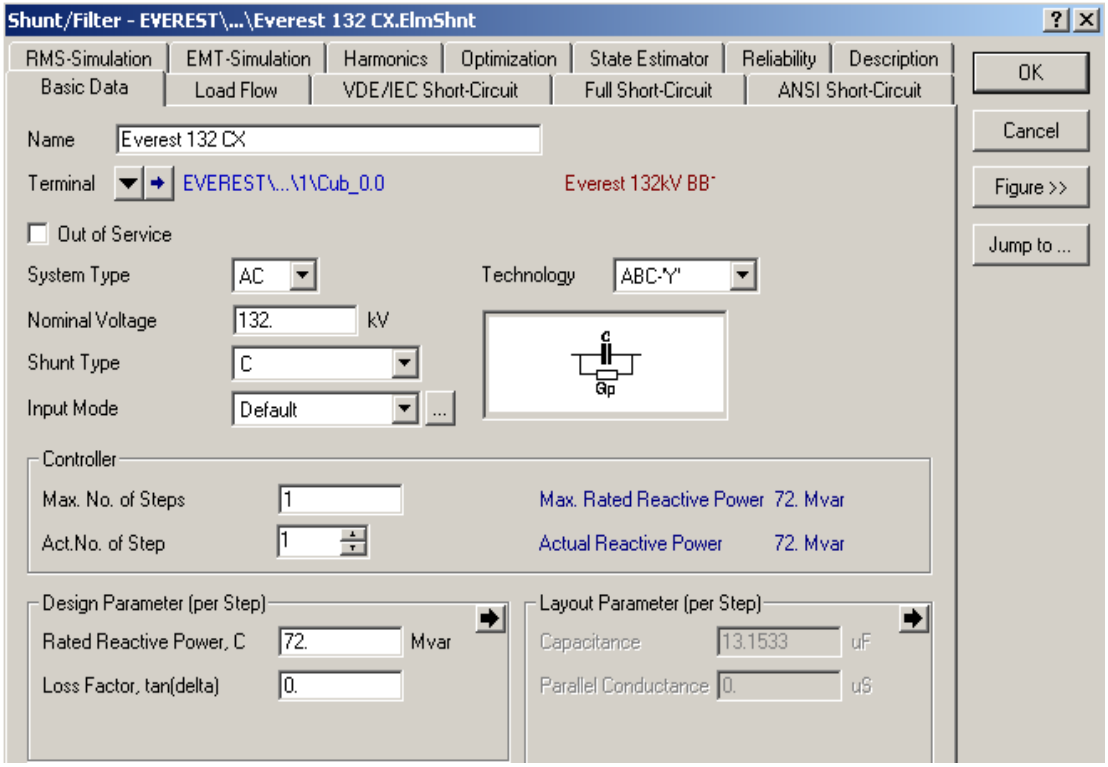

Figure 3.11: Load flow data required as part of type data for the Everest Capacitor Bank Model-1

The basic data required includes the following: system type (AC or DC), nominal voltage, shunt type (C, R, RL, RC or RLC), technology, the number of steps and the capacitor's rated reactive power. Following is a Figure showing the load flow data that is required.

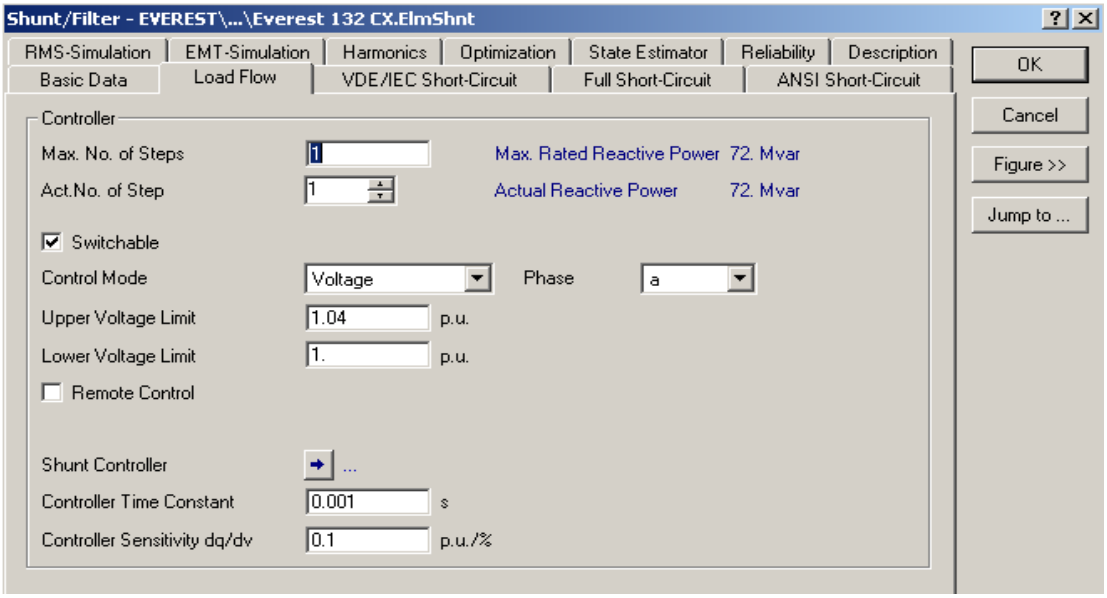

Figure 3.12: Load flow data required as part of type data for the Everest Capacitor Bank Model-2

3.1.6 Modelling of Bus bars

The only data that Dig-silent requires to model bus-bars or terminals is the basic data. The load flow data is not required in this case and no types need to be specified. The actual data used to build all bus bar models was obtained from Eskom"s Phoenix plant database that is used to store specific plant data. The following Figure indicates the input data that is needed to model bus-bar. It should be noted that all the bus-bars within the study system were modelled using this model.

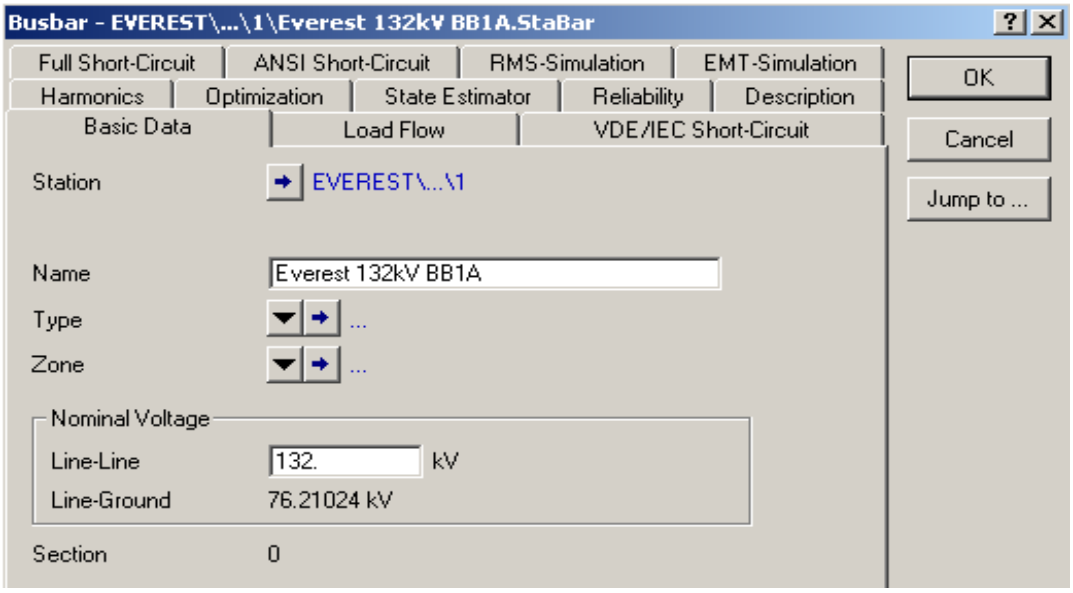

Figure 3.13: Load flow data required as part of type data for a Bus bar Model

The input data required to model bus-bars includes the following: Name, system type (AC or DC), phase technology and the line to line nominal voltage.

3.1.7 Modelling of Filter Bank

The main purpose of the harmonic filter is to reduce the harmonics amplitude at resonance point. This filter has been designed and tuned to reduce the 5th harmonics amplitude.

Figure 3.14 below shows the data that was used in Dig-Silent when modelling the shunt filter.

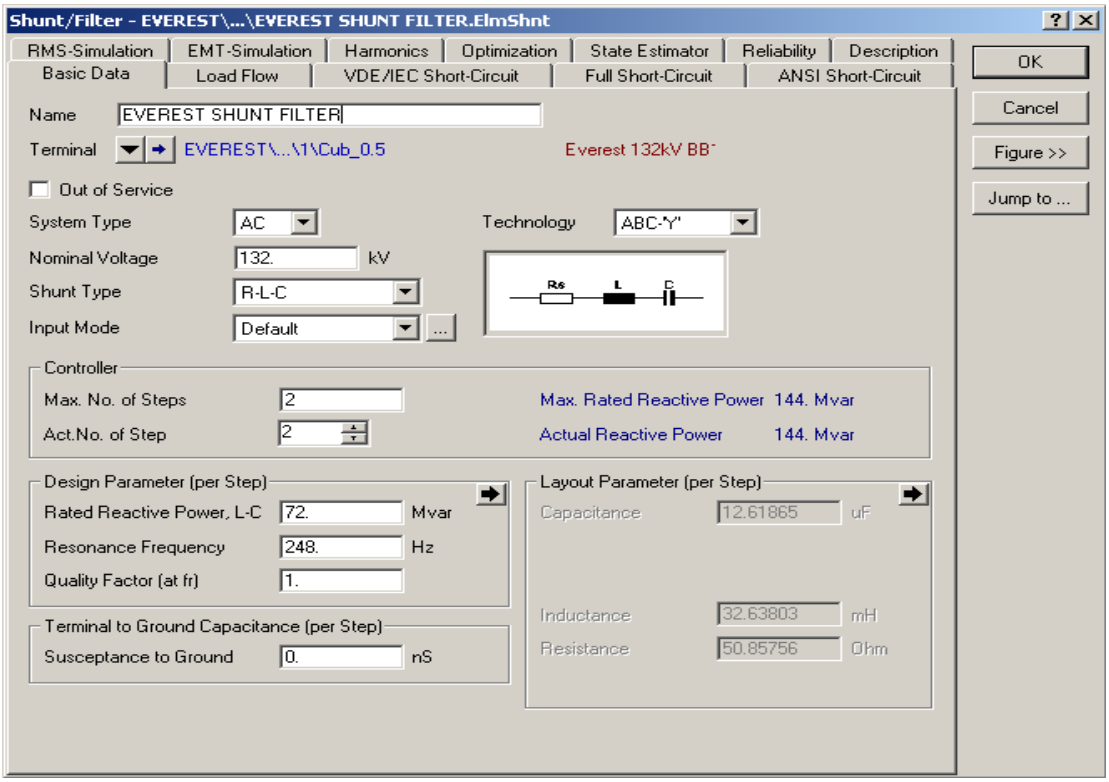

Figure 3.14: Load flow data required as part of type data for a shunt filter Model - 1

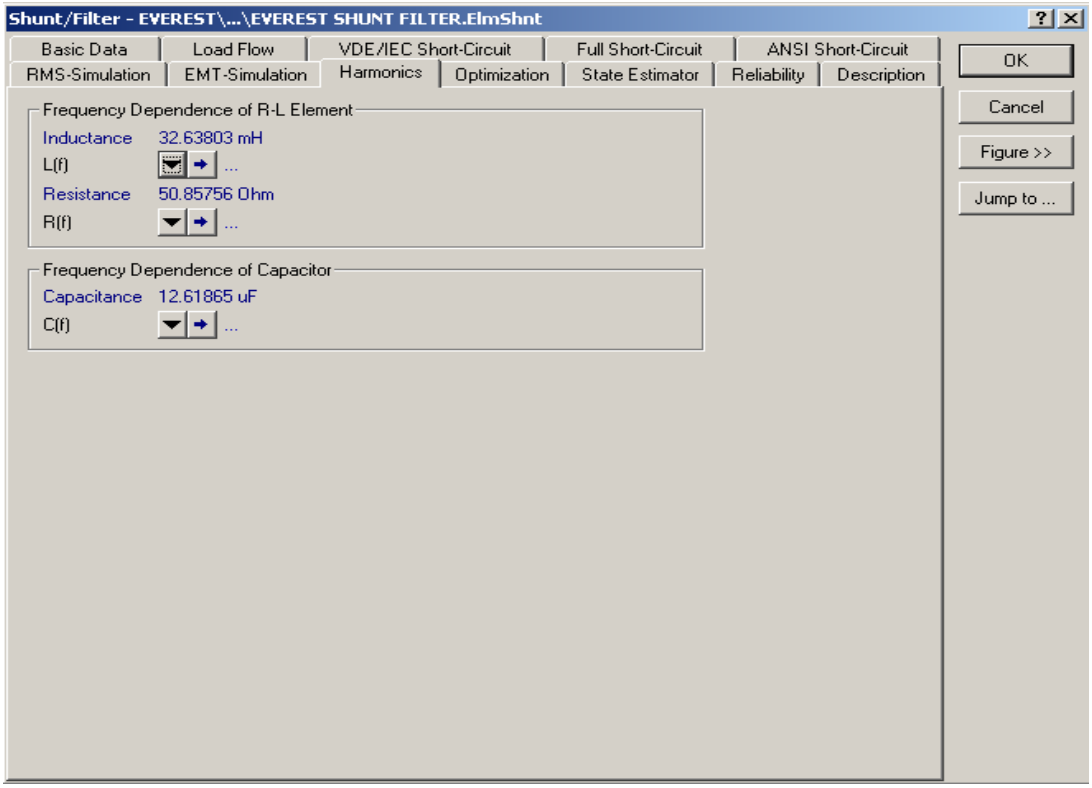

Figure 3.15: Load flow data required as part of type data for a shunt filter Model - 2

3.2 Capacitor Bank Performance History Analysis

The performance history of the capacitor bank was analysed using the fault information obtained from the TIPPS database. This database contains a record of high voltage equipment and lines performance. The information obtained was from year 1998 to 2010, and was then used for correlation with the high THD data recorded in the network. This failure Trend is shown in figure 4.27 to follow.

3.3 Accuracy of the Dig Silent Power Factory Model

3.3.1 Fault Level Comparison

A fault level study was done on the designed model in order to compare the three phase and single phase fault levels simulated at the Everest 132kV source with the actual data. The results are as shown on table 3.3 below.

Type	Voltage (kV)	Fault Level - Actual (kA)	Fault Level - Simulated (kA)	% Error
3 Phase	132	16.041	15.985	0.349
1Phase	132	16.483	16.542	-0.358

Table 3.3: Comparison of fault levels at Everest Substation

Both the three phase and single phase fault levels simulated at Everest 132kV source were found to be almost the same as the actual data as shown on table 3.3 above. This close comparison of the fault levels shows the accuracy of the designed Dig-Silent model in terms of the equipment parameters that were used in setting up the model.

3.3.2 Rule of Thumb Method

To determine the harmonic number at which resonance peak occurs can be determined by taking the square root of the ratio of System Fault level (MVA) and Capacitor Rating (MVAR) – given by:

$$‘h_r = \sqrt{S_{pc}/Q_c} \quad (13)$$

When two capacitors are in service, the dominant harmonic will be:

= √3654.7MVA/ (72MVAR x2) = 5.04; where

„h_r – harmonic order

S_{pc} – Fault level at point of connection

Q_c – Capacitor Reactive power rating

When one capacitor is in service, the dominant harmonic will be:

„hr = √Spc/Qc = √3654.7MVA/(72MVAR) = 7.12;

This result indicates resonant points of 5^{th} (two capacitors in service) and 7^{th} (one capacitor in service) harmonic which confirms resonance points already depicted from metering data and simulation results. This method therefore also confirms the accuracy of model, which means that simulation results obtained can be trusted and used to make firm decisions.

3.4 Determination of the Harmonic Compliance at Everest using IEEE519-1992

This section is aimed at analysing the compliance of the Everest network based on the limits prescribed in IEEE519-1992 [13].

The total demand at Everest is 100MVA as shown in table 3.1 above. Calculating I_L from this figure we obtain:

$S = \sqrt{3} \times V \times I$ ..... (14)

Where:

S = Apparent Power

V = Line Voltage

I = Line Current

100MVA = $\sqrt{3}$ X 132kV X I_L

Therefore, (I_L) = 437.39Amps

In table 3.4 below (I_s) is given as 16kAmps

Hence I_s / I_L = 16kA / 437.39A

Therefore, I_s / I_L = 36.6

According the IEEE519 1992 Harmonic limit tables, for (I_s) / (I_L) between 20 and 50, harmonic orders below 11^{th} should not exceed 3.5.

Maximum Harmonic Current Distortion in Percent of I_L

Is/IL	**<11**	**11<h<17**	**17<h<23**	**23<h<35**	**35<h**	**TDD**
<20	2	1	0.75	0.3	0.15	2.5
20<50	3.5	1.75	1.25	0.5	0.25	4

Table 3.4: Current Distortion Limits for General Sub transmission Systems [13].

Analysing the harmonic current measurements taken at various Everest networks, it is evident that the limit of 3.5 is often exceeded, with some feeders reaching as high as 12% harmonic current distortions. The situation is much worse during low load conditions and at times when both capacitors are in service.

3.5 Harmonic Currents Measurements

3.5.1 Individual Harmonics Profiles

Harmonic currents metering instruments were installed at all outgoing 132kV feeders at Everest substation. The following figure show individual harmonics profiles recorded at Everest – Newsteyn 132kV feeder, Everest – Duiker 132kV Feeder, Everest – Anglo Erfdeel 132kV Feeder and Everest – Anglo Dankbaarheid 132kV Feeder. The abovementioned feeders are connected to the affected bus bars and are mainly supplying mining loads.

The meters were installed for a period of three weeks (08/02/08 to 22/03/08), however most of the data was corrupt by the time of retrieval and only three days data was retrievable. The three day‟s data though not sufficient, but does give an indication of the characteristic harmonics of the loads supplied from Everest substation‟s 132kV feeders. The figures below depict a high 5th harmonic currents flowing in these networks.

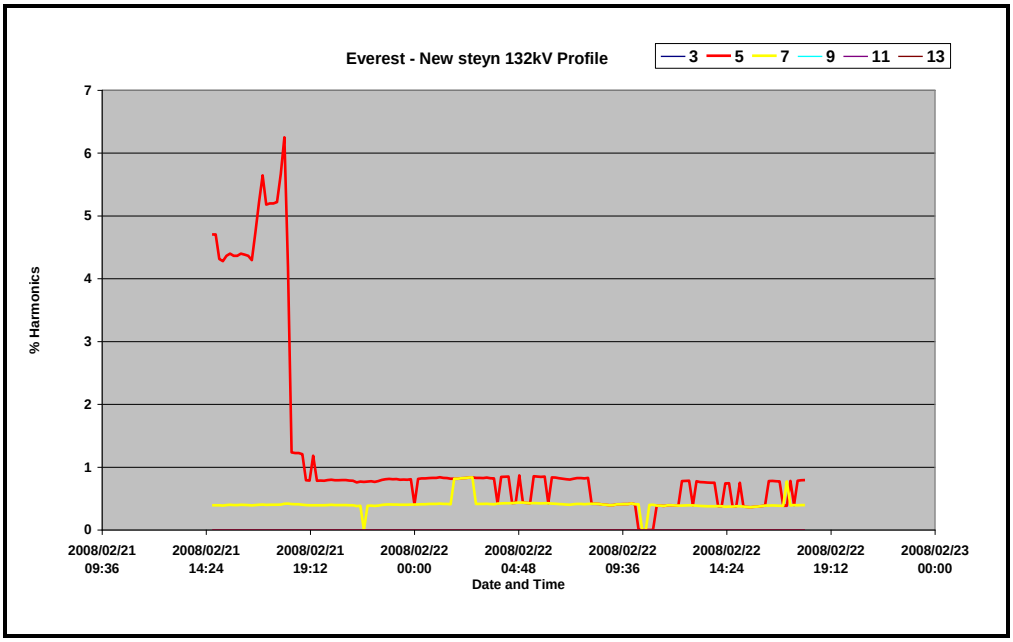

Figure 3.16: Individual harmonic currents profiles recorded at Everest – Newsteyn 132kV feeder

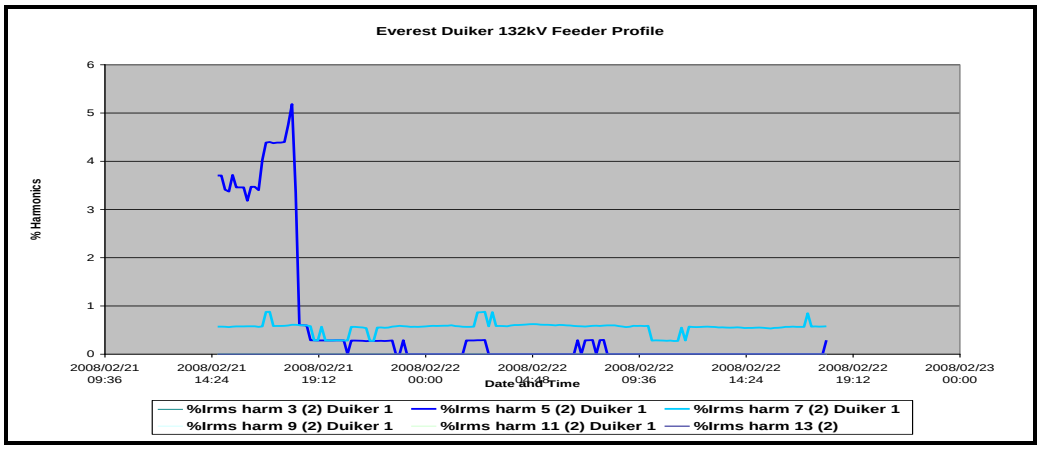

Figure 3.17: Individual harmonic currents profiles recorded at Everest – Duiker 132kV feeder

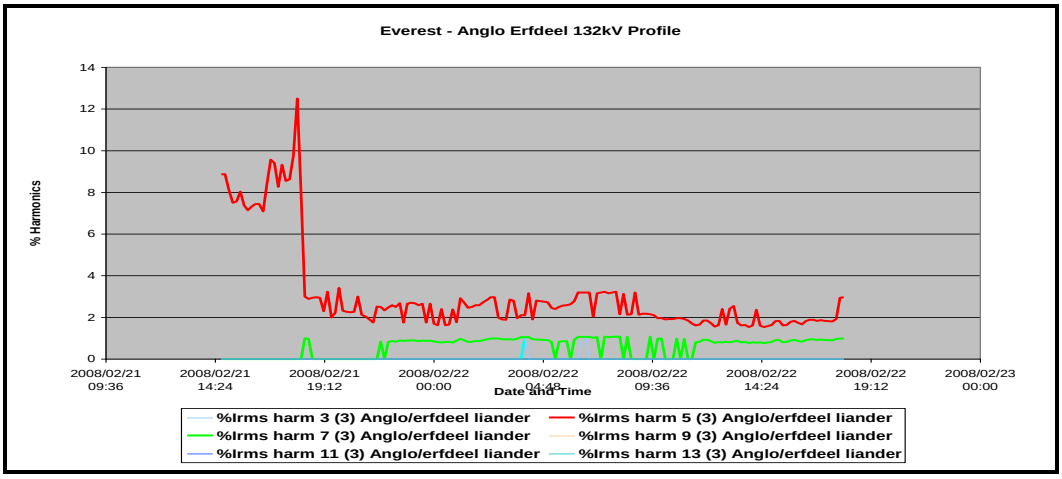

Figure 3.18: Individual harmonic currents recorded at Everest – Anglo Erfdeel 132kV feeder

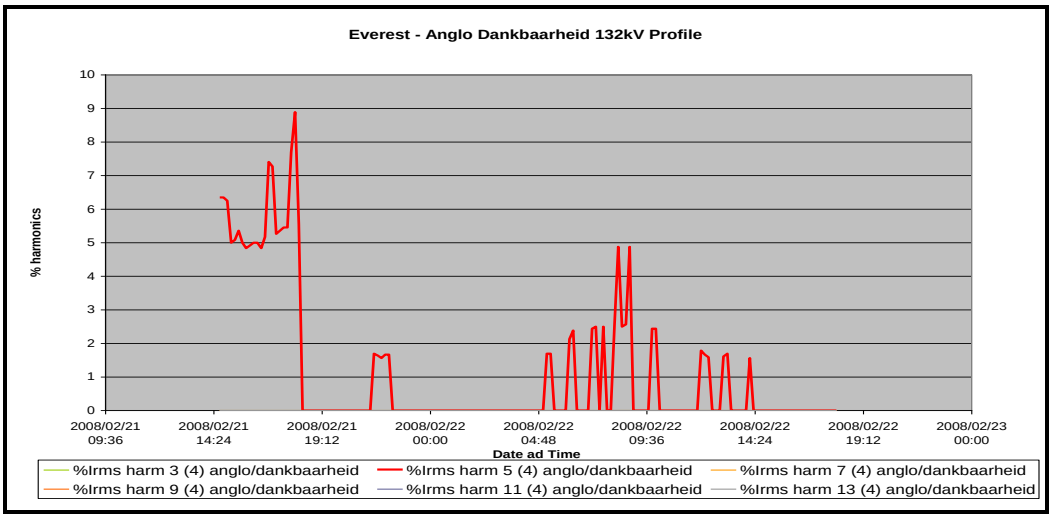

Figure 3.19: Individual harmonic currents recorded at Everest – Anglo Dankbaarheid 132kV feeder

The profiles above indicate a peaking 5th harmonic current between 16h10 and 18h00 on 2008/02/21, and then followed by a sudden/abrupt drop in the harmonic currents in all measured feeders. To analyse the possible cause for the sudden drop in distortion levels, network control data logs were obtained from EMS system for the day and time that this incident occurred to identify any network event that could have caused this incident, as seen in in figure 3.20 below.

The Everest 132kV feeder's sudden change/drop in harmonic current profile on 21/02/2008 occurred when network control switched off the capacitor bank in response to high THD alarms (highlighted in red in figure below). There had been numerous high THD alarms sent through to control on that day, as can be seen above at 16:01 and16:40 that afternoon (highlighted in blue in figure below). At about18:03 network control therefore took a decision to switch out capacitor 2 by opening the capacitor breaker in order to get the harmonic distortion to an acceptable level. The profiles show that when this action was taken, it is then that the high harmonics subsided. This is further confirmed below by time stamp 18:10:01 when the THD levels went back to normal.

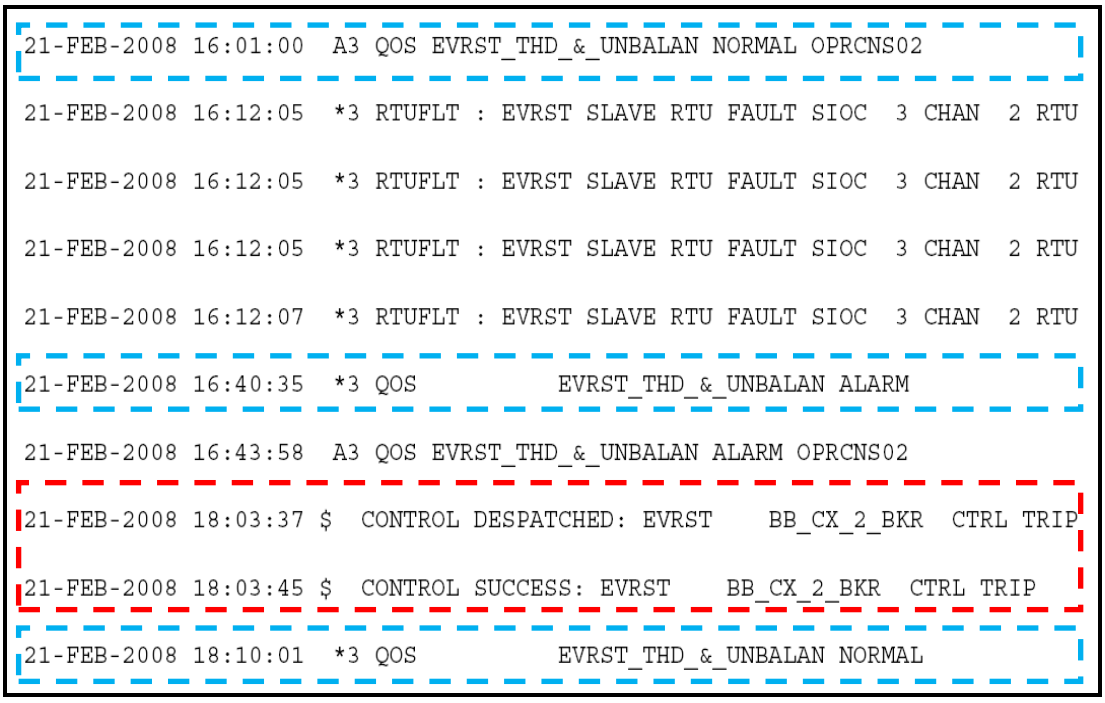

Figure 3.20: Everest network operating time stamps from EMS

CHAPTER 4: DISCUSSION OF RESULTS

4.1 Simulation of Original Network

The Transmission network around the Everest substation was modelled in Dig-silent Power Factory to determine the harmonic distortions and the system harmonic impedance as seen from the 132kV bus-bar at Everest substation. Figure 3.2 shows the network that was modelled in the Dig-silent power system simulation tool.

4.1.1 Everest Original Network Configuration

The Everest network was simulated at original condition (i.e.) before the network changes were effected. The 132kV bus bars were run closed with bus couplers and bus sections closed, and all other in-feeds from Theseus and Leander transmission stations were opened. The capacitor banks were switched in and out when necessary. Figure 4.1 below depicts the network state.

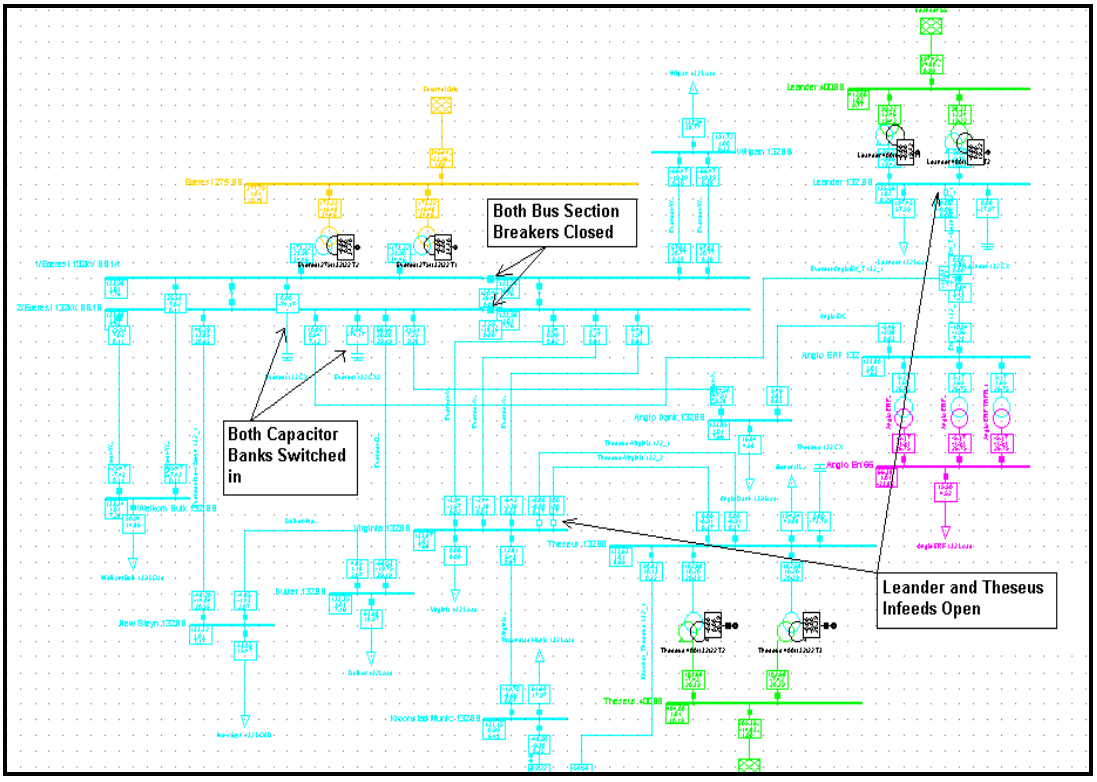

Figure 4.1: Everest original network configuration

4.1.2 Everest Original Network Configuration – Harmonic Distortion

The figure below shows harmonic distortion at Everest 132kV bus-bar 1A. When both capacitors are in service at Everest substation and with all load supplied from the 132kV bus bar.

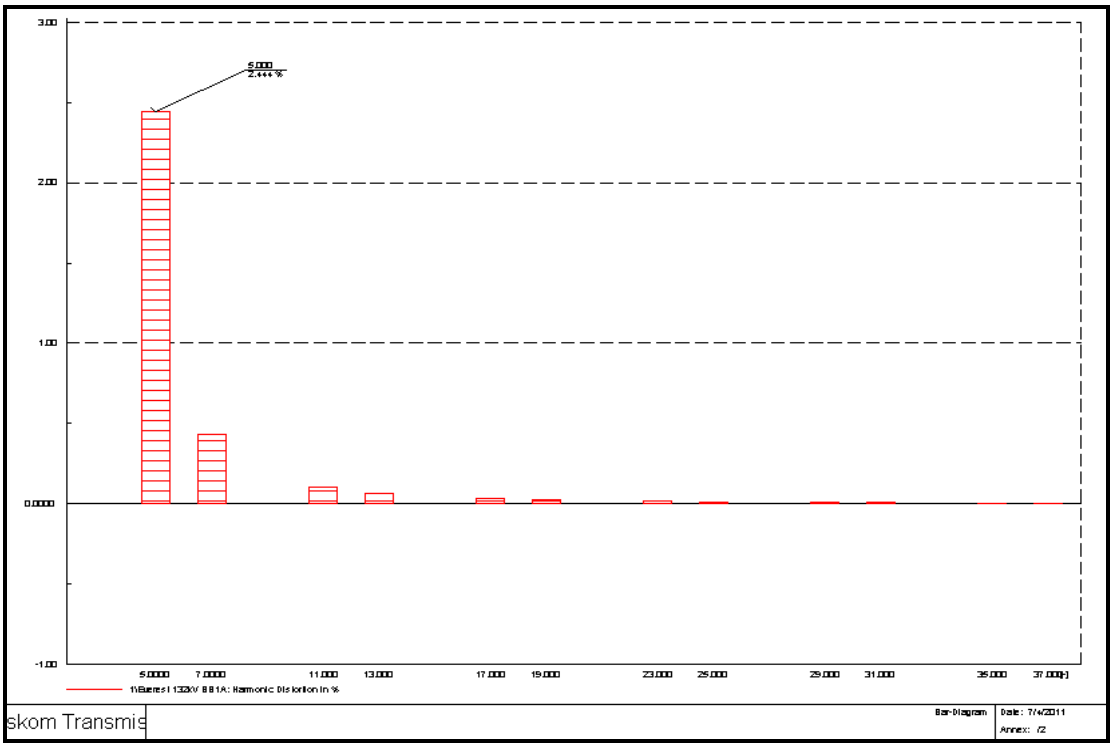

Figure 4.2: Everest original network configuration Harmonic distortion

The figure above shows that the 5th harmonic was the most prevalent with the distortion level at 2.44%.

4.1.3 Everest Original Network Configuration – Frequency sweep

The figure below shows network impedance as seen from Everest 132kV bus-bar 1A. When all the 132kV feeders are supplied off Everest substation and both capacitor banks are in service, the 5th harmonic impedance level is at 136 ohms while the 7th harmonic impedance level is at 35 ohms. The resonance point occurs around the 5th harmonic.

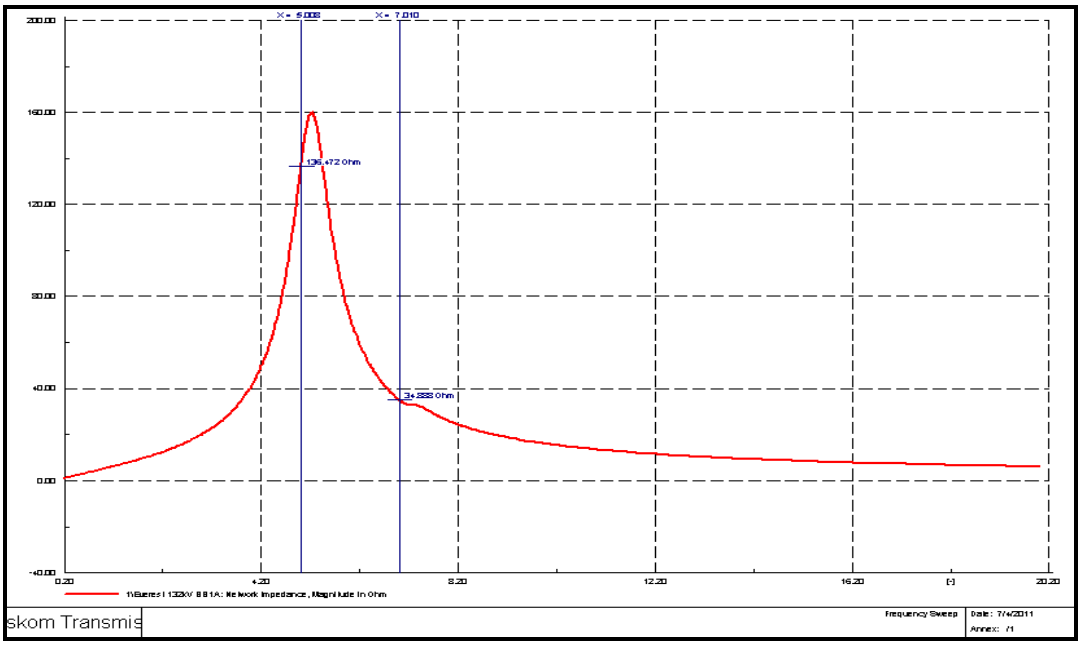

Figure 4.3: Everest original network - Frequency Sweep– Both Capacitors in service

5th Harmonic Impedance Amplitude (Ω)	7th Harmonic Impedance Amplitude (Ω)	5th Harmonic HD (%)	7th Harmonic HD (%)	Voltage (pu)	Trfr1 Loading (MVA)	Trfr2 Loading (MVA)
136	35	2.44	0.43	1.01	175	175

Table 4.1: Network Parameter at original configuration – Both Capacitors in service

Table 4.1 above depicts the summary of the network parameters when the network is at its original state. The loading is evenly shared between the transformers and the voltage levels were acceptable

As already stated above during the time when the network was operated with all the feeders supplied from Everest substation, the capacitor banks were switched in and out of the network when necessary.

The following figure depicts the network when only one capacitor bank was in service.

4.1.4 Everest Original Network Configuration – One Capacitor in service

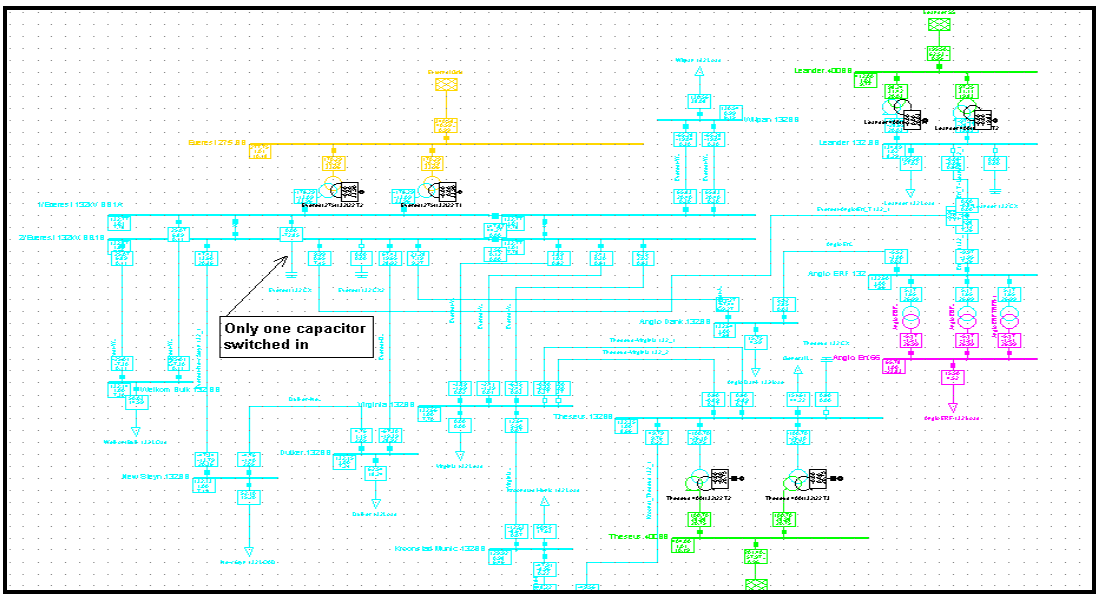

Figure 4.4: Everest original network configuration – One capacitor in service

4.1.5 Everest Original Network Configuration – Harmonic Distortion-One capacitor in

The figure below shows harmonic distortion at Everest 132kV bus-bar 1A when one capacitor bank is in service at Everest substation, with all load supplied from the 132kV bus bar. The figure below shows harmonic distortion levels of 0.75% for the 5th harmonic and 2.15% for the 7th harmonic. The resonance point shifts towards the 7th harmonic for this configuration. There is also a 400% increase in the 7th harmonic distortion level when only one capacitor bank is in service compared to when both capacitors are switched in.

.

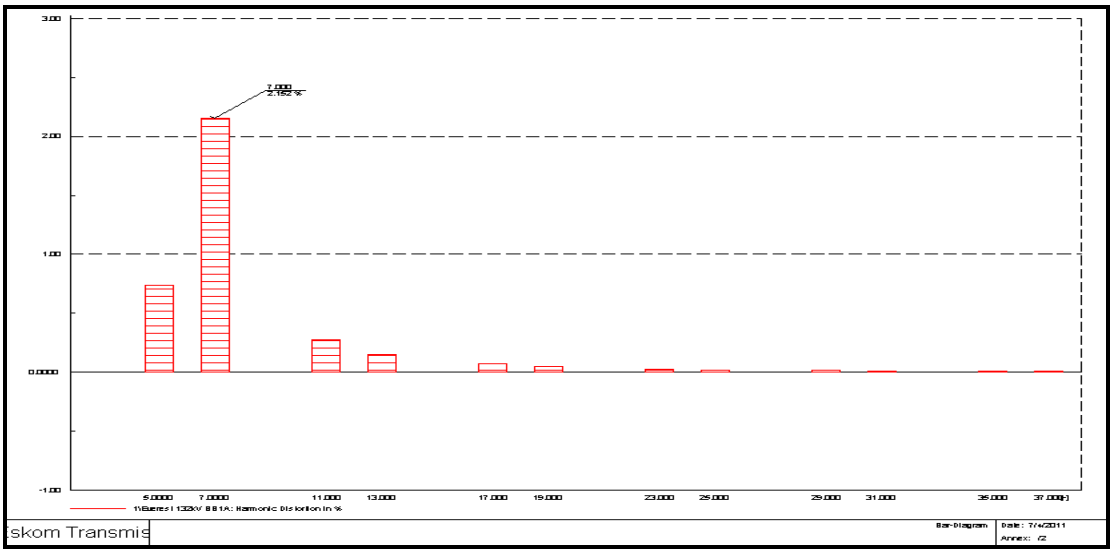

Figure 4.5: Everest original network Harmonic Distortion– One capacitor in service

4.1.6 Everest Original Network Configuration – Frequency Sweep-One capacitor in

The figure below shows network impedance as seen from Everest 132kV bus-bar 1A. When all the 132kV feeders are supplied off Everest substation and both capacitor banks are in service, the 5th harmonic impedance level is at 40 ohms, while the 7th harmonic is at 170 ohms. There is a 386% increase in 7th harmonic impedance amplification when only one capacitor bank is in service compared to when both capacitors are switched in.

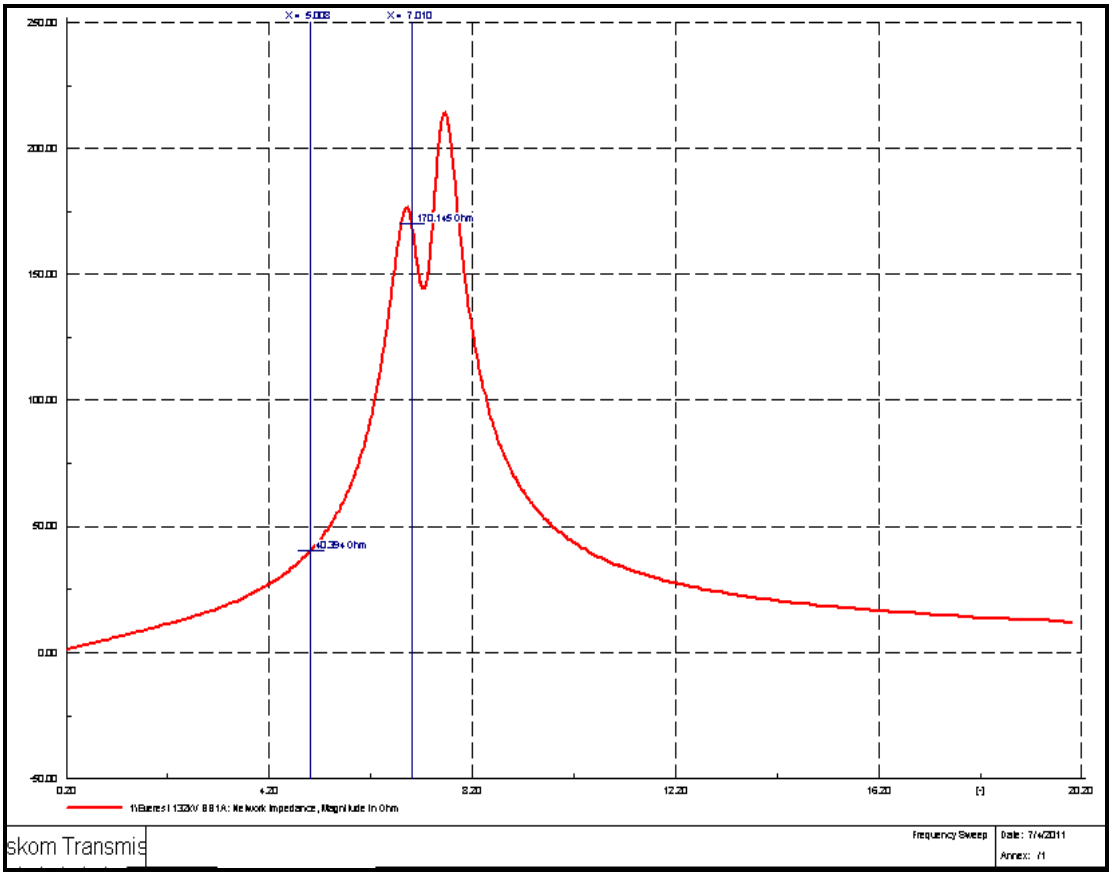

Figure 4.6: Everest original network- Frequency Sweep– One capacitor in service

5th Harmonic Impedance Amplitude (Ω)	7th Harmonic Impedance Amplitude (Ω)	5th harmonic HD (%)	7th harmonic HD (%)	Voltage (pu)
40	170	0.75	2.15	1.01

Table 4.2: Network Parameter at original configuration – One capacitor Bank in service

Table 4.2 above depicts the summary of the network harmonics parameters when the network is at its original state with one capacitor switched out.

4.1.7 Everest Original Network Configuration – No Capacitor in service

The figure below shows the network when none of the capacitors are switched in to service.

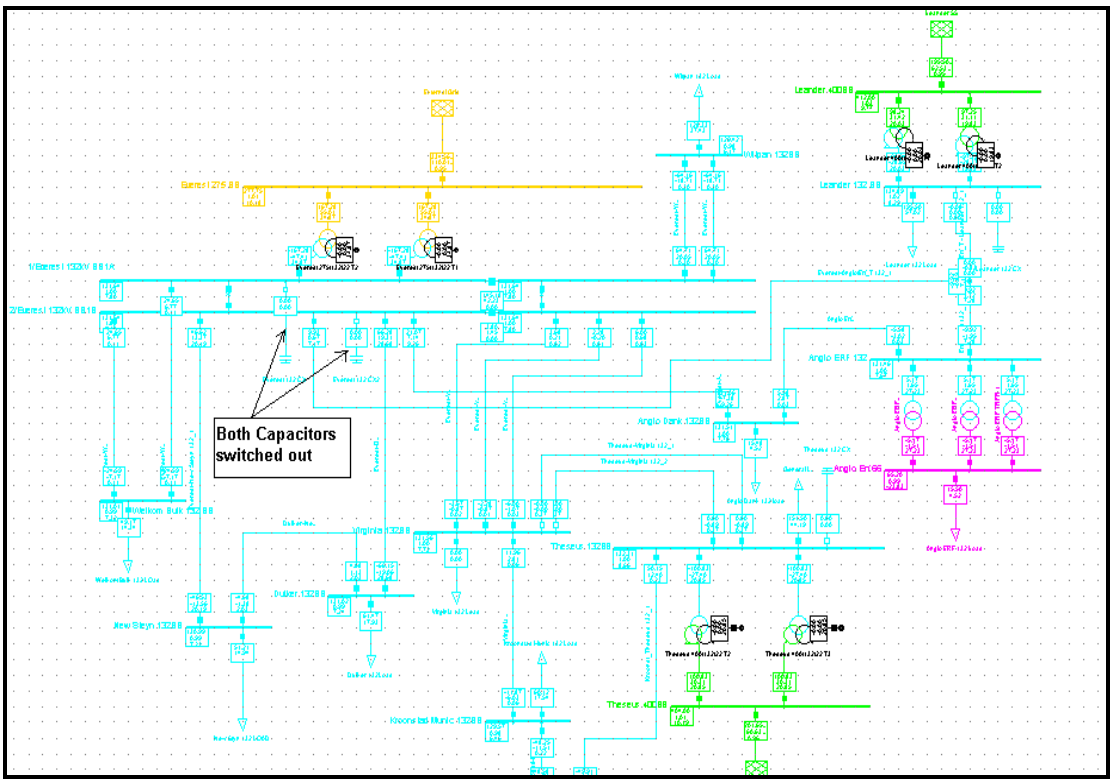

Figure 4.7: Everest original network Configuration– No capacitors in service

4.1.8 Everest Original Network – Harmonic Distortion-No capacitor switched in

The figure below shows harmonic distortion at Everest 132kV bus-bar 1A. When no capacitor bank is in service at Everest substation and with all load supplied from the 132kV bus bar. The figure shows a negligible 5th and 7th harmonic distortion levels. There is a considerable reduction in the harmonic distortion levels when no capacitor banks are in service as compared to when one capacitor switched in. The highest harmonic distortion of 3.93% is observed at the 19th harmonic, but is not a concern for this network as lower order harmonics are most critical.

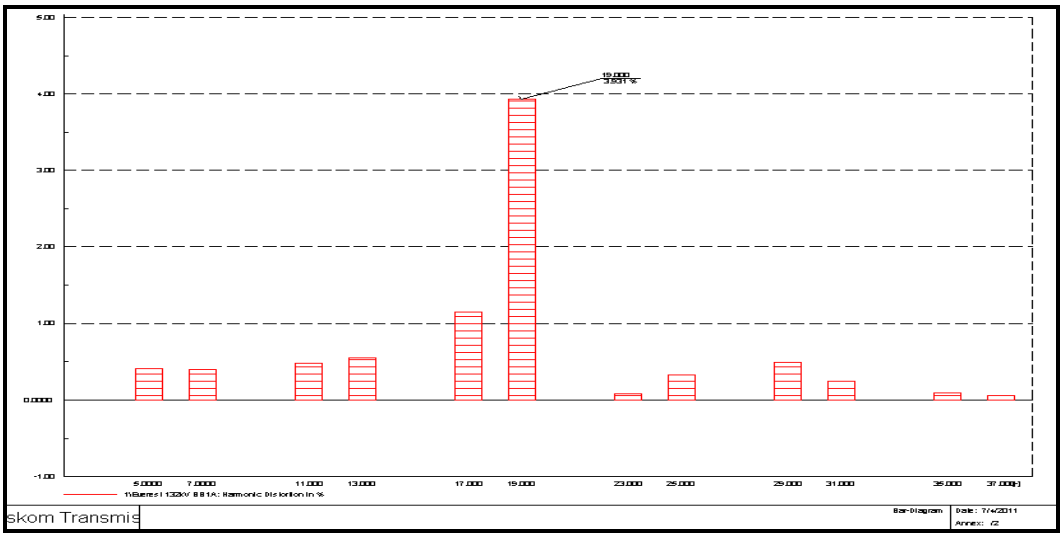

Figure 4.8: Everest original network- Harmonic Distortion– No capacitors in service

4.1.9 Everest Original Network – Frequency Sweep-No capacitor Switched in

The figure below shows network impedance as seen from Everest 132kV bus-bar 1A. When all the 132kV feeders are supplied off Everest substation and both capacitor banks are switched out of service, the impedance amplitude level at 5th harmonic is at 22.1 ohms, while the 7th harmonic impedance is 31.8 ohms. As expected the harmonic impedance is linear and there is a 45% and 81% reduction in 5th and 7th harmonic impedance amplitudes respectively, when no capacitor bank is in service compared to when one capacitor is switched in.

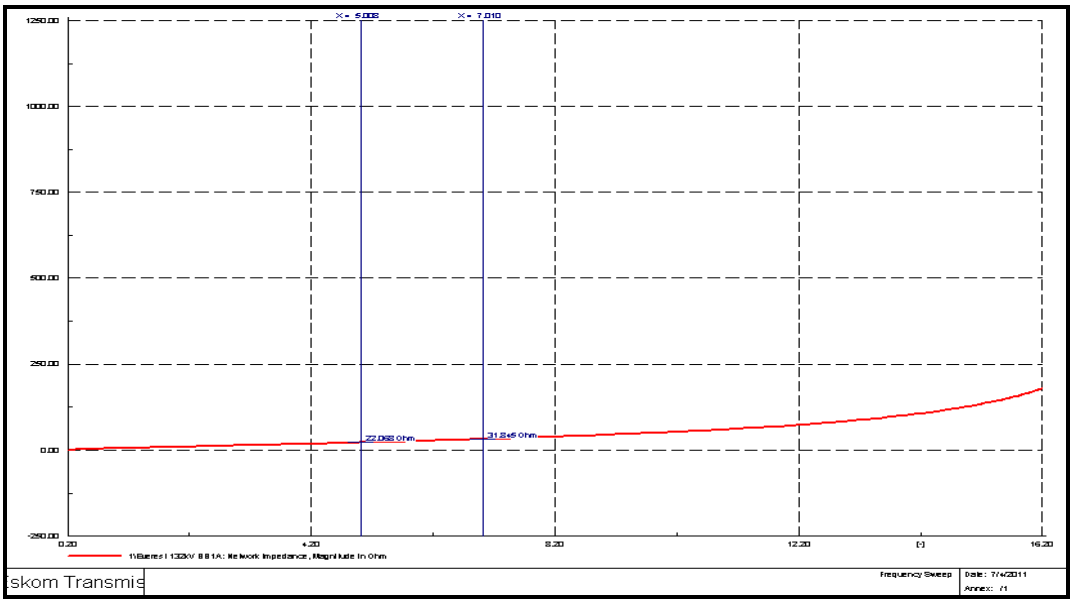

Figure 4.9: Everest original network- Frequency Sweep– No capacitors in service

5th Harmonic Impedance Amplitude (Ω)	**7th Harmonic Impedance Amplitude (Ω)**	**5th harmonic HD (%)**	**7th harmonic HD (%)**	**Voltage (pu)**
22.1	31.8	0.4	0.4	1

Table 4.3: Network Parameter at original configuration – No capacitor Banks in service

Table 4.3 above depicts the summary of the network harmonics parameters when the network is at its original state with both capacitors switched out.

4.2 Simulation of Network after Reconfiguration

As stated earlier that the reconfiguration of the Everest was implemented in year 2004/5 after complaints from some customers about the poor quality of supply. Some of the feeders supplying harmonic producing loads were shifted to other stations away from Everest substation. This was achieved by the opening of the bus section breakers at Everest 132kV bus bars and by closing of the Theseus – Virginia Terminal 132kV breakers. When this was done the load damping previously provided by these networks was removed resulting in worsening quality of supply at Everest.

4.2.1 Network State after Reconfiguration

The figure below also depicts the Everest network as it is currently operated

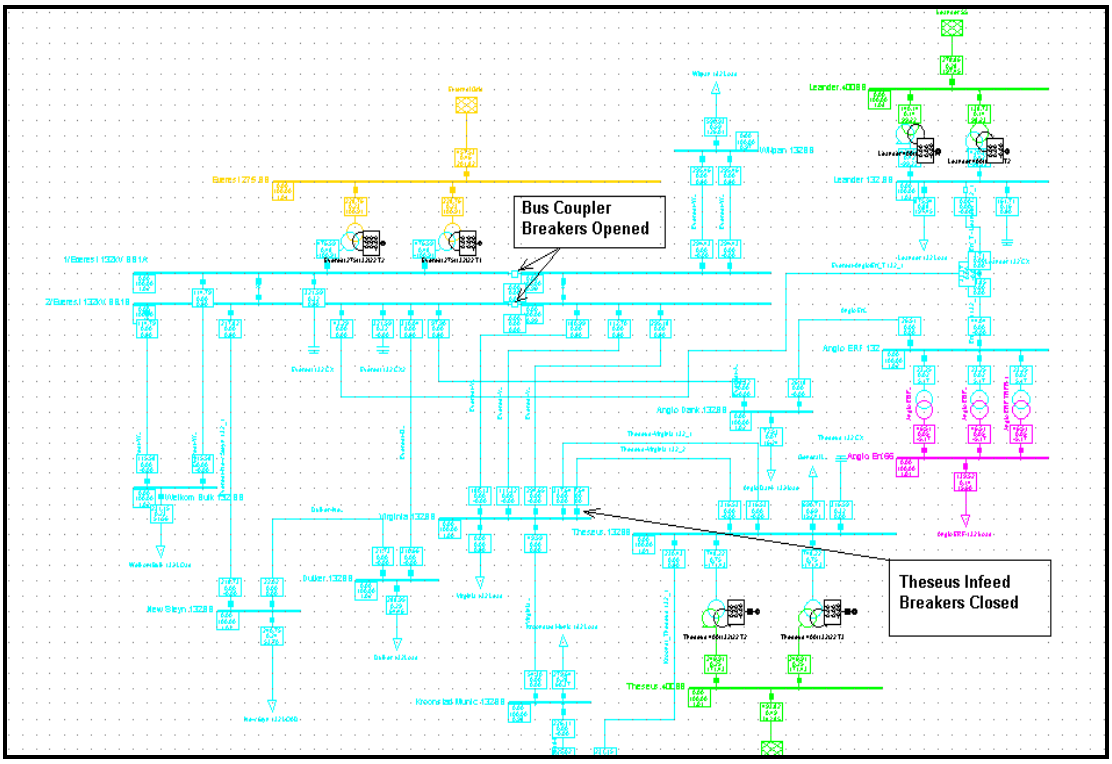

Figure 4.10: Everest current network configuration

With the configuration above, the network is operated such that the capacitor banks are switched in and out of the network when necessary.

The network was then simulated for the following conditions to determine the impact:

- Both capacitors in service at Everest substation
- One capacitor in service at Everest substation
- No Capacitors in service at Everest network

4.2.2 Simulation of Network with both Capacitors in service – Harmonic Distortion

The figure below shows harmonic distortion at Everest 132kV bus-bar 1A. When both capacitors are in service at Everest substation the 5th harmonic is amplified the highest. The figure shows a harmonic distortion level of 3.96% for the 5th harmonic and 0.4% for the 7th harmonic.

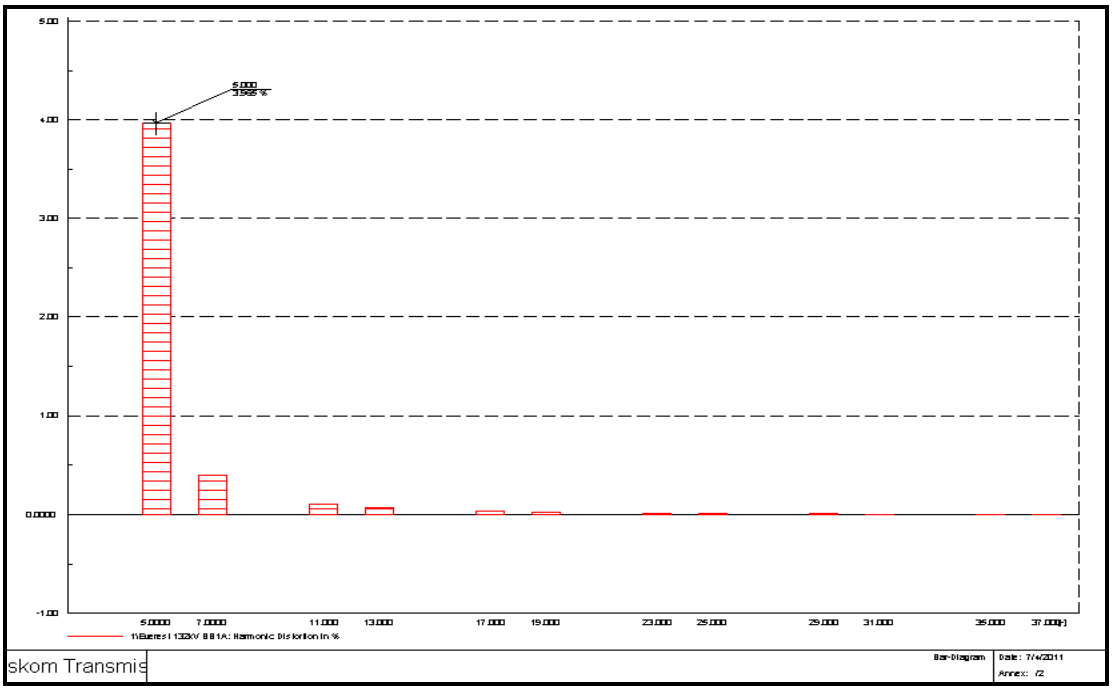

Figure 4.11: harmonic distortion at Everest 132kV bus-bar 1A - both capacitors are in service

4.2.3 Simulation of Network with both Capacitors in service – Frequency Sweep

The figure below shows the network impedance at Everest 132kV bus-bar 1A if both capacitors are in service. The shunt capacitors at Everest resonate with the network at approximately the 5th harmonic. The harmonic currents measured in the load current depict a characteristic harmonic of 5th. The characteristic harmonic almost coincides with the resonant frequency, therefore dangerous voltage levels may arise which may lead to increased aging rate and or failure rate for the capacitors at Everest Substation [25].

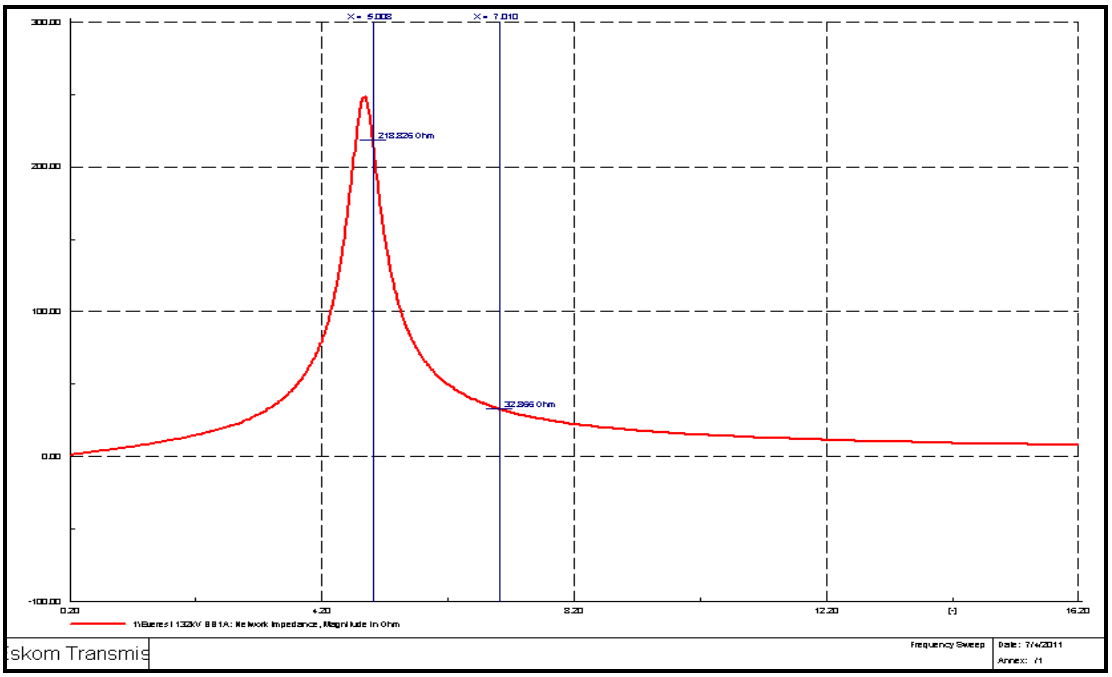

Figure 4.12: Network impedance at Everest 132kV bus-bar 1A if both capacitors are in service

Figure 4.12 above shows the network impedance as seen from Everest 132kV bus-bar 1A. When some of the harmonic producing loads are moved away from Everest substation, the 5th harmonic impedance level is at 219 ohms, while the 7th harmonic impedance level is at 32.9 ohms.

5th Harmonic Impedance Amplitude (Ω)	7th Harmonic Impedance Amplitude (Ω)	5th Harmonic HD (%)	7th Harmonic HD (%)	Voltage (pu)	Trfr1 Loading (MVA)	Trfr2 Loading (MVA)
219	32.9	3.96	0.4	1.02	111	111

Table 4.4: Network Parameter at Current configuration – Both capacitor Banks in service

Table 4.4 above depicts the summary of the network parameters when the harmonic producing loads were removed from Everest substation, while both capacitors were switched in. The loading through the transformers has reduced by 37% due to the moving of some loads away from Everest substation while the voltage level is at nominal value.

4.2.4 Simulation of Network with one Capacitor in service – Harmonic Distortion

The figure below shows harmonic distortion at Everest 132kV bus-bar 1A. When one capacitor is in service at Everest substation the 5th harmonic distortion level is 0.97%, while the 7th harmonic distortion level is 4.72%. The 7th harmonic distortion level increases by 1080%, while the 5th harmonic distortion level has experienced a 76% reduction compared to when the current network was operated with both capacitors in service. This is mainly due to the change in network impedance brought about by the change in network configuration.

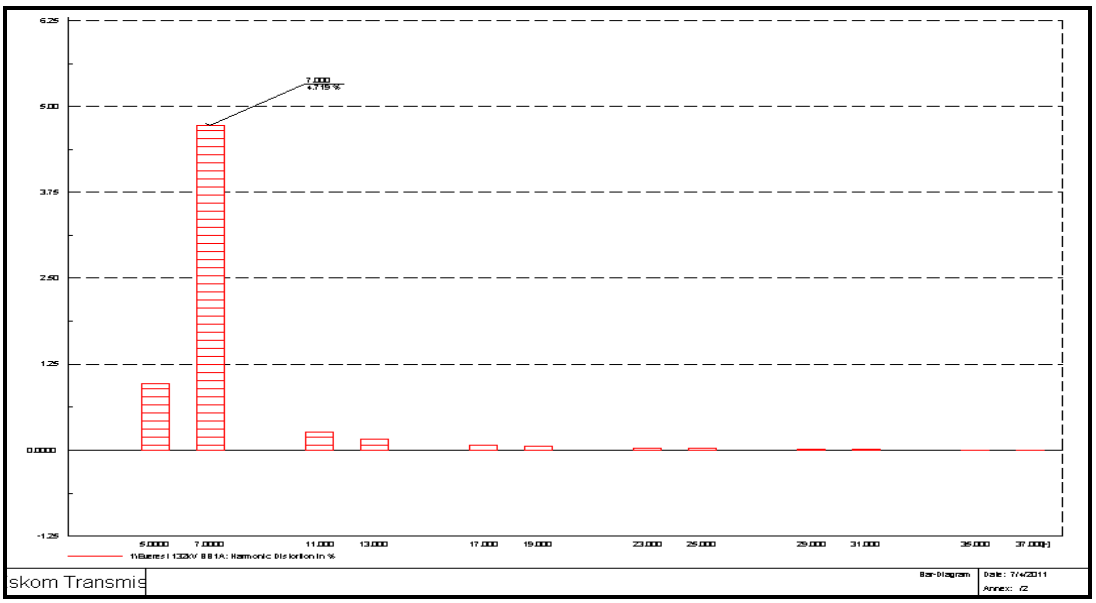

Figure 4.13: harmonic distortion at Everest 132kV bus-bar 1A. When one capacitor is in service

4.2.5 Simulation of Network with one Capacitor in service – Frequency Sweep

The figure below shows the network impedance at Everest 132kV bus-bar 1A when one capacitor bank is in service. The remaining shunt capacitor resonates with the network at approximately the 7th harmonic. The harmonic currents measured in the load current depicted a characteristic harmonic of 5th. This 5th Harmonic impedance amplification is to be monitored to determine impact.

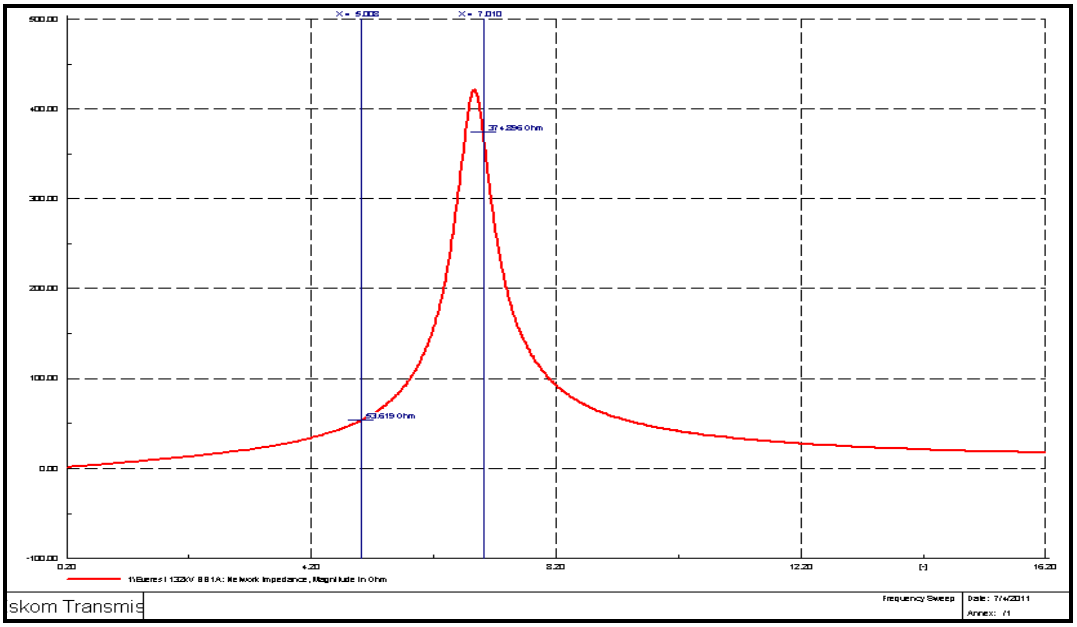

Figure 4.14: Frequency Sweep at Everest 132kV bus-bar 1A. When one capacitor is in service

Figure 4.14 above shows the network impedance as seen from Everest 132kV bus-bar 1A. When some of the harmonic producing loads are moved away from Everest substation, the 5th harmonic impedance level is at 54 ohms, while the 7th harmonic impedance level is at 375 ohms. There is a 75% and 1040% reduction in 5th and 7th harmonic impedance amplitude respectively, when one capacitor bank is in service compared to when both capacitors is switched in. This is mainly due to the network harmonic impedance change and the moving of the resonance point from 5th to around the 7th harmonic.

5th Harmonic Impedance Amplitude (Ω)	**7th Harmonic Impedance Amplitude (Ω)**	**5th Harmonic HD (%)**	**7th Harmonic HD (%)**	**Voltage (pu)**
54	375	0.97	4.72	1.01

Table 4.5: Network Parameter at Current configuration – One capacitor Banks in service

4.2.6 Simulation of Network with no Capacitors in service – Harmonic Distortion

The figure below shows harmonic distortion at Everest 132kV bus-bar 1A. When one capacitor is in service at Everest substation the 5th harmonic distortion level is 0.48%, while the 7th harmonic distortion level is also 0.46%. This represents a 51% and 90% reduction in

5^{th} and 7^{th} harmonic distortion levels respectively compared to when the current network was operated with both capacitors in service

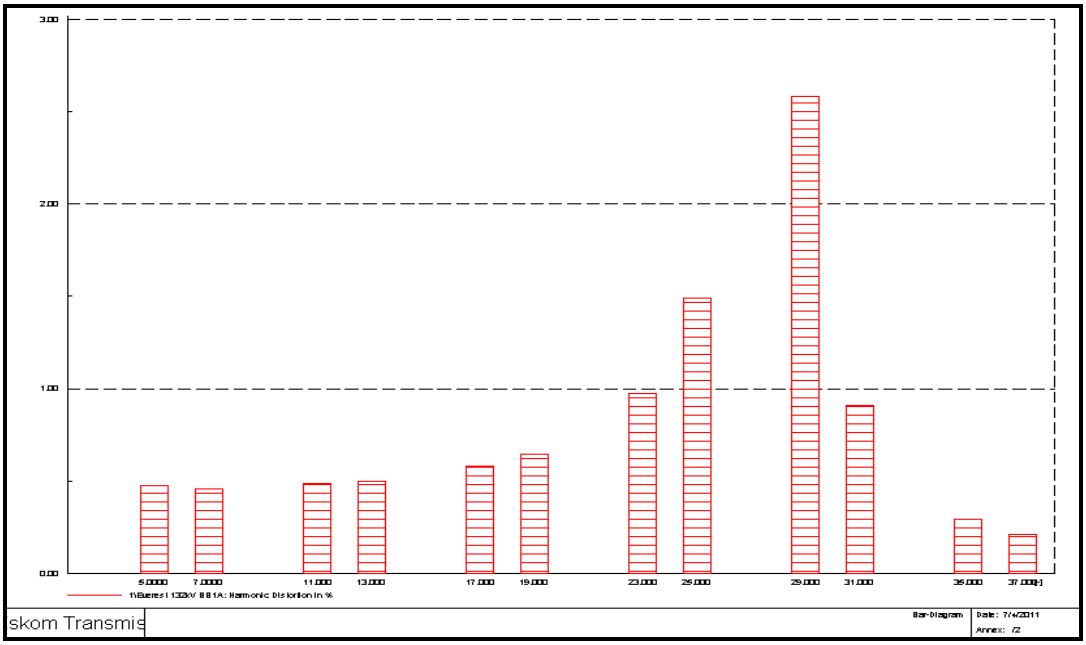

Figure 4.15: harmonic distortion at Everest 132kV bus-bar 1A - No capacitors in service

4.2.7 Simulation of Network with no Capacitors in service – Frequency Sweep

The figure below shows the network impedance at Everest 132kV bus-bar 1A when one capacitor bank is in service.

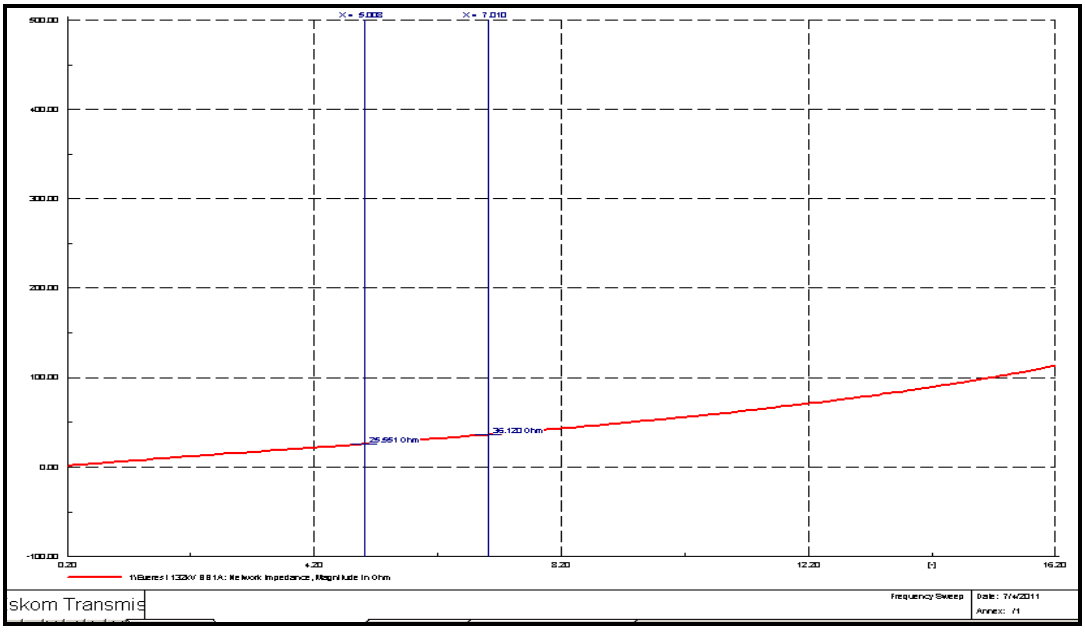

Figure 4.16: Network impedance at Everest 132kV bus-bar 1A if No capacitors are in service

Figure 4.14 above shows the network impedance as seen from Everest 132kV bus-bar 1A. When some of the harmonic producing loads are moved away from Everest substation, the 5th harmonic impedance level is at 25.5 ohms and the 7th harmonic impedance level is at 36.1 ohms. This represents a 53% and 90% reduction in 5th and 7th harmonic impedance amplitude respectively compared to when the current network was operated with one capacitor in service.

5th Harmonic Impedance Amplitude (Ω)	**7th Harmonic Impedance Amplitude (Ω)**	**5th Harmonic HD (%)**	**7th Harmonic HD (%)**	**Voltage (pu)**
25.5	36.1	0.48	0.46	1

Table 4.6: Network Parameter at Current configuration – No capacitor Banks in service

4.2.8 Simulation Results Analysis

The table below shows comparison of the change in network operating conditions before and after the Everest network reconfiguration.

Network Condition **Both Capacitors switched in**	**5th Harmonic Impedance Amplitude (Ω)**	**7th Harmonic Impedance Amplitude (Ω)**	**5th Harmonic HD (%)**	**7th Harmonic HD (%)**	**Voltage (pu)**	**Trfr1 Load (MVA)**	**Trfr2 Load (MVA)**
Original Network	136	35	2.44	0.43	1.01	175	175
Current Network	219	32.9	3.96	0.4	1.02	111	111
% Change	61	6	62	7		-37	-37

Table 4.7: Network operating condition comparison- Both Capacitors switched in

The table above shows the results of the network simulated with both capacitors switched in for the Everest network conditions before and after the reconfiguration. When the reconfiguration was done 37% of the load was shifted away from Everest. The 5th harmonic impedance amplitude increased by 61% after network configuration, while the 7th harmonic impedance amplitude reduced by 6%. This is mainly due to changed network impedance and the reduced load damping. This high harmonic impedance for the current network

configuration introduces high harmonic voltages which can be harmful to the capacitor banks.

Network Condition One Capacitor switched in	5^{th} Harmonic Impedance Amplitude (Ω)	7^{th} Harmonic Impedance Amplitude (Ω)	5^{th} Harmonic HD (%)	7^{th} Harmonic HD (%)	Voltage (pu)
Original Network	40	170	0.75	2.15	1.01
Current Network	54	375	0.97	4.72	1.02
% Change	35	121	29	120	

Table 4.8: Network operating condition comparison- One Capacitor switched in

Table 4.8 above shows the results of the network simulated with only one capacitor switched in for the Everest network conditions before and after the reconfiguration. The 5^{th} and 7^{th} harmonic impedance amplitude increased by 35% and 121% respectively after the network configuration. Also for the current network there is a 75% reduction in 5^{th} harmonic impedance compared to when the network is operated with both capacitors in service. This reduction in 5^{th} harmonic amplitude represents a much less harmful operating condition for capacitors and network as a whole.

Network Condition No Capacitor switched in	5^{th} Harmonic Impedance Amplitude (Ω)	7^{th} Harmonic Impedance Amplitude (Ω)	5^{th} Harmonic HD (%)	7^{th} Harmonic HD (%)	Voltage (pu)
Original Network	22.1	31.8	0.4	0.4	1
Current Network	25.5	36.1	0.48	0.46	1
% Change	15	14	20	15	

Table 4.9: Network operating condition comparison- No Capacitors switched in

Table 4.9 above shows the results of the network simulated with no capacitors switched in for the Everest network conditions before and after the reconfiguration. The 5^{th} and the 7^{th}

harmonic impedance amplitude increased by 15% and 14 % respectively after network configuration. Current Network operation without the capacitor banks seems to be ideal as the 5th harmonic impedance is very low and there is minimal risk of high harmonic voltages developing. However this configuration may sometimes not be practical as voltage support will still be required.

4.3 Filter Bank Consideration

If a filter bank is considered instead of the conventional capacitor bank and tuned just below the 5th harmonic, a significant reduction is realised.

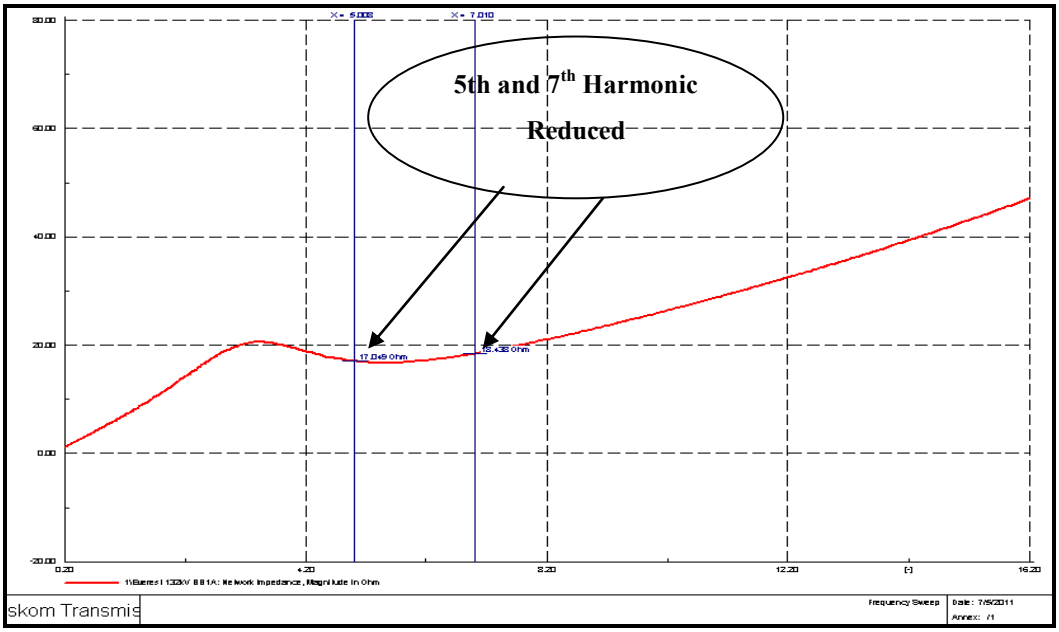

Figure 4.17: Everest 132kV Filter Response

The harmonic trap filter was tuned just below the 5th harmonic this then enabled the 5th harmonic currents to be absorbed by the trap filter. A harmonic trap filter tuned at 5th harmonic is capable of also absorbing significant amounts of 7th harmonic currents since trap filters are broad band. Also the higher harmonic frequencies are significantly reduced by the series impedance.

4.4 Impact of Changing Capacitor Bank Size

The harmonic number at which the resonance frequency occurs can be derived from the system fault level at PCC and capacitor MVAR rating as discussed earlier in section 3.3.2. According to equation (13), the capacitor MVAR rating is inversely proportional to the harmonic number at which the resonance frequency occurs. Therefore changing capacitor sizes can have an appropriate desired effect in terms of reducing harmonic impedance amplification and shifting resonance points.

An investigation was conducted on Dig-silent Power factory simulating tool to determine the precise impact of just changing capacitor size to reduce harmonics compared to other mitigation measures already discussed earlier in 2.7. Instead of having two 72MVAR (144MVAR combined) capacitors, the system was modelled with single capacitor units of varying sizes which ranged from (180, 200, 220 and 240MVAR) connected to the 132kV bus-bar and the impact registered accordingly. A single bank arrangement was chosen because currently at Everest the harmonic problems are most prevalent when both 72MVAR units are switched inn; hence a single bank arrangement afforded an opportunity to assess the worst case scenario and then determine the optimal size of capacitor MVAR that would move the resonance point away from the critical 5th harmonic.

4.4.1 Capacitor Size Changed to 180MVAR

The system was first modelled with one 180MVAR capacitor bank in service on the 132kV bus-bar in Everest substation. The impact of having this capacitor bank in the network is depicted in figure 4.18 below.

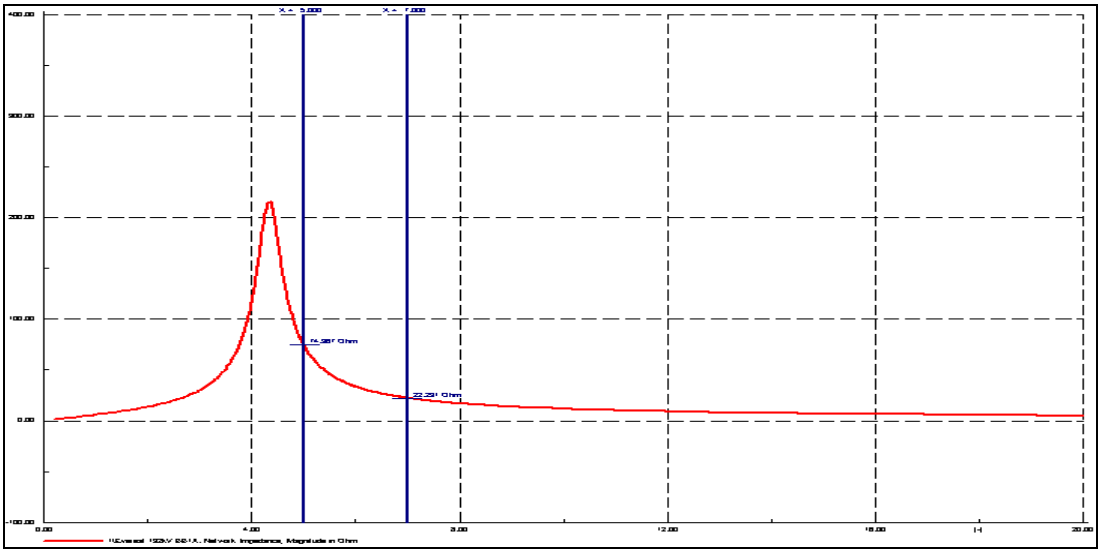

Figure 4.18: Frequency Sweep at Everest 132kV bus-bar 1A – 1 x180MVAR capacitor in

Figure 4.18: above shows the network impedance as seen from Everest 132kV bus-bar 1A. When a 1800MVAR capacitor is connected to the 132kV bus-bar; the resonance point moves away from the 5th harmonic towards the fourth harmonic which is less critical. The 5th harmonic Impedance is recorded as 74 Ω; while the 7th harmonic impedance is 22.21Ω.

Figure 4.19 below depicts the impact of having a 180MVAR capacitor on the harmonic distortion.

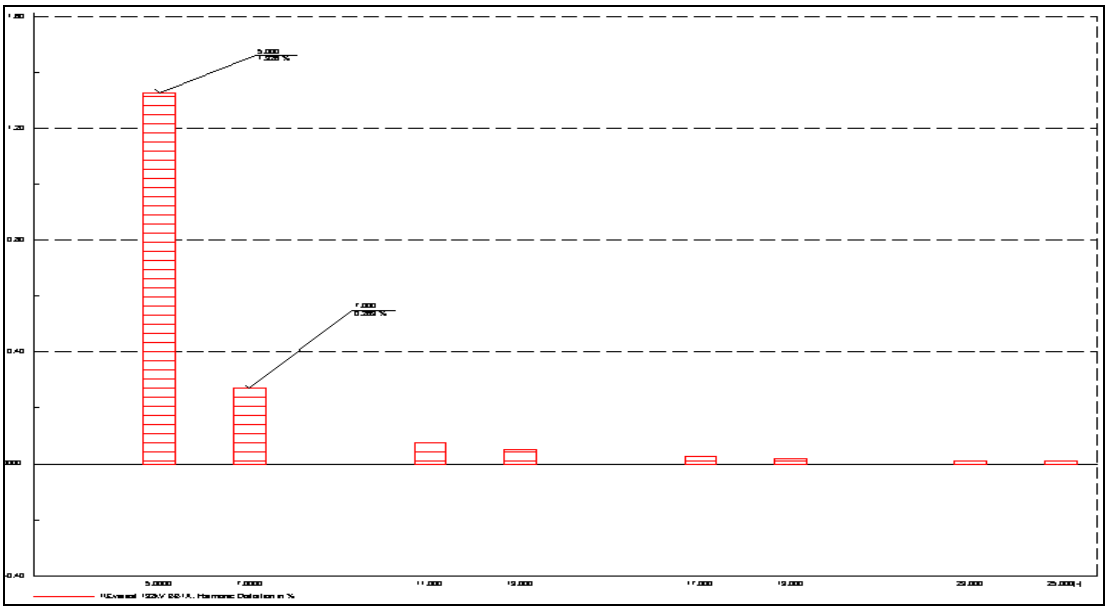

Figure 4.19: harmonic distortion at Everest 132kV bus-bar 1A - 180MVAR capacitor in service

Figure 4.19: above shows the harmonic distortion as seen from Everest 132kV bus-bar 1A. When a 180MVAR Capacitor is connected to the 132kV bus-bar; the 5th harmonic distortion is 1.326%; while the 7th harmonic impedance is 0.269% as seen in table 4.10 below.

When compared with the case when 2 x 72MVAR capacitors (144MVAR combined) are switched in, there is a 66% reduction in the 5th harmonic impedance and a 32% reduction in the 7th harmonic impedance. The 5th harmonic distortion experienced a 66% reduction while the 7th harmonic distortion experienced a 32% reduction as seen in table 4.10 below.

Capacitors	5th Harmonic Impedance	7th Harmonic Impedance	5th Harmonic Distortion	7th Harmonic Distortion
144MVAR	219	32.9	3.96	0.4
180MVAR	74	22.2	1.33	0.27
% Difference	66.2	32.5	66.4	32.5

Table 4.10: The effect of the change in capacitor size from 144 to 180MVAR

4.4.2 Capacitor Size Changed to 200MVAR

The system was modelled with one 200MVAR capacitor bank in service on the 132kV bus-bar in Everest substation. The impact of having this capacitor bank in the network is depicted in figure 4.20 below.

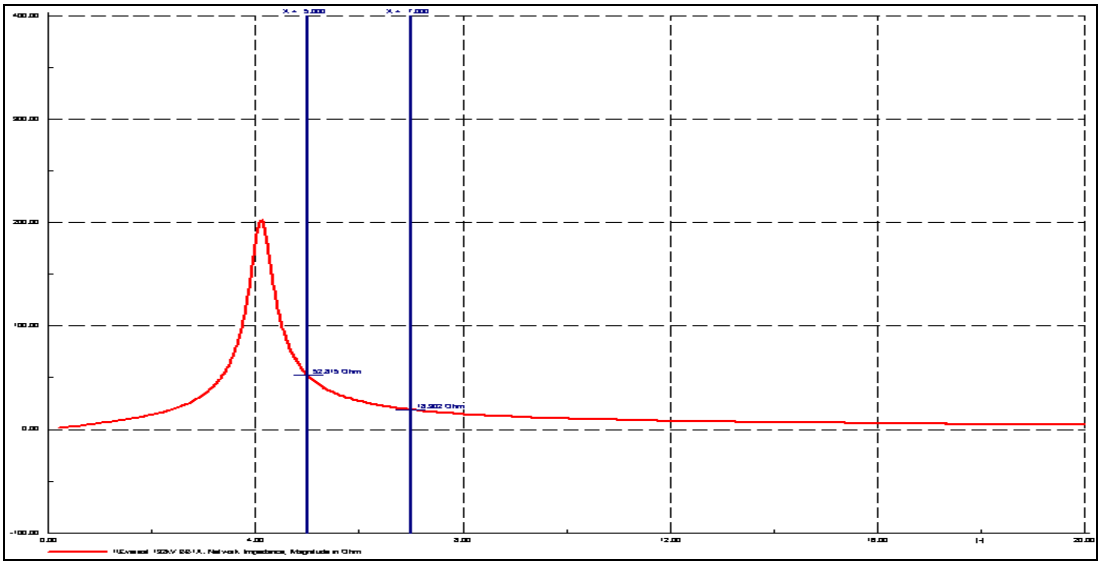

Figure 4.20: Frequency Sweep at Everest 132kV bus-bar 1A – 1 x200MVAR capacitor is in

Figure 4.20: above shows the network impedance as seen from Everest 132kV bus-bar 1A. When a 200MVAR Capacitor is connected to the 132kV bus-bar; the resonance point moves away from the 5th harmonic towards the fourth harmonic which is less critical. The 5th harmonic Impedance is recorded as 52.815 Ω; while the 7th harmonic impedance is 18.902Ω. Figure 4.21 below depicts the impact of having a 200MVAR capacitor on the harmonic distortion.

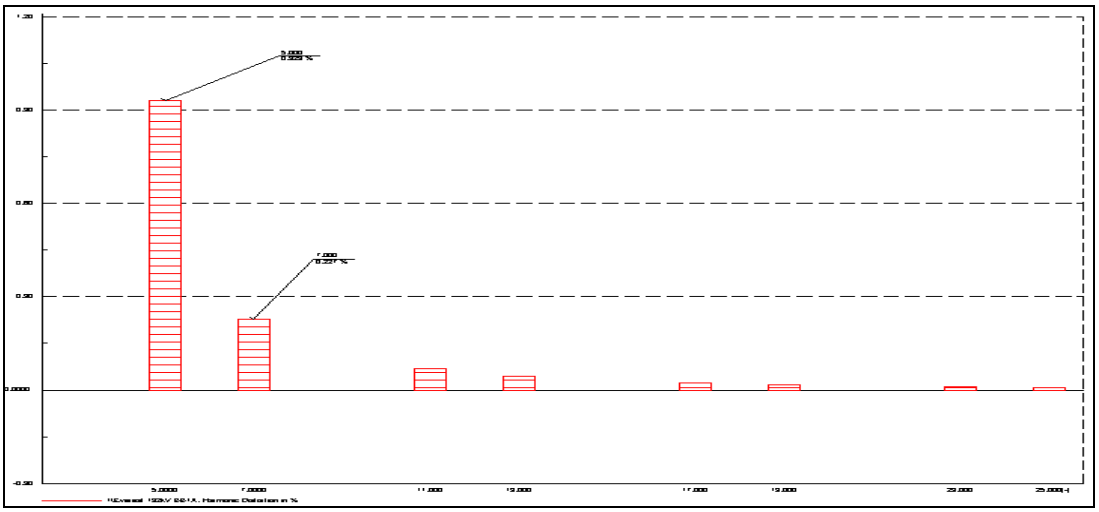

Figure 4.21: harmonic distortion at Everest 132kV bus-bar 1A – 1 x200MVAR capacitor in

Figure 4.21: above shows the harmonic distortion as seen from Everest 132kV bus-bar 1A. When a 200MVAR Capacitor is connected to the 132kV bus-bar; the 5th harmonic distortion is 0.929%; while the 7th harmonic impedance is 0.227% as seen in table 4.11 below.

When compared with the case when 2 x 72MVAR capacitors (144MVAR combined) are switched in, there is a 76% reduction in the 5th harmonic impedance and a 43% reduction in the 7th harmonic impedance. The 5th harmonic distortion experienced a 76% reduction while the 7th harmonic distortion experienced a 43% reduction as seen in table 4.11 below.

Capacitors	5th Harmonic Impedance	7th Harmonic Impedance	5th Harmonic Distortion	7th Harmonic Distortion
144MVAR	219	32.9	3.96	0.4
200MVAR	52.8	18.9	0.93	0.23
% Difference	75.9	42.6	76.5	42.5

Table 4.11: The effect of the change in capacitor size from 144 to 200MVAR

4.4.3 Capacitor Size Changed to 220MVAR

The system was modelled with one 220MVAR capacitor bank in service on the 132kV bus-bar in Everest substation. The impact of having this capacitor bank in the network is depicted in figure 4.22 below.

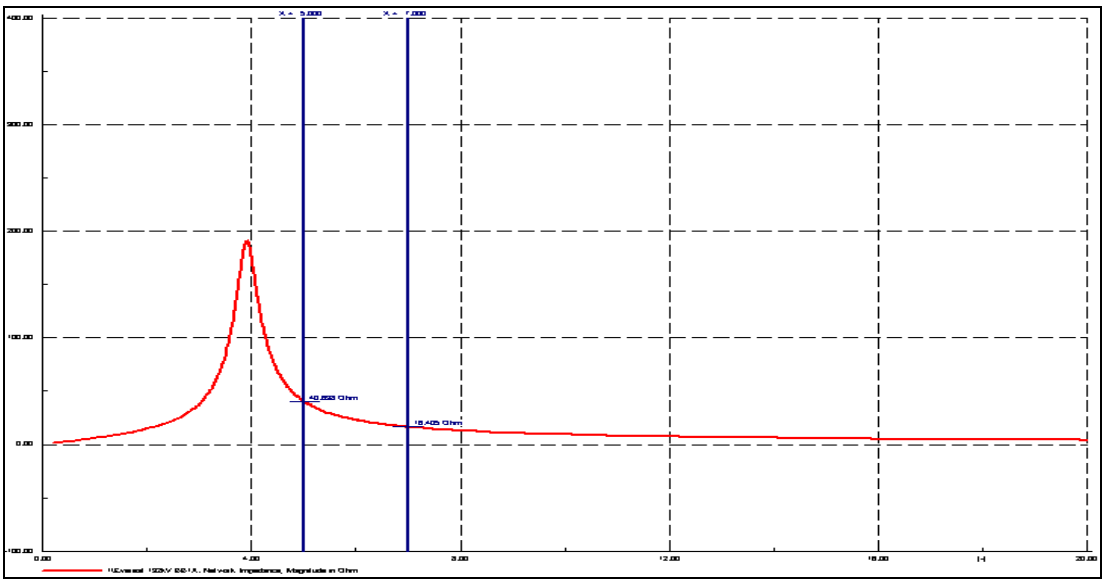

Figure 4.22: Frequency Sweep at Everest 132kV bus-bar 1A – 1x220MVAR capacitor in

Figure 4.22 above shows the network impedance as seen from Everest 132kV bus-bar 1A. When a 220MVAR Capacitor is connected to the 132kV bus-bar; the resonance point moves

away from the 5th harmonic towards the fourth harmonic which is less critical. The 5th harmonic Impedance is recorded as 40.64 Ω; while the 7th harmonic impedance is 16.41Ω. Figure 4.23 below depicts the impact of having a 220MVAR capacitor on the harmonic distortion.

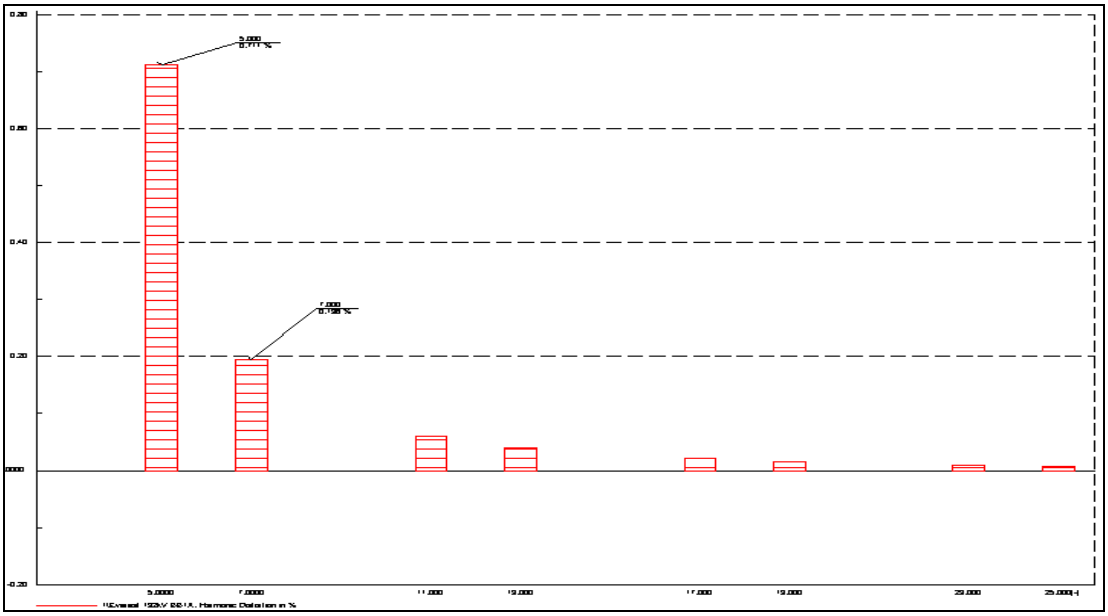

Figure 4.23: Harmonic distortion at Everest 132kV bus-bar 1A - 220MVAR capacitor in service

Figure 4.23: above shows the harmonic distortion as seen from Everest 132kV bus-bar 1A. When a 220MVAR Capacitor is connected to the 132kV bus-bar; the 5th harmonic distortion is 0.71%; while the 7th harmonic impedance is 0.196% as seen in table 4.12 below.

When compared with the case when 2 x 72MVAR capacitors (144MVAR combined) are switched in, there is a 81% reduction in the 5th harmonic impedance and a 50% reduction in the 7th harmonic impedance. The 5th harmonic distortion experienced a 82% reduction while the 7th harmonic distortion experienced a 50% reduction as seen in table 4.12 below.

Capacitors	5th Harmonic Impedance	7th Harmonic Impedance	5th Harmonic Distortion	7th Harmonic Distortion
144MVAR	219	32.9	3.96	0.4
220MVAR	40.64	16.41	0.71	0.2
% Difference	81.4	50.1	82.1	50.0

Table 4.12: The effect of the change in capacitor size from 144 to 220MVAR

4.4.4 Capacitor Size Changed to 240MVAR

The system was modelled with one 240MVAR capacitor bank in service on the 132kV bus-bar in Everest substation. The impact of having this capacitor bank in the network is depicted in figure 4.24 below.

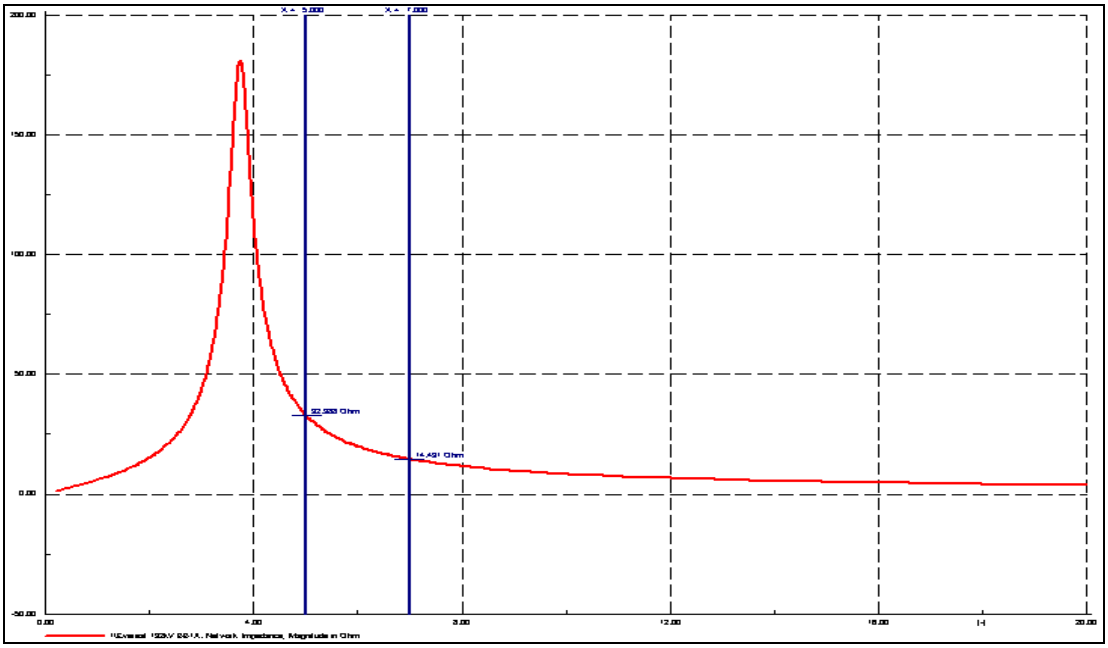

Figure 4.24: Frequency Sweep at Everest 132kV bus-bar 1A – 1x 240MVAR capacitor in

Figure 4.24: above shows the network impedance as seen from Everest 132kV bus-bar 1A. When a 240MVAR Capacitor is connected to the 132kV bus-bar; the resonance point moves away from the 5th harmonic towards the third harmonic which is less critical. The 5th harmonic Impedance is recorded as 32.988 Ω; while the 7th harmonic impedance is 14.491Ω.

Figure 4.25 below depicts the impact of having a 240MVAR capacitor on the harmonic distortion.

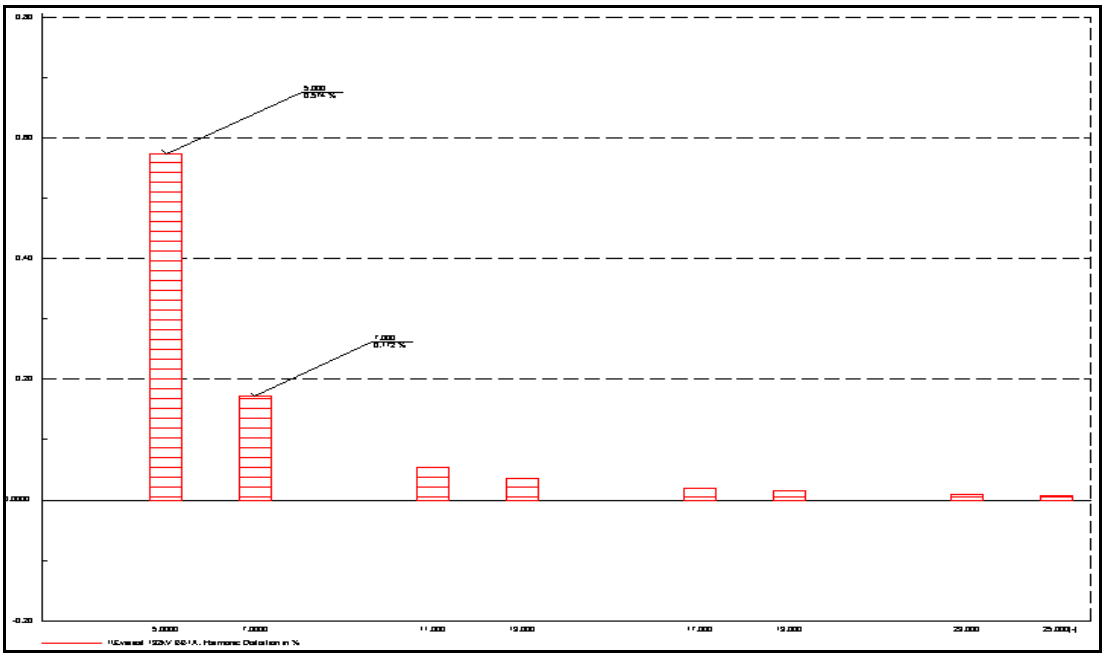

Figure 4.25: Harmonic distortion at Everest 132kV bus-bar 1A – 1 x240MVAR in

When a 240MVAR Capacitor is connected to the 132kV bus-bar; the 5th harmonic distortion is 0.574%; while the 7th harmonic impedance is 0.172% as seen in table 4.13 below.

When compared with the case when 2 x 72MVAR capacitors (144MVAR combined) are switched in, there is a 84.9% reduction in the 5th harmonic impedance and a 57.5% reduction in the 7th harmonic impedance. The 5th harmonic distortion experienced a 84.8% reduction while the 7th harmonic distortion experienced a 57.5% reduction as seen in table 4.13 below.

Capacitors	5th Harmonic Impedance	7th Harmonic Impedance	5th Harmonic Distortion	7th Harmonic Distortion
144MVAR	219	32.9	3.96	0.4
240MVAR	33	14.5	0.6	0.17
% Difference	84.9	55.9	84.8	57.5

Table 4.13: The effect of the change in capacitor size from 144 to 240MVAR

4.4.5 Discussion of Impact of changing capacitor size

The simulations conducted above clearly show an improvement or reduction in the 5th harmonic impedance and voltage distortion. There is an inverse proportionality between the size of the capacitor and the harmonic impedance and voltage distortion. In the above cases, increasing the capacitor sizes resulted in the reduction of the 5th and 7th harmonic impedance and voltage distortion. Figure 4.26 below clearly depicts this relationship.

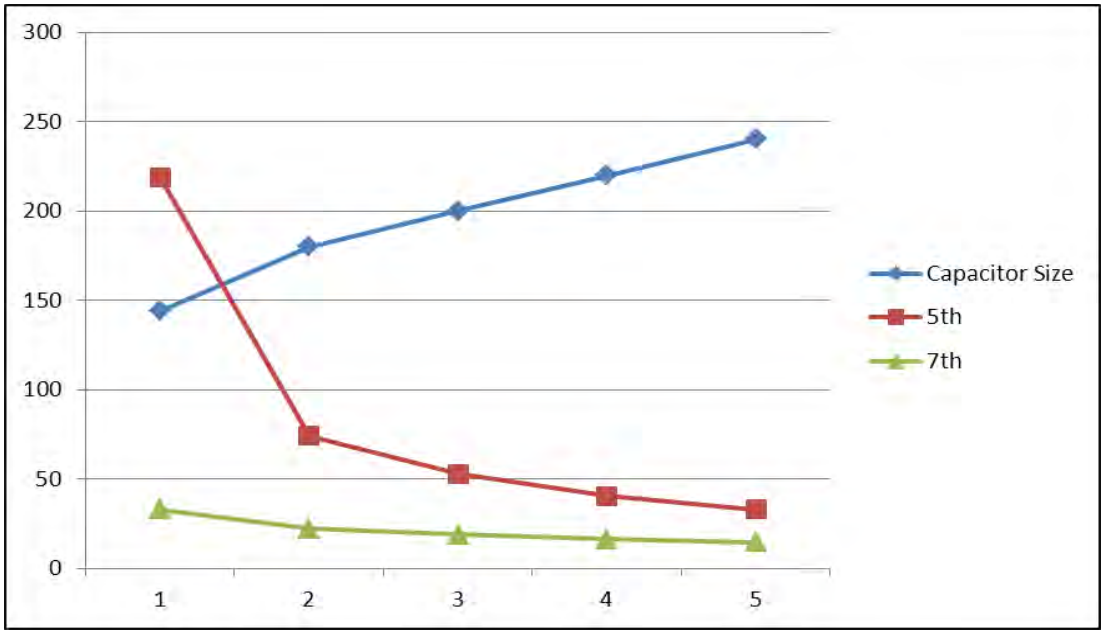

Figure 4.26: Comparison of the effect of change in capacitor size on harmonics

This therefore confirms that indeed this is a viable solution for the Everest case, where the choice of the size of the capacitor to be chosen would depend on a number of factors including available budget, because the higher the rating the higher the cost. Although any of the capacitor banks that were investigated (180 – 240MVAR) would be suitable for the Everest case; however this solution is not preferred mainly because it does not offer the flexibility that a tuned harmonic filter offers. When network configuration changes for whatever reason, a fixed capacitor bank may no longer be suitable as it may introduce resonance points at critical frequencies. The solution of changing the capacitor size is therefore not recommended for the Everest case.

4.5 Everest Network Analysis

This section covers the Everest network performance analysis for the last five years to ascertain inconsistencies and variations in performance.

4.5.1 Everest Capacitor Failure Trend

The following picture depicts the failure trend of the 132kV capacitor banks at Everest substation from year 1998 to December 2010. During this period, a total of 23 failures were experienced by the Everest capacitor banks. These failures to some extent can be attributed to high harmonic voltages that are prevalent at Everest substation.

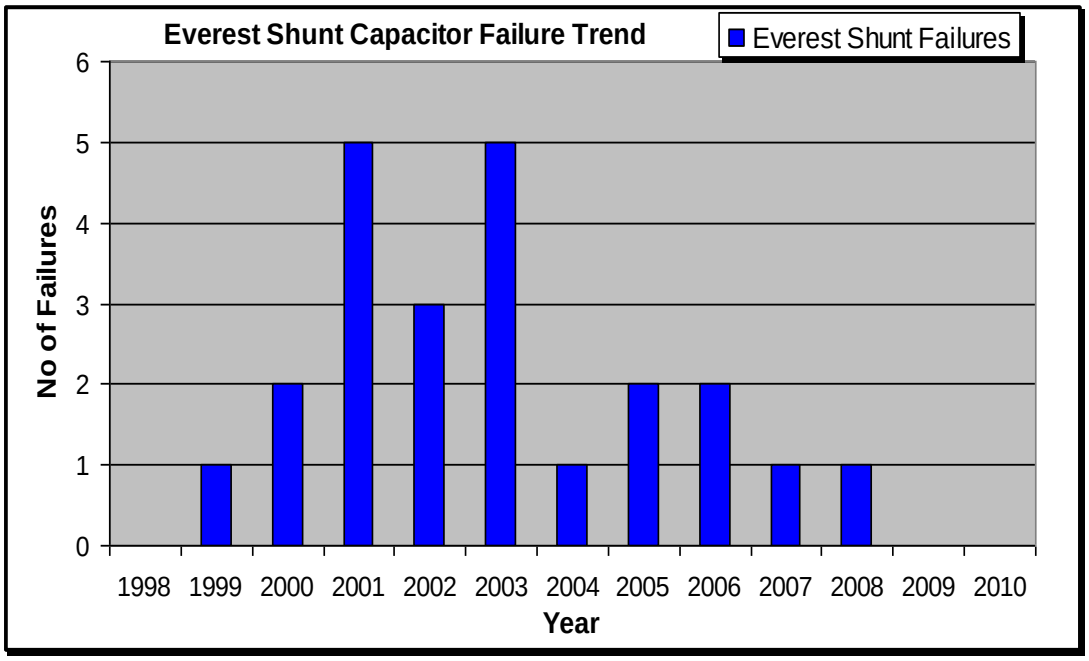

Figure 4.27: The failure trend of the 132kV capacitor banks at Everest

There have been 23 capacitor bank failures in Everest substation since year 1998. In year 2001 and 2003 a total number of five shunt capacitor failures were experienced respectively. These failures resulted from violent blowing of shunt fuses or internal shunt capacitor cans failure. In year 2008 during the compilation of this study, a request was made to the Eskom network control to limit the simultaneous switching in of both Everest Capacitor Banks. The capacitor banks were to be only utilised during emergency conditions for voltage support. This resolution was immediately endorsed by control and by the end of 2009 financial year no shunt capacitor failures had been experienced. However, adherence to this arrangement needs to be continuously monitored as the high harmonic currents flowing in the Everest network may influence capacitor bank performance.

4.5.2 Everest Capacitor Failure & THD Correlation

The Table below depicts the correlation of capacitor bank failures over the years and the THD value at the time of failure.

Incident No	Date	Start Time	Incident Comment	Incident Cause	THD at the Time (%)
1	15/01/1999	11:17	Everest, No.1 132kV Capacitor Bank Incident	Blown Fuse	4.2
2	23/08/2000	04:34	Everest, Shunt Capacitor 2 132kV Tripped	Blown Fuse	4.1
3	24/08/2000	09:26	Everest, Shunt Capacitor 2 132kV Tripped	Blown Fuse	4
4	09/02/2001	20:16	Everest, Shunt Capacitor 2 132kV Tripped	Blown Fuse	4.2
5	11/08/2001	18:20	Everest, Shunt Capacitor No1 132kV Breaker Tripped	Blown Fuse	2.8
6	19/09/2001	09:02	Everest, Shunt Capacitor No2 132kV Breaker Tripped	Blown Fuse	2.7
7	19/09/2001	09:30	Everest, Shunt Capacitor No2 132kV Breaker Tripped on Closing	Blown Fuse	2.7
8	19/09/2001	10:48	Everest, Shunt Capacitor No2 400kV Breaker Tripped on Closing	Blown Fuse	2.7
9	05/06/2002	21:18	Everest, Shunt Capacitor No1 132kV Tripped	Blown Fuse	1.8
10	13/11/2002	07:10	Everest, Shunt Capacitor No2 132kV Tripped	Blown Fuse	1.8
11	11/12/2002	21:53	Everest, Shunt Capacitor No1 132kV Tripped	Blown Fuse	2.8
12	24/01/2003	18:13	Everest, Shunt Capacitor No1 132kV Tripped	Blown Fuse	2.8
13	13/02/2003	23:11	Everest, Shunt Capacitor No1 132kV Tripped	Blown Fuse	3
14	23/04/2003	23:30	Everest, Shunt Capacitor No2 132kV Tripped	Blown Fuse	2

15	24/04/2003	14:53	Everest, Shunt Capacitor No2 132kV Trip on closing	Blown Fuse	2.8
16	23/09/2003	14:42	Everest, Shunt Capacitor No1 132kV Tripped	Blown Fuse	2.7
17	04/06/2004	11:06	Everest, Shunt Capacitor No1 132kV Tripped	Blown Capacitor Can	2.3
18	03/03/2005	07:44	Everest, Shunt Capacitor No2 132kV Opened	Blown Fuse	2.3
19	22/05/2005	09:42	Everest, Shunt Capacitor No2 132kV Opened	Blown Fuse	1.7
20	26/10/2006	22:27	Everest, Shunt Capacitor No2 132kV Tripped	Two Fuses Blown	2.3
21	11/11/2006	12:33	Everest, Shunt Capacitor No2 132kV Tripped	Blown Fuse	No data
22	31/07/2007	06:43	Everest, Shunt Capacitor No2 132kV Tripped	Blown Capacitor Can	3

Table 4.14: Everest Capacitor Bank Failure and THD correlation

The analysis of the data above reveals that majority of the Everest Capacitor Bank failures were due to fuse failures. The allowable THD level at Everest 132kV bus bar is 3%, however the THD level was above 3% during some of the failures that occurred from year 1999 to 2001. All failures that occurred after year 2001, the THD levels were below the 3% acceptable level at the time of the Capacitor failure. Literature indicates that continuous exposure to high levels of harmonics will lead to overheating of capacitor banks and eventually lead to insulation failure over time. Although most of the failures above occurred during the time when THD levels were within limits, but it is suspected that high levels of harmonics occurring prior to the failures could have been a root cause.

4.5.3 Everest THD and Individual Harmonic Trends

The figure below shows the THD profile for the year 2005 recorded at Everest 132kV bus bar which depicts the THD NRS limit of 3% already exceeded. The THD exceedance points shown in the picture are due to the capacitors at Everest switched in to the network and forming resonant points with the system reactance. The highest THD level reached in 2005 was 4.5%.

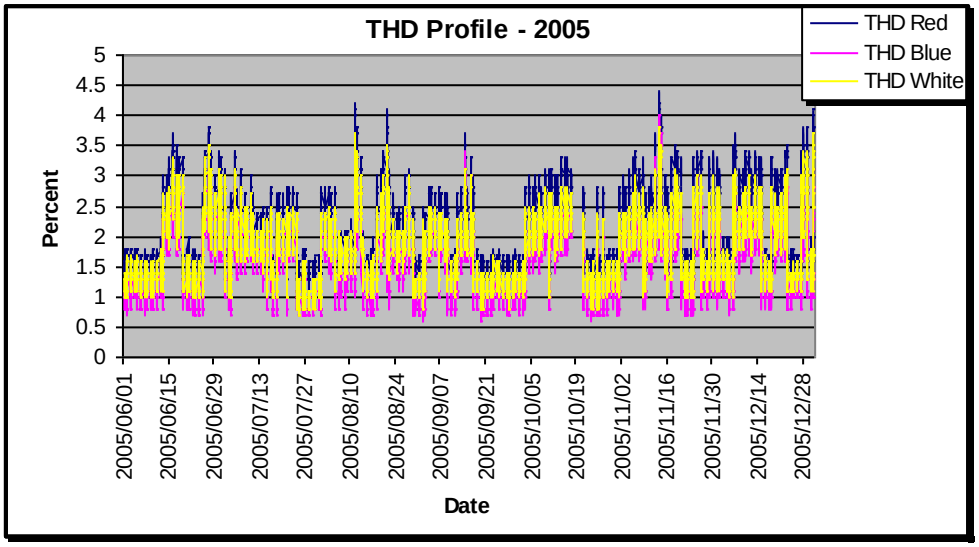

Figure 4.28: THD profile for the year 2005 recorded at Everest 132kV bus bar

The figure below shows the worsening THD profile recorded at Everest 132kV bus bar, the highest figure for THD recorded in 2006 was 6.5%.

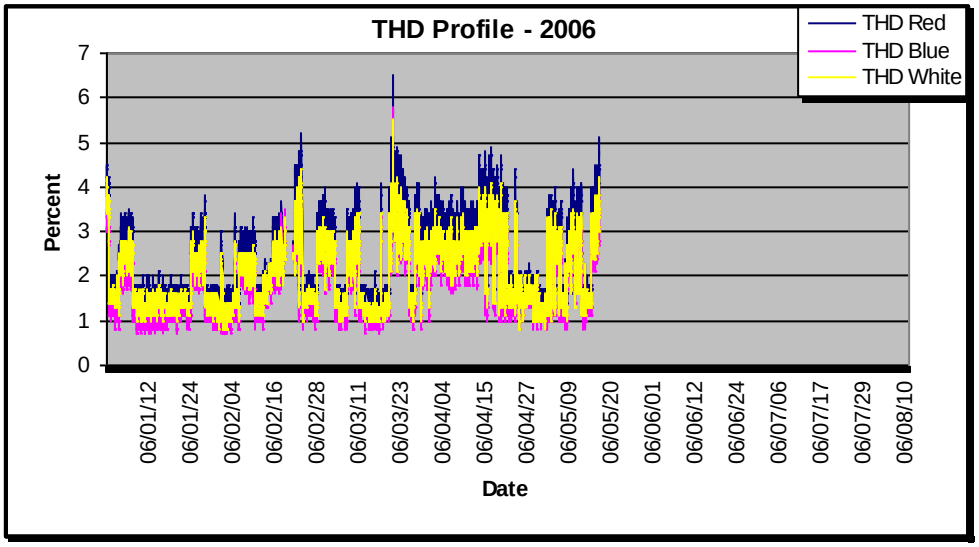

Figure 4.29: THD profile for the year 2006 recorded at Everest 132kV bus bar

The figure below shows the THD profile for year 2007 recorded at Everest 132kV bus bar, the highest recorded figure for THD recorded in 2007 was 5%. The times when the capacitors were switched out are visible from the picture below and show lower THD levels.

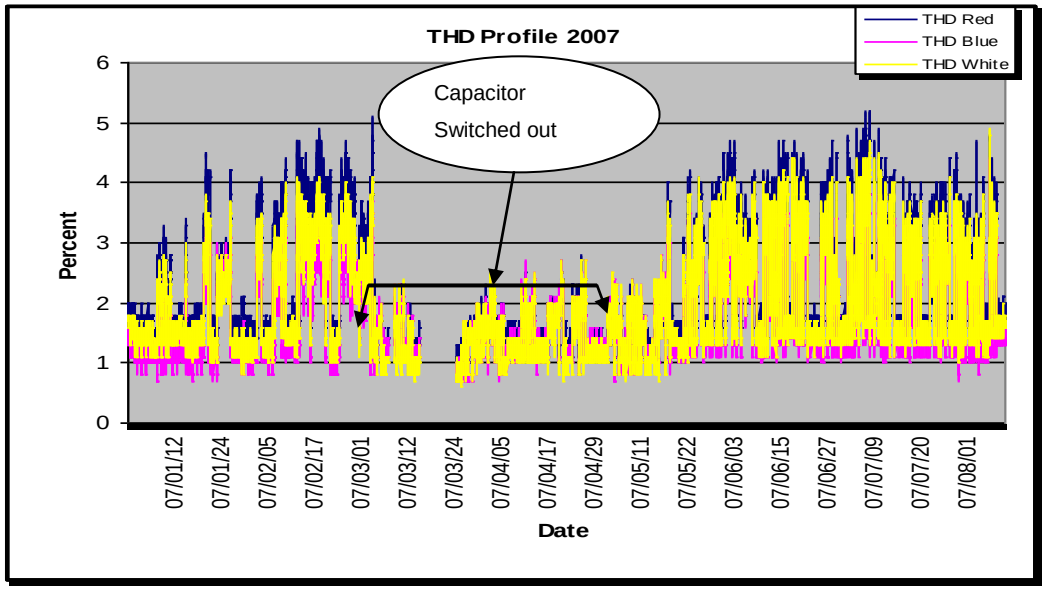

Figure 4.30: THD profile for the year 2007 recorded at Everest 132kV bus bar

The figure below shows the THD profile for year 2008 recorded at Everest 132kV bus bar, the highest recorded figure for THD recorded in 2008 was 8%. The times when the capacitors were switched out are visible from the picture below and show lower THD levels.

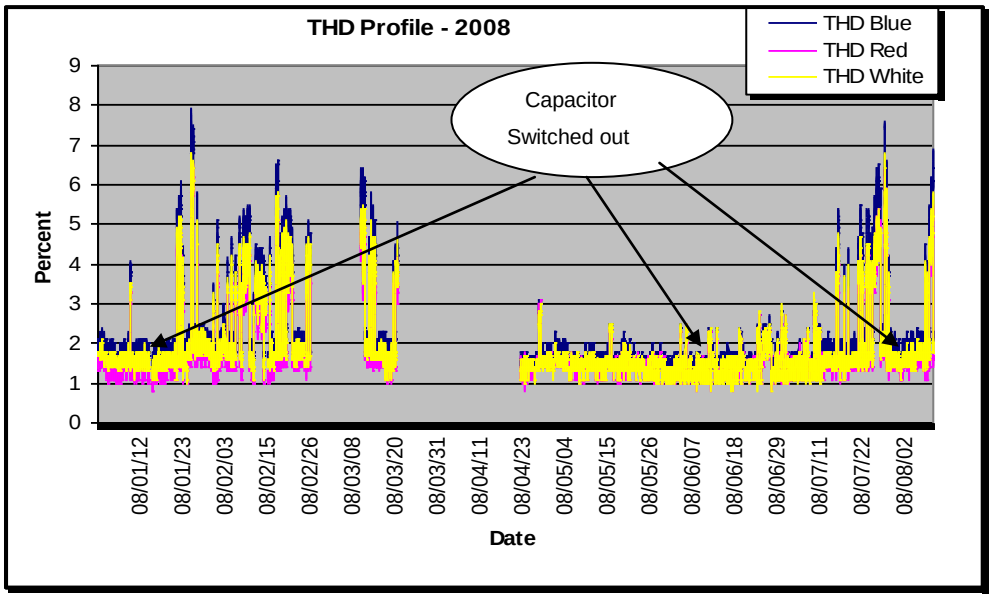

Figure 4.31: THD profile for the year 2008 recorded at Everest 132kV bus bar

The increasing THD exceedances can be attributed to changing network conditions that have altered Fault levels at Everest 132kV bus bars. The harmonic producing loads at Everest are responsible for injecting harmonic currents into the system.

The figure below shows the THD profile for year 2009 recorded at Everest 132kV bus bar, the highest recorded figure for THD recorded in 2009 was 7%. The times when the capacitors were switched out are visible from the picture below and show lower THD levels.

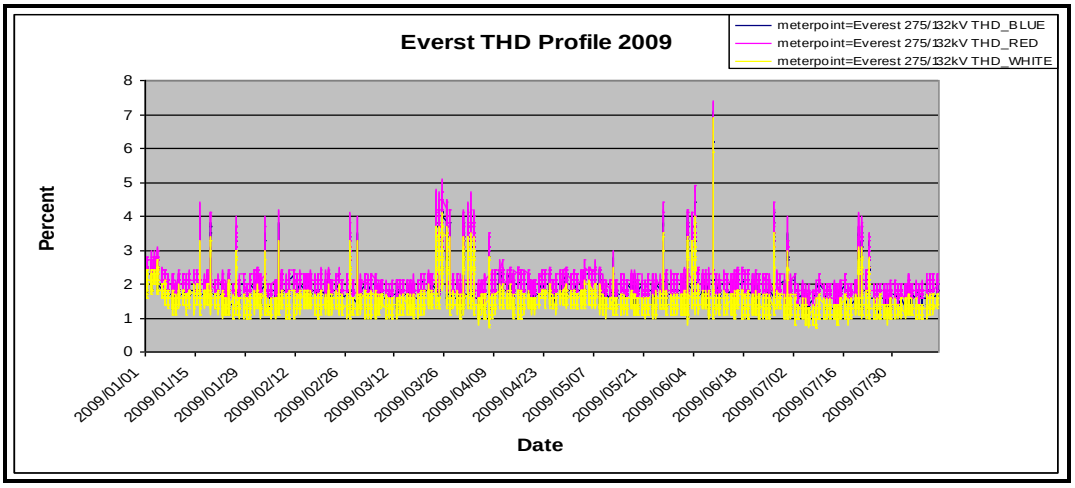

Figure 4.32: THD profile for the year 2009 recorded at Everest 132kV bus bar

The figure below shows the THD profile for year 2010 recorded at Everest 132kV bus bar, the highest recorded figure for THD recorded in 2010 was 3.5%. The times when the capacitors were switched in and out are visible from the picture below and show lower or higher THD levels.

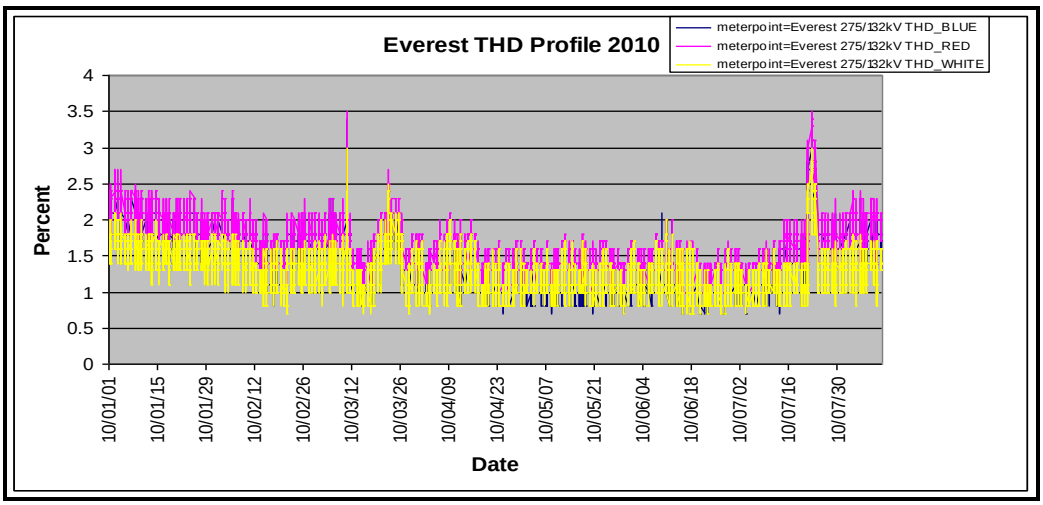

Figure 4.33: THD profile for the year 2010 recorded at Everest 132kV bus bar

Power quality measuring instruments known as an Impedo graph were installed at Everest 132kV bus bar 1A and relevant lines to enable the measurement of individual harmonic currents and voltages. The impedo graphs were installed at Everest from the 29th June 2012 to 10th July 2012. The impedo graphs were installed on feeders which predominantly supply industrial customers and mines, these included:

1) Everest – Anglo Dankbarheid 132kV line
2) Everest – Anglo Erfdeel 132kV line
3) Everest – Duiker 132kV line
4) Everest – New Steyn 132kV line

As highlighted earlier in section 3.5.1 the harmonic current measurements were previously conducted on the same feeders from 08/02/2008 to 23/02/2008, although there were problems encounted with the data size and quality. The latest measurements do provide a clearer individual harmonic current and voltage trends. However direct comparison with the previous measurements will be limited, since the previous measurements were not conclusive. During the recent measurements, some of the meters experienced problems and only recorded a few days of data, compared to other meters. This could have been due to the sensitivity of the data interrogation software within these meters; also the meters could have been abruptly moved from their position during switching or cleaning in the control room thus interrupting the recording process.

The following figures indicate the harmonic voltage and current measurements obtained from each line during this period.

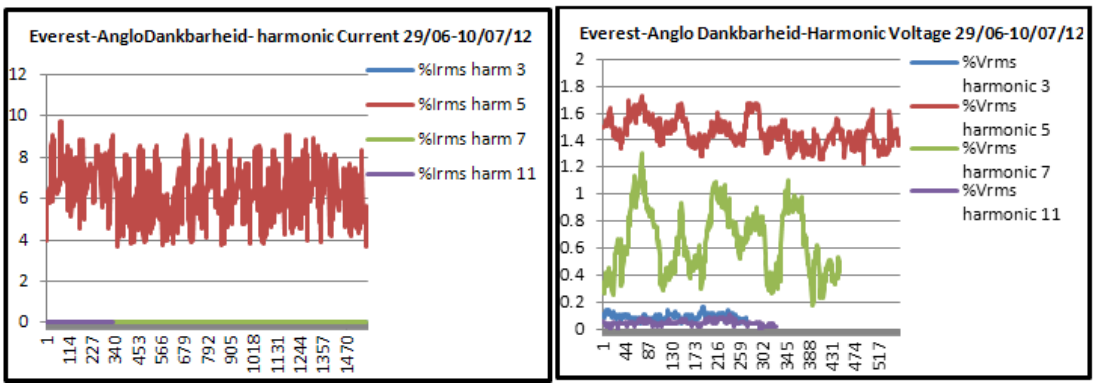

Figure 4.34: Everest - Anglo Dankbarheid 132kV line individual harmonics profiles

The impedograph connected to the Everest Anglo Dankbarheid line seem to have recorded all the data during the period with no interruptions.

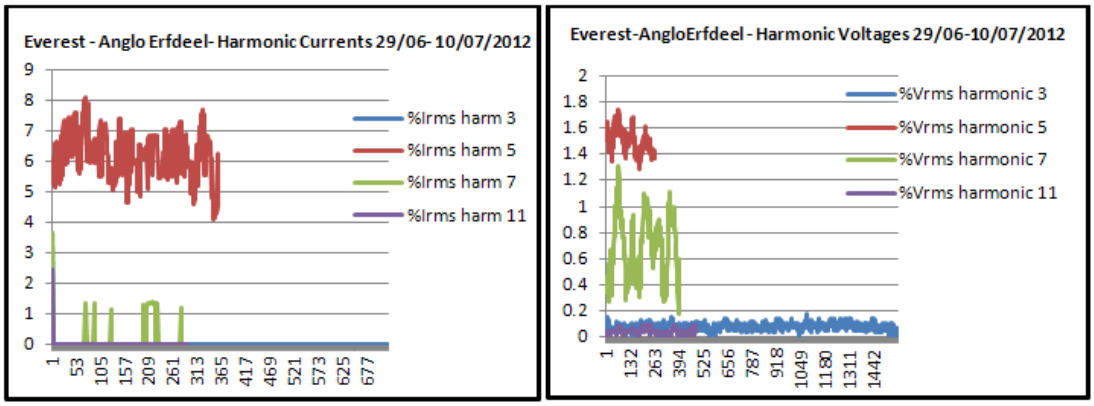

Figure 4.35: Everest - Anglo Erfdeel 132kV line individual harmonics profiles

The impedograph connected to the Everest Anglo Erfdeel line seem to have recorded almost half of the data within the period; it is evident that it suffered an interruption.

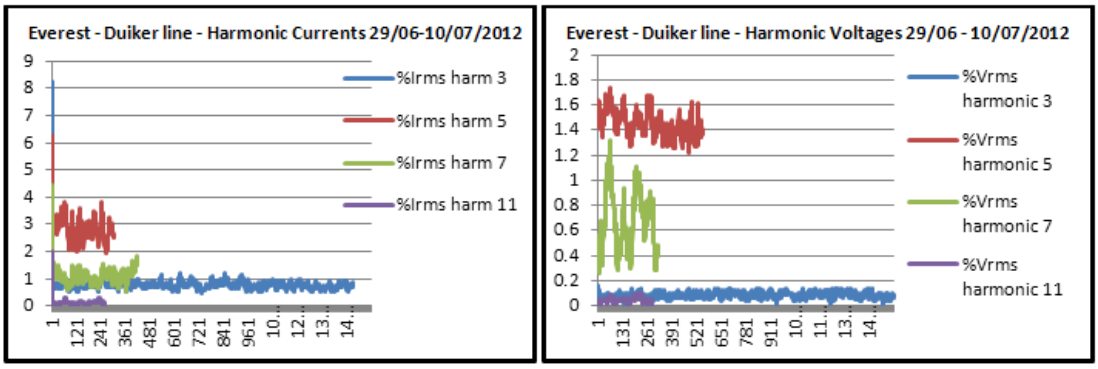

Figure 4.36: Everest - Duiker 132kV line individual harmonics profiles

The impedograph connected to the Everest - Duiker line seem to have recorded less than half of the data within the period; it is evident that it also suffered an interruption.

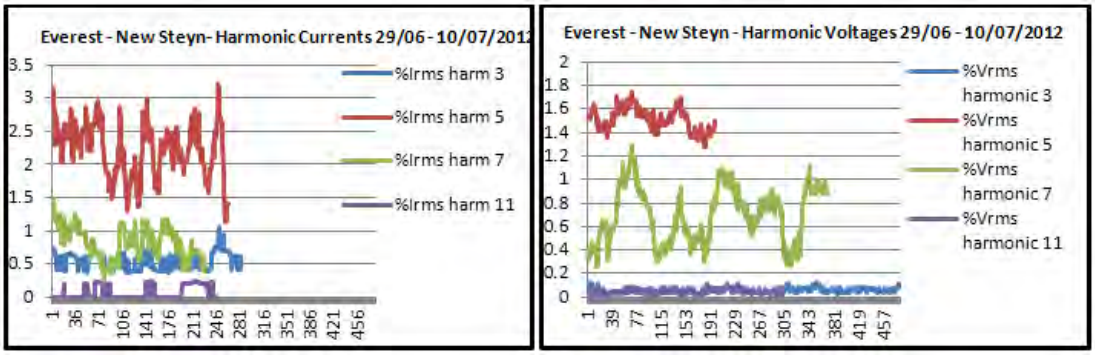

Figure 4.37: Everest - New Steyn 132kV line individual harmonics profiles

The impedograph connected to the Everest – New Steyn line seem to have recorded almost half of the data within the period; it is evident that it also suffered an interruption.

The harmonic current and voltage profiles shown above indicate the 5th harmonic currents varying from 1.5% to 9.5% of the fundamental current, while the 5th harmonic voltages seem to vary from 1.2% to 1.7% of the fundamental voltage in all the feeders. The 7th harmonic currents vary from an average 0% to 1% of the fundamental current, while the 7th harmonic voltages seem to vary from 0.2% to 1.3% of the fundamental voltage in all the feeders. The individual harmonic current profiles were mainly influenced by the amount of non-linear load currents drawn by the mining and industrial customers during the period. The individual harmonic voltage profiles were mainly influenced by the flow of the harmonic currents through the system impedances. The profiles provide a confirmation that the harmonic voltage distortions were within allowable limits, and this is further emphasised in figure 4.38 below.

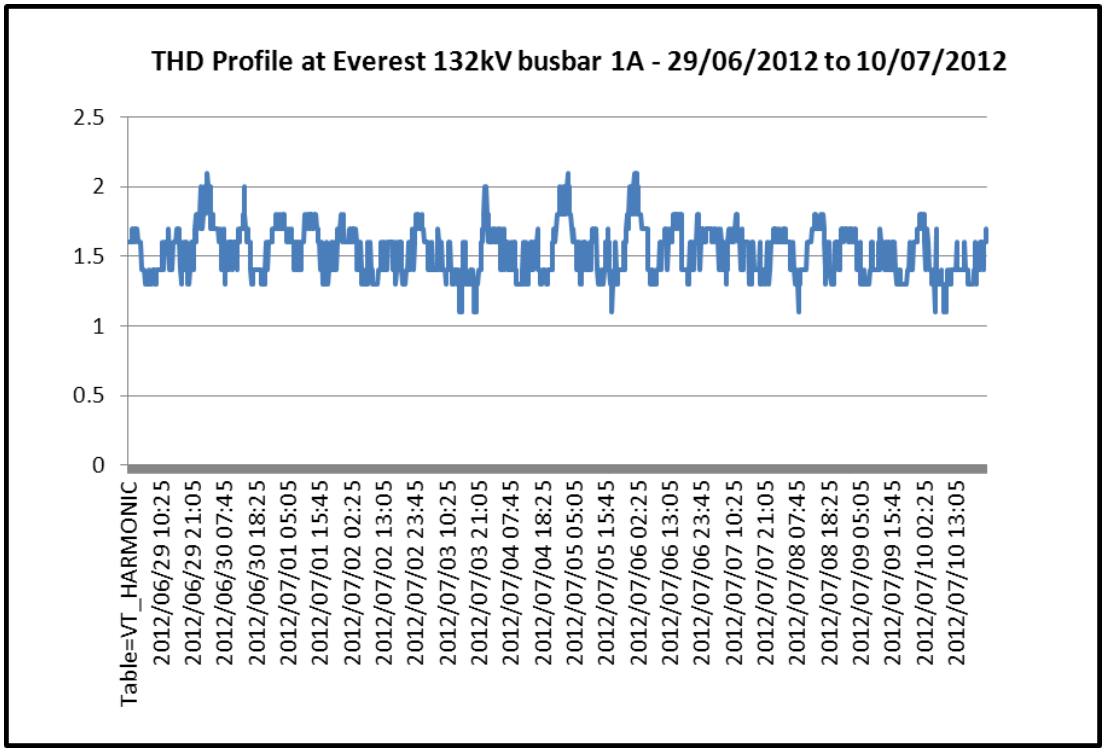

Figure 4.38: THD Profile at Everest 132kV bus-bar 1A - 29/06/2012 to 10/07/2012

Figure 4.38 above confirms that there was no sudden swing in distortion levels normally evident during capacitor switching and confirm that the harmonic voltage distortion levels are within the NRS 048 specified limit of 3%.

4.5.4 Further Assessment of Network Operating Guideline

As discussed earlier, harmonic current and voltage measuring instruments were installed at Everest feeders and 132kV bus-bar 1A in order to also ascertain the improvements since the implementation of the recommended capacitor switching arrangement or guideline. The switching guideline highlighted the need to avoid switching in both capacitor banks at Everest network in order to prevent 5th harmonic voltage amplification. This guideline was adopted and implemented since 2008; therefore the harmonics measuring instruments installed were aimed at firstly assessing the compliance to the switching arrangement/guideline by network control and also to correlate the field measurements with the dig-silent simulations.

The total harmonic distortion (THD) measurements were taken at Everest 132kV bus bar 1A to determine the improvement in THD if the new switching arrangement was adhered to. The THD profile was downloaded from the vectograph meter that is permanently connected to the Everest 132kV bus bar 1A which mainly registers the voltage regulation and disturbances. Figure 4.39 below depicts the THD as seen from Everest 132kV bus bar 1A from 01/01/2011 to 30/06/2012.

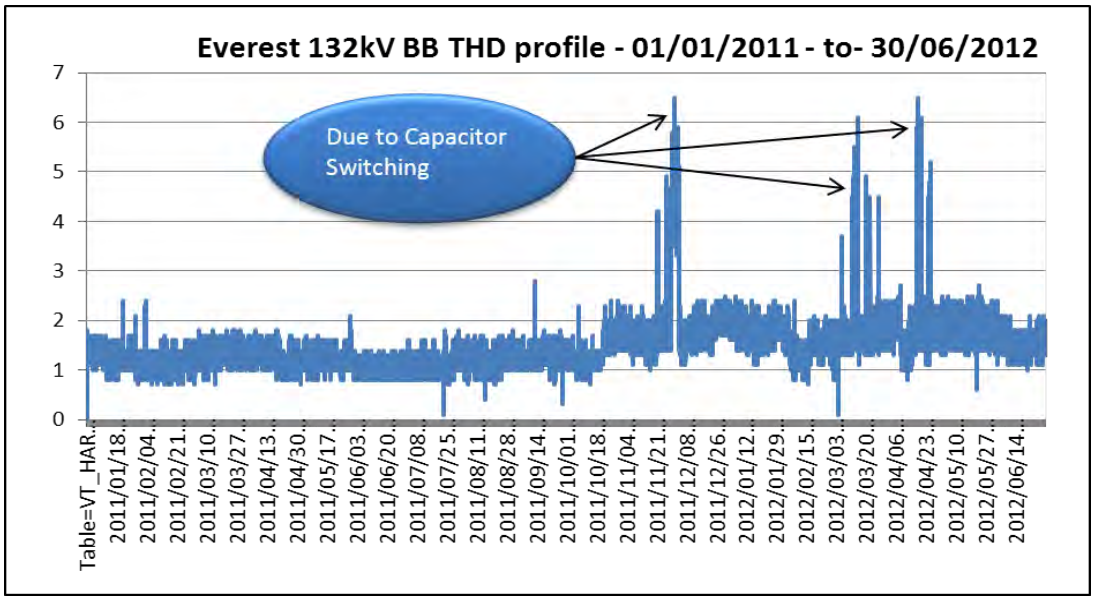

Figure 4.39: Everest 132kV bus-bar 1A THD Profile 01/01/2011 – 30/06/2012

Figure 4.39 above depicts a TDH profile at Everest 132kV bus bar 1A from 01/01/2012 to 30/06/2012, indicating distortion levels mostly below 3% in the entire period. However there were times during November 2011, March 2012 and April 2012 when both capacitors were

switched in for brief moments thus resulting in amplified harmonic voltages as shown in the figure above exceeding 3% THD NRS 048 limit. Eskom network controllers are often under pressure to switch in both Everest capacitor banks when the Koeberg generation has an outage that necessitates utilisation of voltage support sources from other parts of the networks linking with the Cape corridor. Nonetheless, the THD profile undoubtedly confirms that Eskom network controllers in most cases have continuously adhered to the recommendation to limit switching both capacitors in.

4.5.5 Dig-silent Simulation versus Field Measurement Correlation

A more sophisticated power quality measuring instrument known as an Impedo graph was installed at Everest 132kV bus bar 1A to enable the measurement of individual harmonic currents and voltages. In this case the impedo graph was required to enable accurate measurement and recording of especially the 5th and 7th harmonic voltage distortions for comparison with dig silent simulated values. The impedo graph was installed at Everest from the 29th June 2012 to 10th July 2012. During this period the capacitor banks were unfortunately never switched in to service. Therefore this limited the comparable scenarios, meaning that the only comparable scenario is that which correlates the simulated and measured voltage harmonic distortions when both capacitors are out of service. Figure 4.40 below highlights this correlation.

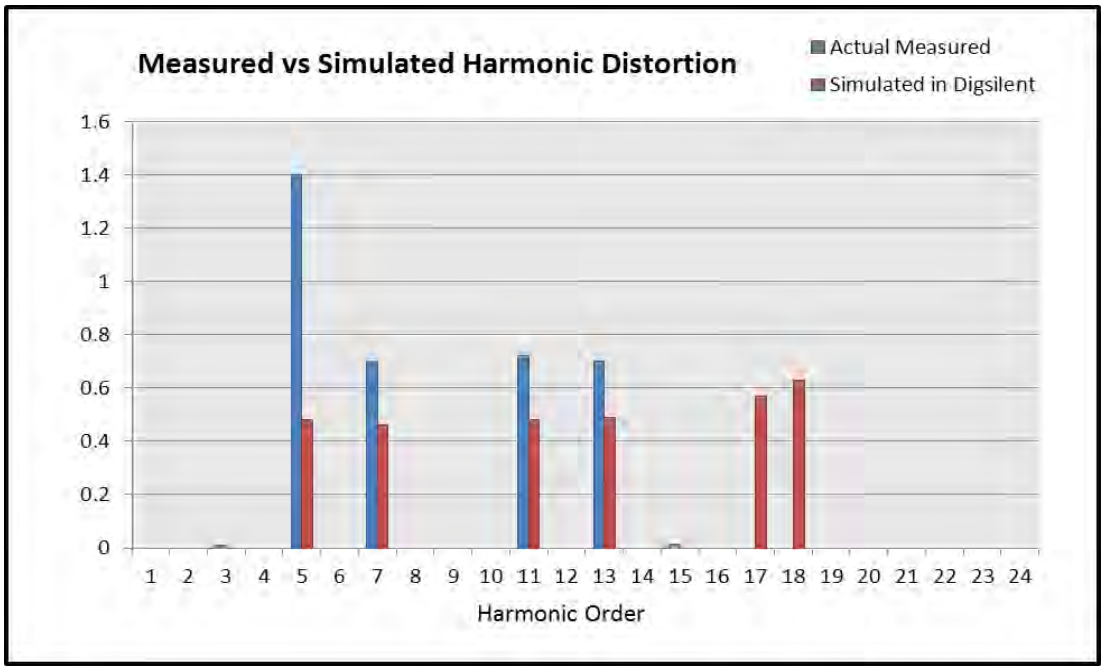

Figure 4.40: Measured vs Simulated Voltage Harmonic Distortion at Everest 132kV BB

Figure 4.40 above shows a deviation between the simulated and actual measured 5thand 7th harmonic voltage distortions. This variance could have resulted from the changed harmonic current flows during that period which then impacted on the harmonic voltage profiles. It was also reported that there was a maintenance outage on the New Steyn feeder during that period, which could have also contributed to the variance.

To achieve a more conclusive correlation assessment between dig silent and the field measurement would require that the harmonic measuring instruments be left in the field for many months in order to capture all the important network events like capacitor switching in this particular case. The ideal case would be to record harmonic voltage distortion during the time when one capacitor is switched in, when both capacitors are switched in and when both capacitors are switched out. Due to time limitations and resource constraints this was not feasible, however the preceding discussions about the adherence to network operating guideline in section 4.5.4 does give comfort that the harmonic distortions are significantly reduced since the implementation of the operating guideline.

CHAPTER 5: CONCLUSION AND RECOMMENDATIONS

5.1 Conclusion

This dissertation has highlighted the results of the study in to the impact of changing network configuration on the power quality at Everest Substation. The entire transmission and distribution network around Everest substation was modelled using Dig-silent Power Factory Simulation Tool. The simulated network fault levels were compared with the actual to confirm the accuracy of the model. The rule of thumb methods was also used to double check and confirms the accuracy of the model.

The history of the network indicates that the problem at Everest substation was initiated in 2005/6 when bus bars were split and other loads removed from Everest to shield the sensitive customers from harmonic pollution caused by mining and other industrial loads. This then drastically reduced the load damping that these loads were providing to the Everest harmonics situation. The results of the frequency sweep simulations indicated that changing the network configuration does influence the network's quality of supply. In the case where both the Everest capacitor banks are switched in, the resonant point is created around the 5^{th} harmonic. Also the 5^{th} harmonic impedance amplitude increased by 61% after network configuration, for the condition when both capacitors are switched in. This was mainly due to changed network impedance and the reduced load damping. This high harmonic impedance for the current network configuration introduces high harmonic voltages which can be harmful to the capacitor banks.

When One Capacitor bank is switched in, the resonant point is created around the 7^{th} harmonic. The 5^{th} harmonic impedance amplitude increased by 35% after network configuration for the condition when one capacitor is in service. Also for the current network configuration there is a 75% reduction in 5^{th} harmonic impedance compared to when the network is operated with both capacitors in service. This reduction in 5^{th} harmonic amplitude represents a much less harmful operating condition for capacitors and network as a whole.

The study revealed that the ideal network configuration is when the network is operated with no capacitor banks in service. The 5^{th} harmonic impedance amplitude is drastically reduced when both capacitor banks are switched out of service. Current Network operation without the capacitor banks seems to be ideal as the 5^{th} and 7^{th} harmonic impedances are very low and there is minimal risk of high harmonic voltages developing. However this configuration

is not practical as the voltages may drop below the nominal value of 132kV, necessitating the use of capacitor banks for voltage support.
An option of upgrading the Everest bank in to a filter bank tuned at the 5th harmonic was also assessed. The study showed that this option would yield positive results where the 5th harmonic currents will be absorbed by the filter. While this option might be advantageous in terms of solving the problem, however due to the high costs of implementation is at this stage not recommended.

Another option of increasing the size of the capacitor bank was assessed. The results of this assessment indicate that the resonant point can be shifted by installing an appropriately sized capacitor bank. Although any of the capacitor banks that were investigated (180 – 240MVAR) would be suitable for the Everest case; however this solution is not preferred mainly because it is costly and it does not offer the flexibility that a tuned harmonic filter offers. When network configuration changes for whatever reason, a fixed capacitor bank may no longer be suitable as it may introduce resonance points at critical frequencies. The solution of changing the capacitor size is therefore not recommended for the Everest case.

The most practical approach recommended is to operate the Everest network with no capacitors in service and only switch in capacitors when necessary. Network operation without the capacitor banks seems to be ideal as the 5th and 7th harmonic impedances are very low and there is minimal risk of high harmonic voltages developing. One capacitor bank can be switched in when necessary, the study shows that when this is done the resonant point is created around the 7th harmonic. This configuration does not pose a major threat as the problematic harmonic level is the 5th. There is a 75% reduction in 5th harmonic impedance amplitude for the current network configuration compared to when the network is operated with both capacitors in service.

In year 2008 during the compilation of this study, a request was made to the Eskom network control to limit the simultaneous switching in of both Everest Capacitor Banks. The capacitor banks were to be only utilised during emergency conditions for voltage support. This arrangement saw a reduction in the number of harmonic distortion violations experienced at Everest substation as seen in figures 4.31 to 4.33 and 4.38.

The performance of the Everest capacitor banks were assessed based on their history of operation and failure mode. The analysis revealed that the Everest capacitors banks failures

were sporadic in nature and could not be directly linked to high harmonic distortions at Everest. However, literature surveyed indicates that exposure to excessive harmonic voltages and currents over time may have a negative impact on equipment performance. Further tests need to be conducted to conclusively prove that excessive harmonics are the main cause of failures.

5.2 Recommendations for Further Work

Future work may involve the assessment of Quality of Supply contracts that Eskom has with various mines and other industries around the Welkom area to ascertain whether customers are complying with emission limits.

Another study that may involve the installation of temperature monitoring devices at Everest Capacitor banks during times when both capacitors are switched in and the harmonic voltages are greatest. This will provide a temperature rise trend that will enable conclusive linking of capacitor bank failures to excessive harmonic levels.

Also a study that may be undertaken is to understand the impact of the campaign initiated by Eskom in 2008 to encourage all industrial and mining customers to reduce their load by 10%, how it has impacted the overall Welkom network in terms of harmonics.

CHAPTER 6: REFERENCES

[1] V. E Wagner, J.C Balda, D. C Griffith, “Effects of Harmonics on Equipment” IEEE Transactions on Power Delivery, Vol. 8, No.2, April 1993, pp. 672-680

[2] T Ramolapeli, “Welkom CLN Harmonics Investigation” Eskom Transmission Performance Audits and Compliance Investigation Report, June 2009

[3] P. Pretorius and R Koch, “ENEL805S: EMC & Power Quality Course Notes, University of kwa-Zulu Natal, Durban, South Africa

[4] American Bureau of Shipping, “Control Of Harmonics In Electrical Power Systems”, May 2006.

[5] Robert G Ellis “Harmonic Analysis of Industrial Power Systems” –Based Method for Identifying Harmonic Sources”, IEEE Transactions on Industrial Applications, Vol 32, No2, March/April 1996.

[6] Hsiung-Cheng Lin and Chao-Hung Chen, “Inter-Harmonic Identification using Group-Harmonic Weighting Approach Based on the FFT”, The 33rd Annual Conference of the IEEE Industrial Electronics Society (IECON) Nov. 5-8, 2007, Taipei, Taiwan.

[7] Chang, G.W., Chen, C.Y., and Wu, M.C., "Measuring harmonics by an improved FFT-based algorithm with considering frequency variations", Proc. of 2006 IEEE International Symposium on Circuits and Systems, 2006, pp.1203-1206.

[8] IEEE Standard 1057-2007, “Standard for Digitizing Waveform Recorders”, the Institute of Electrical and Electronics Engineers, 2007

[9] Li C, Xu W, Tayjasanant T; “A “Critical Impedance” –Based Method for Identifying Harmonic Sources”, IEEE Transactions of Power Delivery, Vol 15, No2, April 2000.

[10] B Peterson, “Spitskop Harmonic Analysis” Eskom Transmission Services Performance Audits and Compliance Investigation Report QoS-2008-10025, August 2008

[11] A. T Stanchev and S. J Ovcharov, “The Power Quality and the Measurement of harmonics,” Available at: http://ecad.tu-sofia.bg – accessed 23 July 2009

[12] Louis Hapeshis, “Power System Harmonic Mitigation for Water and Wastewater Treatment Plants”, Available at: http://www.squared.com– accessed 23 July 2009

[13] IEEE Standard 519-1992, “Recommended Practices and Requirements for Harmonic Control in Electrical Power Systems”, the Institute of Electrical and Electronics Engineers, 1993

[14] John F. Hibbard and Michael Z. Lowenstein, “Meeting IEEE 519-1992 Harmonic Limits,” Available at: http://www.transcoil.com/meetieee.pdf accessed 18 April 2010

[15] Izzeldin Idris Abdalla, K. S. Rama Rao, N. Perumal; “Harmonics Mitigation and Power Factor Correction with a Modern Three-phase Four-Leg Shunt Active Power Filter”, IEEE International Conference on Power and Energy, 29 November – 1 December 2010, Kuala Lampur, Malaysia.

[16] D. Basic, V.S. Ramsden, P. K. Muttik; “Performance of combined power filters in harmonic compensation of high power cyclo-converter drives”, IEEE Transactions of Power Electronics and Variable Speed Drives, 21-23 September 1998,

[17] Zhou Wei, Mu Longhua; “Compensation Characteristics of a Novel LC Shunt Resonance Type Hybrid Active Power Filter”, IEEE International Conference on Electrical Engineering, China, 2009

[18] P.Pillay, M. Manyage, “Definitions of Voltage Unbalance” IEEE Power Engineering Review, May 2001

[19] P. Pacific Gas and Electric Company, “Voltage Unbalance and Motors” Notes, October 2009. Available at: www.pge.com/includes/docs/pdfs accessed on 10 November 2010

[20] Shu-Chen Wang, Yu-Jen Chen, and Chi-Jui Wu, “Design and Implementation of Three-Phase Voltage Flicker Calculation Based on FPGA”, IEEE International Journal of Circuits, Systems and Signal Processing. Issue 2, Vol. 1, 2007

[21] S. A. Deokar and L. M. Waghmare, “Induction motor voltage flicker analysis and its mitigation measures using custom power devices”: A case study”, IEEE International Journal of Engineering Science and Technology. Vol. 2(12), 2010, 7626-7640

[22] Math H. and J. Bollen, “Voltage Recovery after Unbalanced and Balanced Voltage Dips in Three-Phase Systems” IEEE Transactions on Power Delivery, Vol. 18, No. 4, October 2003

[23] D Maule, C Lyons Ltd, “Voltage Dip Mitigation” Copper Development Association, Version 0b November 2001

[24] D. Van Hertem, M. Didden, J. Driesen, and R. Belmans, “Optimal mitigation of voltage dips and interruptions,” in Proc. IEEE Young Researchers Symposium in Electrical Power Engineering, Delft, The Netherlands, Mar. 2004.

[25] E.F Fuchs, D.J Roesler, K.P Kovacs, “Aging of Electrical Appliances due to Harmonics of the Power System‟s Voltage, “ IEEE Transactions on Power Delivery, Vol. PWRD-1, No.3 July 1986, pp. 301 - 307.

[26] www.digsilent.co.za